"*When we feared the dragons, were we fearing a part of ourselves? One way or another, there were dragons in Eden.*" Carl Sagan, 1977.

University of Alberta

The development and biomechanics of theropod teeth and comparisons with other reptiles: a functional analysis

by

Miriam Reichel

A thesis submitted to the Faculty of Graduate Studies and Research
in partial fulfillment of the requirements for the degree of

Doctor of Philosophy
in
Systematics and Evolution

Biological Sciences

Spring 2012
Edmonton, Alberta

Dedication

This thesis is dedicated to Hans Joachim Voget, a man who did not believe in giving up, and who always encouraged me to continue jumping forward, just like a frog, even when I was uncertain of where I would land.

Abstract

Teeth are important for taxonomic studies. They are often the only remains found of certain vertebrates in the fossil record. This is because they are more resistant to weathering than most bones, they are small, and they are generally abundant. Most reptiles have homodont dentition, and the study of their teeth was neglected for a long time due to the lack of structures that facilitate their taxonomic identification. Recently it has been shown that many reptiles have teeth with morphological traits that reliably allow them to be identified to a narrow range of taxonomic groups. Additionally, the study of function and morphometrics of teeth in theropods and other reptiles has shown potential for understanding feeding behaviors. The objectives of this thesis are to describe the function and biomechanics of theropod dinosaur teeth, and compare them to other reptiles. Detailed analyses of histological sections of theropod and varanid lizard teeth show that in both taxa carinal development starts before enamel deposition. A concentration of dentinal tubules near the posterior carinae of all taxa may be related to the presence of larger carinae and denticles on the posterior side of teeth. Finite element analyses of tooth crowns of tyrannosaurids, varanids and *Stegosaurus*, plus the enamel microstructures in various reptile teeth show that an increased bending resistance is observed in taxa with labiolingually thickened teeth and columnar enamel microstructures. Additionally, the morphometric analyses

of tyrannosaurid teeth, and the variation of carinal placements along the tooth rows help quantifying heterodonty. The highest degree of heterodonty was found in *Tyrannosaurus*, and this could be a result of the gigantism observed in this taxon. In conclusion, carinae (and denticles) develop in a variety of different taxa for reasons including phylogenetic relationships, tooth proportions, and tooth biomechanics. Also, heterodonty in tyrannosaurids is quantifiable, and each tooth family produces teeth that are specialized for different functions. The innovative techniques developed for these studies allowed a new approach to the study of reptile teeth. As the search for good modern analogs to fossil taxa continues, comparisons with distantly related taxa show great potential for functional analyses, besides taxonomic studies.

Acknowledgements

There is an extensive list of people that helped me immensely during the course of my grad studies at the University of Alberta. I cannot come up with a specific order of importance, because each person that helped me was “the most important one” in his or her very own way. However, I would like to start by thanking the person that helped me decide to study at the University of Alberta in the first place. A very special thank you to my supervisor Dr. Philip J. Currie, who answered my first e-mail contact from Brazil by a hand-written letter with very encouraging prospects for studies with theropod dinosaurs. Thank you for your extensive help with my research manuscripts, grant applications and countless entertaining moments in field trips and dinner parties.

I would also like to warmly thank Dr. Eva Koppelhus for making sure that many of the technical details and deadlines of research projects and academic requirements were met. She has also been a great friend in times of need and my “second mother” when my biological mother could not be around. Additional thanks to Dr. Michael Caldwell, for being my first personal contact (still back in Brazil) with a University of Alberta professor, and for introducing me to the “Power Plant” on the very first day I arrived at the University. Thank you Dr. Caldwell for also helping me with great insight on my research, for allowing me access to equipment and specimens that made a great part of this thesis possible, and for being part of my thesis committee. Thank you Dr. Alison Murray, for being part of

my thesis committee, for offering help especially during the final stages of my program, and for reviewing manuscripts in their early stages.

I would also like to thank a number of people I met at the Biological Sciences Department at the University of Alberta. Thank you very much Dr. Eric Snively for helping me with Finite Element Analyses and all things mathematics, thank you Dr. Rob Holmes, for helping me with photographic equipment, Dr. Erin Maxwell for great insight in tooth histology, Clive Coy for helping with preparation techniques and being a great colleague in the field, Darrin Molinaro, for help on tooth development research, Al Lindoe, for humorous field trips and great suggestions on preparation techniques, and Dr. Phil Bell, for being a great friend, for understanding southern hemisphere culture, and for teaching me about proper fieldwork and lunch time techniques. Thank you to all students in the vertebrate paleontology lab, especially Michael Burns and Aaron Leblanc, for help with materials described in the tooth development and enamel microstructure chapters, for help in the field (especially in the Danek Bonebed, which is challenging, to say the least), and for great time travels. Additional thanks to Dr. Randy Mandryk and Dr. Arlene Oatway at the Microscopy Lab for help with the varanid lizard histological sections.

People in other departments at the University of Alberta also had important contributions to my research. Thank you Mark Labbe at the Earth and Atmospheric Sciences Thin Sectioning lab for preparing great quality sections of small theropod and Komodo Dragon teeth. Thank you

Manuel Lagravere at the Dentistry/Pharmacy Centre for the CT scans. Thanks to De-Ann Rollings and George Braybrook for the SEM images, the great home-made deer jerky and for finding last-minute time slots to fit me into their busy schedule.

Thanks to the crew at the *T. rex* Discovery Centre in Eastend, Saskatchewan, for lending some of the materials used for comparisons in this study. The *T. rex* tooth (SMNH 2523.8) described in Chapter 1 was collected in 1994 by Tim Tokaryk and Grant Schutte.

Thank you very much to all the people from other institutions in Canada and worldwide who made these projects possible. Thank you Dr. Anthony P. Russell from the University of Calgary for lending the *Varanus rudicollis* specimen for dissection and sectioning. Thank you to the Toronto Zoo staff (Dr. Andrew M. Lentini, Dyann Powley, Pam Pritchard, and Bob Johnson) for collecting 47 Komodo Dragon shed teeth from their cages and sending them to the University of Alberta Vertebrate Paleontology Lab. Thank you Dr. Matthew Vickaryous for suggestions and a protocol for sectioning techniques on teeth. Thank you Dr. Ariana Paulina Carabajal (Premji) for being great company in the field in Argentina and, most of all, a great friend. Thank you to Dr. Vladimir Alifanov and Brandon Strilisky, for allowing access to the PIN and RTMP collections, respectively. Special thanks to Zinaida and Sergei Gagina for great help and companionship during my trip to Moscow. Thanks Dr. Anne Schulp for input and suggestions at early stages of the project involving

mosasaurid teeth. Thanks to H. J. Kirby Siber for organizing the Symposium on Stegosauria and arranging for student travel funding. Additional thanks to Emanuel Tschopp, Jean-Paul Billon-Bruyat for help with *Stegosaurus stenops* photographs. Thanks to Emily Rayfield and Daniela Schwarz-Wings for reviews and helpful comments on the *Stegosaurus* manuscript. Thanks to the reviewers and Associate Editors of CJES for their comments and suggestions on both the *Albertosaurus* Bonebed and the carinal angles on tyrannosaurid teeth manuscripts. Special thanks to all volunteers who cooperated with hard work at the wonderful, yet challenging fieldwork at various localities within Alberta, as well as the volunteers who helped preparing countless specimens at the University of Alberta Vertebrate Paleontology Lab.

None of the projects would have been possible without financial aid. Thank you very much to the Dinosaur Research Institute, Alberta Ingenuity Fund, and Natural Sciences and Engineering Research Council of Canada for providing funding for these projects.

I would also like to thank my family for supporting my love for science and for feeding my curiosity for the natural and historical sciences. Special thanks to my husband Matthew C. Bodner, for believing in my career, and for showing me that true strength lies in persistence and optimism.

Table of Contents

List of Tables

List of Figures

List of Abbreviations

Institutional Abbreviations

AMNH – American Museum of Natural History, New York, NY, USA.

BHI, Black Hills Institute, Hill City, South Dakota, USA.

BMRP – Burpee Museum of Natural History, Rockford, Illinois, USA.

DS-RCR – Sauriermuseum Aathal, Switzerland.

PIN – Paleontological Institute of the Russian Academy of Sciences; Moscow, Russia.

SMNH – Saskatchewan Museum of Natural History, Regina, Saskatchewan, Canada.

TMP – Royal Tyrrell Museum of Palaeontology, Drumheller, Alberta, Canada.

UALVP – University of Alberta Laboratory of Vertebrate Paleontology, Edmonton, Alberta, Canada.

USNM – National Museum of Natural History (Smithsonian Institution), Washington, D.C., USA.

Morphometric Abbreviations

ACH – anterior carina height.

ANG – angle between carinae.

BW – basal width.

FABL – fore-aft basal length.

FABL/BW – proportion between fore-aft basal length and basal width.

Chapter 1

Introduction

Teeth are one of the most studied structures of vertebrate fossils. There are several reasons for this. First, they are abundant and durable. They can also be diagnostic, and hold a significant amount of information about the diet of the organisms they once belonged to.

Some vertebrates, such as sharks and reptiles, will shed teeth in great numbers throughout their lives, because they go through a number of functional tooth sets as they age, a characteristic called polyphyodonty. Another reason for the abundance of vertebrate teeth in the fossil record is that the enamel covering them is hard, and the least diagenetically altered structure in the vertebrate skeleton (Thomas and Carlson 2004). Tooth enamel has low organic composition and high crystallinity (Straight et al. 2004), which are characteristics that decrease the effects of post-burial alterations that are commonly found in bones (Kolodny et al. 1996). It is common to find isolated teeth in excellent preservation amongst vertebrate microfossil assemblages consisting of numerous disarticulated fossil bone remains, such as those commonly found in Dinosaur Provincial Park (Eberth and Currie 2005).

The information held by fossil teeth can be used for phylogenetic studies based on tooth morphology (especially for mammals, which have complex, specialized teeth that allow them to be identified to species level), and provide clues about diet, functional morphology, and paleoecology.

Taxonomic and evolutionary studies based on tooth morphology are abundant for mammals (McKenna 1975; Sigogneau-Russell 1983; Hahn et al. 1989; Kermack et al. 1998; Cifelli 2001; Luo et al. 2001, 2007; van Nievelt and Smith 2005; Renvoisé et al. 2009), fish (Gayet et al. 2003; Shimada 2005; Nyberg et al. 2006; Purdy and Francis 2007) and some reptiles (Currie et al. 1990; Sankey et al. 2002; Smith 2005; Brusatte et al. 2007; Larson 2008). Phylogenetic studies on reptile teeth are not as common as those of mammals and sharks, because for a long time it was believed that reptiles had limited morphological variation in their teeth.

Among dinosaurs, theropod teeth have often been ignored or poorly described in papers regarding osteology and systematics of theropod taxa, mainly because of their lack of easily identifiable structures (Farlow et al. 1991; Sander 1997). Although referred to as not more than “laterally compressed blades” (Dong et al. 1975; Bonaparte and Novas 1985), some authors (Abler 1992; Smith 2005; Smith et al 2005; D’Amore 2009) recognized that theropod dentition is not homogenous and that significant information (both taxonomic and functional) can be obtained when

examining theropod teeth more carefully. Indeed, Currie et al. (1990) recognized that many isolated theropod teeth can be identified to the species level, and sometimes even correspond to the different regions of the jaws. With the increasing number of tooth descriptions in reptiles, the need for a standardized nomenclature in these descriptions arose. The tooth nomenclature proposed by Smith and Dodson (2003) suggests the use of “mesial” to refer to anterior teeth (or portions of teeth), and “distal” to refer to posterior teeth (or portions of teeth). However, “mesial” and especially “distal” are also used for other frames of reference in tooth descriptions, and therefore can cause more potential confusion than “anterior” and “posterior”. Therefore, the preferred terms for the purposes of the analyses throughout this thesis will be “anterior” and “posterior”.

Studies about diet, functional morphology and paleoecology based on teeth have become more common in recent years and range from form-and-function analyses based on tooth measurements (Szalay 1994; Hungerbühler 2000; Renesto and Vecchia 2000; Freeman and Lemen 2006; D’Amore 2009) to elaborate stable isotope analyses (Zazzo et al. 2000; Feranec 2003; Clementz et al. 2003, 2008; Thomas and Carlson 2004; Fricke et al. 2011). These studies led to reconstructions of food chains, plant preferences of herbivores, and paleoenvironmental conditions, including levels of humidity and temperatures.

Other detailed tooth studies that have emerged recently are analyses of reptile enamel microstructures (Sander 2000; Hwang 2005; Stokosa 2005), relating those structures to phylogeny and evolutionary patterns, in addition to some biomechanical inferences. These studies became more feasible with the use of Scanning Electron Microscopy (SEM), because the prismless enamel microstructures that characterize most reptile teeth are not observable under polarized light, in contrast with mammalian prismatic enamel (Sander 2000; Hwang 2005), because the light microscope cannot resolve individual crystallites. Prismatic enamel has been suggested for theropod dinosaurs such as *Carcharodontosaurus saharicus* and *Spinosaurus sp*. (Buffetaut et al. 1986). However, the structures described as “prismatic” are identical to the columns of diverging crystallites described by Sander (1999), Hwang (2005), and Stokosa (2005) for many reptile taxa, including theropod dinosaurs. Additionally, an image claiming to be “naturally preserved external face of Canadian carnosaur showing a prismatic aspect” (Buffetaut et al. 1986) is in fact similar to the surface of dentine in cross-section, and the “prisms” are likely to be dentine tubules.

Regardless of the presence or absence of prisms, all amniotes have enamel that is purely ectodermal (Edmund 1969). In fact, it has been suggested that dental tissues at first developed not in the mouth, because the first vertebrates were jawless, but on the surface of their body, as a protective exoskeleton, or dermal armor (Smith and Sansom 2000). This

type of enamel is exclusively secreted by ameloblasts and is therefore termed monotypic enamel (Smith 1989). It is characterized by appositional growth, documented by its incremental lines and crystallites deposited perpendicular to the tooth surface by ameloblasts (Sansom et al. 1992). Bitypic enamel is also a hypermineralized tissue that occurs on teeth and scales, but it is produced by both neural-crest derived cells (such as odontoblasts) and ameloblasts (Smith 1989). Bitypic enamel is also known as enameloid and is best known in chondrichthyians and some amphibians. In polarized light, it is possible to see dentine tubules extending into the enameloid cap in some actinopterygians, and the enameloid and dentine are also less birefringent than enamel (Smith 1992).

An important review by Sander (2000) describes a debate about the appropriate term to be used to best describe reptilian enamel. According to this review, previously used terms, such as ‘pseudoprismatic’ (Poole 1956; Lester and Koeningswald 1989) and ‘preprismatic’ (Carlson 1990; Koeningswald and Clemens 1992) imply an evolutionary interpretation that these taxa would be related to mammals (which have prismatic enamel), which is not the case for the taxa analyzed in these studies. Alternatively, the terms ‘nonprismatic’ and ‘aprismatic’ (Lester and Koeningswald 1989; Carlson 1990; Koeningswald and Clemens 1992) imply that all other types of enamel are prismatic (Sander 2000). The latest consensus on the term ‘prismless’ (Clemens 1997; Sander 1997; Wood and Stern 1997) seems

appropriate for enamel that lacks prisms, such as in most reptiles. Therefore, this term will be preferred for the discussions in the studies described here.

Further confusion is observed when attempting to classify the enamel microstructures found in reptile enamel, especially when considering the different hierarchies in which they are organized. In order to establish the hierarchy and better describe prismless enamel, five levels of organization have been recognized: the crystallite level, the module level, the enamel type level, the schmeltzmuster level, and the dentition level (Koenigswald and Sander 1997; Sander 1999; Sander 2000). These levels were established with the premise that the structural units of each level are grouped into “building blocks” of the next higher level (Sander 2000).

In the crystallite level, the crystallites may be placed at different angles in relation to the enamel-dentine junction (EDJ). Sander (2000) describes crystallites as being normal to the EDJ (and parallel to each other), or at high angles in relation to the EDJ (in converging, diverging or helicoidal arrangements).

In the module level, Sander (2000) describes columnar units (that may be composed of either diverging or converging crystallites), microunits (bundles of diverging crystallites only a few crystallites long), and compound units (groups of columnar units or microunits). A few

aspects of this classification generate confusion. First, at which point can a microunit be considered a columnar unit, and vice-versa? It seems that more details about the differences between these two units are necessary in order to understand what the relationship between them is, if there is any. A second point of confusion is the inclusion of compound units into the module level. As previously described, the structural units of each level are the building blocks of the next higher level (Sander 2000); in this sense, the compound units do not fit the model, because, as the name says, they are compounds of units included in the module level, which would put the compound units at a level above the module level.

The classification of enamel types by Sander (2000) divides prismless enamel into five categories; these are parallel crystallite enamel, columnar enamel, microunit enamel, compound unit enamel, and wavy enamel. An important addition by Hwang (2005) is the basal unit layer, which is a thin layer of polygonal columnar units adjacent to the enamel-dentine junction. This basal unit layer is the first enamel formed during amelogenesis. Hwang (2005) created another category, the “diverging parallel crystallite enamel”, to describe the enamel type found in *Coelophysis bauri*. This category, however, seems to be similar, if not equal, to the microunit enamel described by Sander (2000) for *Nothosaurus* sp. Therefore, the term ‘microunit enamel’ will be given preference throughout this manuscript. Stokosa (2005) also divides the category “columnar enamel” into “poorly developed” and “well developed”,

after comparing the columnar enamel of *Albertosaurus* and *Tyrannosaurus*. Although there is a clear difference between the enamel of these taxa, it seems that this difference is due to scale, so that the crystallites in *Tyrannosaurus* are significantly smaller than in *Albertosaurus*. However, their arrangement and resulting columnar units are similar, and likely result from the same depositional process. A summary of the enamel types described by Sander (2000) and Hwang (2005) can be found in Table I.1. Additionally, an example of the hierarchies described by Sander (2000) is illustrated for a hypothetical tyrannosaurid tooth in Figure I.1.

Amelogenesis is poorly understood in prismless amniote enamel. The assembly of enamel matrix seems to occur extra-cellularly, without contiguous cellular intervention (Fincham et al. 2000). Sander (2000) made a detailed analysis of enamel depositional processes that may result in the enamel microstructures observed in most reptiles. In his study, Sander (2000) suggests that in the initial stages of amelogenesis, crystallites mineralize close to the secretory faces of ameloblasts; however, during the main phase of amelogenesis, the mineralization lags behind the advancing secretory epithelium. Because of that lag, there is little cellular control over the mineralization of crystallites, similarly to what happens in inorganic precipitates, eggshells, and prismatic bivalve shells (Sander 2000). Therefore, it is also unlikely that the columns (or modules) observed in reptilian enamel reflect the arrangement, shape, and size of

Table I.1: Enamel types commonly found in prismless enamel (Sander 2000; Hwang 2005), and the hierarchical levels that characterize them.

Crystallites	**Module**	**Enamel type**
Diverging; Converging (rare)	Columnar unit	Columnar enamel
Diverging	Microunit	Microunit enamel
Diverging	Columnar unit + Microunit	Compound unit enamel
Parallel crystallites	No modules	Parallel crystallite enamel
Staggered crystallites	No modules	Wavy enamel

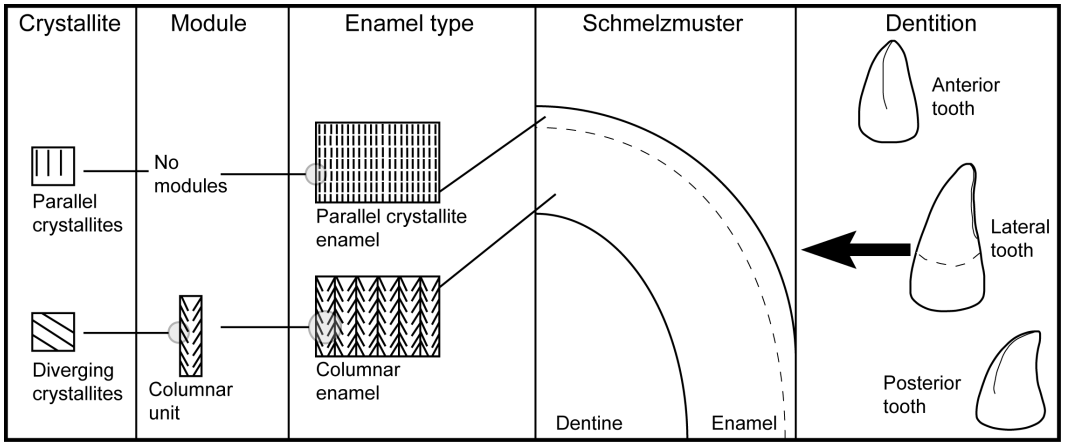

Fig. I.1. The different levels of hierarchy found in tyrannosaurid teeth, after Sander (2000) and Hwang (2005).

the ameloblasts. The main hypotheses on amelogenesis by Sander (2000) describe three main processes that result in different enamel microstructures:

1) In the first hypothesis, the basal unit layer is formed by the early deposition stages of the enamel, in which the crystallite mineralization closely follows the secretion of a proteinaceous matrix, and therefore probably reflects the actual ameloblasts matrix.

2) The second hypothesis describes one of two processes in the main phase of amelogenesis suggested by Sander (2000). In cases where there is columnar enamel (usually with diverging crystallites), Sander (2000) suggests that these structural units do not reflect the ameloblast matrix at all, because the crystallite mineralization lags far behind the secretion front. In this type of deposition, the scarceness of incremental lines could be explained by the fact that the crystallites are not perpendicular to the secretory surface. However, Stokosa (2005) describes well-defined incremental lines in the diverging crystallite enamel of *Tyrannosaurus*.

3) The third hypothesis describes the second depositional process that may occur at the main phase of amelogenesis. This process is the deposition of parallel crystallites, which form the most simple reptilian

enamel type (Sander 2000). In this case, the mineralization of crystallites follows the secretory matrix closely (Sander 2000). Incremental lines occur because all crystallites are perpendicular to the secretory surface, and every time there is a slight change in deposition rates (or in the angle of the secretory matrix) an incremental line occurs.

Stokosa (2005) suggested that enamel types can be related to certain behaviors in carnivorous dinosaurs; for example, the presence of columnar units may be related to bone crushing. In the same paper, a relationship between denticle types and enamel microstructures is suggested for theropod dinosaurs.

The relationship between denticle morphology and enamel microstructures has not yet been tested. In order to do so, a thorough enamel microstructure analysis of numerous theropod taxa with denticulate carinae is necessary. Hwang (2005) and Stokosa (2005) included theropod taxa in their analyses. However, because of the large sample size of isolated theropod teeth in the fossil record, there is potential for more detailed analyses to be done. The variety found in the denticle morphology of theropod dinosaurs, however, has been documented by numerous authors (Currie et al. 1990; Baszio 1997*a*,*b*; Sankey 2001; Sankey et al. 2002; Samman et al. 2005; Currie and Coy 2008; Larson 2008; Longrich 2008; Sankey 2008*a*,*b*). These characteristic structures, along with large sample sizes in micro vertebrate fossil

assemblages, provide great potential for the study of denticles in theropod teeth for taxonomic purposes.

The first detailed taxonomic analysis of small theropod teeth was done by Currie et al. (1990). The identification of theropod teeth to the species level is possible in part because of the distribution and proportions of denticles, which is unique to each taxon, and sometimes to different regions of the jaws. Further analyses of theropod teeth started including the morphometric approach proposed by Currie et al. (1990). Because of that, the number of theropod taxa known for the Aguja, Dinosaur Park, Foremost, Hell Creek, Judith River, Lance, Milk River, and Oldman Formations has increased significantly in the last few decades (Baszio 1997*a*,*b*; Sankey 2001; Sankey et al. 2002; Samman et al. 2005; Currie and Coy 2008; Larson 2008; Longrich 2008; Sankey 2008*a*,*b*).

Although the teeth of theropods provide a great tool for identifying certain taxa, the same is not necessarily true for other clades with serrated teeth. Serrated edges occur in numerous shark taxa, including the Great White Shark (*Carcharodon carcharias*). However, it has been demonstrated that the serrations in this taxon do not occur in a consistent pattern or arrangement, and that each time a tooth is replaced, the serration pattern changes. Therefore, the serrated edges of these teeth are not sufficiently characteristic to enable the identification of a tooth to a

particular position within the jaws of a specimen, or to a particular species (Nambiar et al. 1996).

This high degree of variation in serration patterns shows that the presence of serrations alone does not mean that these structures are always reliable for taxonomic studies. It also suggests that there are different developmental processes involved in the formation of serrated edges on teeth of different taxa.

Tooth development has been well documented for mammals, mostly because of the interest in humans and dentistry. Earlier studies on reptile tooth development mostly addressed tooth replacement rates (Edmund 1960,1962; Westergaard and Ferguson 1990; Kieser et al. 1993, Erickson 1996). However, the development of individual dental tissues in reptiles has been described in few studies (Peyer 1968; Edmund 1969), that have increased in the last decade because of the development of molecular biology (Diekwisch et al. 2002; Caldwell et al. 2003; Harris et al. 2006; Shintani et al. 2006; Beatty and Heckert 2009). Extant crocodilians and lizards are the most commonly studied extant taxa for dental development studies.

Lizards have pleurodont dentition, which makes comparisons for tooth replacement with theropod dinosaurs (which have thecodont dentition) difficult. In crocodiles, the replacement tooth grows into the pulp chamber of the tooth that is about to be shed (Edmund 1962), whereas in

theropod dinosaurs this is not the case. Edmund (1962) described how in *Gorgosaurus* the replacement tooth starts developing lingual to the older tooth; in some specimens, it is possible to see two erupted crowns (of which only one is functional) occupying the same tooth position, before the older one is finally shed. This replacement pattern has unique biomechanical implications and makes comparisons with extant reptile taxa difficult.

Although studies on dental tissue development in reptiles are not nearly as common as in mammals, Peyer (1968) and Edmund (1969) have done a thorough review of the main aspects of reptile tooth development, especially in squamates. Similar to mammals, the histogenesis of a reptile tooth takes place at the boundary between the ectoderm and mesoderm (Peyer 1968). The enamel (originated from the ectoderm) increases outward, while the dentine (originated from the mesoderm) increases inward. Prior to deposition of any hard substances, the mesodermal layer of odontoblasts (which form the dentine) and the ectodermal layer of ameloblasts (which form the enamel) are closely aligned on either side of the basal membrane (Peyer 1968). It has been suggested that because the enamel originates from the ectoderm, teeth would be the last remnants of an exoskeleton in mammals (Lucas 2004).

Little is known about the formation of carinae and denticles in reptiles such as some varanid lizards and theropod dinosaurs. Sander

(2000) analyzed the enamel structures of various amniote taxa. Among all the structures found on the surface of the tooth (such as enamel wrinkles, ridges, ribs, and carinae), Sander (2000) stated that only serrations along the cutting edge of reptile teeth occur at the enamel-dentine junction. Indeed, both theropod and some ornithopod dinosaurs have denticulate cutting edges on their teeth, and they are at the enamel-dentine junction.

Although only denticulate cutting edges are seen in the enamel-dentine junction in many taxa, there are exceptions. Supernumerary carinae (with denticles) are known to occur in theropods (Abler 1992; Erickson 1995; Fiorillo and Gangloff 2000; Candeiro and Tanke 2008; Sereno and Brusatte 2008), as well as in more basal archosauriforms (Beatty and Heckert 2009). In these cases, the serrations are seen at the enamel-dentine junction, but they are not always placed along the cutting edges of the teeth. Additionally, in some cases the irregularities in dentine deposition seen near the denticles are also seen all the way into the pulp cavity. Structures similar to denticles can be seen in the matrix filling the pulp cavity of a *Tyrannosaurus rex* (SMNH 2523.8) tooth. This observation contrasts with the structures seen in teeth of taxa that have sharp longitudinal ridges expressed only in the enamel, but not in the dentine. Examples described by Sander (2000) include the nothosaur *Nothosaurus* sp., the captorhinomorph *Dictyobolus tener*, and the plesiosaur *Liopleurodon ferox*. This fundamental difference between structures found in teeth exposes a problem with nomenclature. Therefore, the terms

“carina” and “denticle” should be reserved for the structures formed by both enamel and dentine. In contrast, the terms “keels” and “serrations” imply a broader concept, concerned only with external morphology, and those terms should be preferred when referring to specimens in which the composition of these structures is unknown. In cases where tooth structures are formed only by enamel, the more appropriate term is “enamel ornamentations”.

As previously mentioned, extensive studies have been done on dinosaur denticulate carinae in relation to their taxonomic significance, but studies relating their form to their function are scarce (Farlow et al. 1991; Abler 1992; D’Amore 2009). Similarly, studies regarding reptile enamel microstructure (Sander 1999; Hwang 2005; Stokosa 2005) have phylogenetic significance, but provide limited information on the function or biomechanics of the different structures observed.

When the functions of teeth are addressed, comparisons with other cutting tools, such as blades, are inevitable. The drawing force of a blade is the force needed to draw the blade across a certain substrate. Frazzetta (1988) noted that a thin smooth blade cuts more readily than a thicker blade. However, Farlow et al. (1991) indicated that biological hard tissues make it difficult to produce a tooth that is thin (and therefore sharp), but at the same time strong enough to resist the stresses of struggling prey. A serrated edge may allow a tooth to do a comparable amount of damage as a thinner smooth blade, and at the same time be less likely to break

(Farlow et al. 1991). Indeed, Abler (1992) observed the action of serrated metal blades and suggested that serrations trap and cut materials in a "grip-and-rip" fashion.

Large theropod teeth tend to have more denticles than small theropod teeth (Farlow et al. 1991). A serrated blade is more likely to bind against the material in which it is embedded than a smooth blade (Frazzetta 1988), and this effect is more pronounced in coarse than in fine serrations. Farlow et al. (1991) suggest that the relatively smaller denticle sizes seen in large rather than in small theropod teeth could reflect an attempt to reduce this problem by maintaining denticles closer to an optimal size in larger teeth.

Tyrannosaurids have a few unique features in their dentition that have yet to be more extensively explored from a biomechanical point of view. Tyrannosaurid teeth have been referred to as dull smooth blades (Abler 1992), and therefore it has been suggested that they function by concentrating large forces onto small areas. Tyrannosaurids did indeed have strong bite forces, estimated as being up to 13,400N (Erickson et al. 1996, Reichel 2010). Additionally, these strong bite forces were often applied to bones (Erickson et al. 1996) or teeth, especially during feeding (Erickson et al. 1996; Molnar 1998). They also engaged in intra-specific face-biting (Tanke and Currie 2000; Bell and Currie 2009). The contact with bone or other teeth frequently resulted in worn or broken tips.

Nevertheless, the wear patterns observed in tyrannosaurid teeth usually do not indicate tooth-to-tooth contact inside the mouth (Molnar 1998) because the wear patterns observed in most teeth are not consistent with the way tyrannosaurid jaws are aligned (Schubert and Unguar 2005).

Tyrannosauridae are only known from the Campanian and Maastrichtian of eastern and central Asia and North America. The latest tyrannosaurid is *Tyrannosaurus rex*. Members of the more inclusive taxon Tyrannosauroidea include more primitive and earlier (Late Jurassic, Early Cretaceous) forms, such as *Dilong* (Xu et al. 2004), *Dryptosaurus* (Carpenter et al. 1997), *Eotyrannus* (Hutt et al. 2001), and *Guanlong* (Xu et al. 2006). A trend towards incrassate (labiolingually thickened) teeth is observed, especially in more derived forms. The early tyrannosauroids and juveniles of tyrannosaurids show zyphodonty (bladelike teeth), but those teeth are still labiolingually thicker than in other theropods (Farlow et al. 1991; Holtz 2004; Longrich et al. 2010).

Abler (1992) observed scratches on the surfaces of fossil teeth and concluded that they are biological rather than preservational, because tyrannosaur tooth surfaces are far more scratched than pedal unguals from the same formation. This suggests that tyrannosaur teeth impacted hard materials such as bones, and even other teeth. It is not uncommon to see fossil bones or tyrannosaurid teeth with tyrannosaurid tooth marks (Abler 1992; Erickson et al. 1996).

Another interesting aspect about tyrannosaurid dentition is their heterodonty, which has been documented by several authors (Currie et al. 1990; Molnar 1998; Holtz 2004; Smith 2005). However, some authors disagree with the term 'heterodonty' being applied to this group (Stokosa 2005; D'Amore, 2009). Stokosa (2005) recognizes that the teeth in tyrannosaurids have different functions according to their position within the jaws, but argues that this is not enough evidence for heterodonty. D'Amore (2009) states that the morphometric variation observed in tyrannosaurid teeth does not suggest specialized functions for specific teeth, and therefore the only factor influencing this variation is the distance of each tooth from the jaw hinge. Nevertheless, tyrannosaurid teeth can generally be grouped into at least five sets; premaxillary, anterior maxillary, posterior maxillary, anterior dentary, and posterior dentary (Samman et al. 2005; Smith 2005). Additionally, Smith (2005) considers the first dentary tooth as another type. According to Smith (2005), *Tyrannosaurus* has a higher degree of heterodonty than *Albertosaurus*. This variation in tooth morphology suggests that there are different functions for each region in the mouth. The anterior portion of a jaw of a tyrannosaurid has teeth that are slightly curved posteriorly and have characteristic D-shaped cross sections. These are often referred to as 'incisiform' in shape. Robust, curved and elongate teeth characterize the middle portions of the jaws. Finally, the posterior regions of the jaws have small, strongly curved and more labiolingually compressed teeth.

The jaw position of a tooth in a tyrannosaurid may dictate the curvature of the tooth. This is because the “line of action” of a tooth (Rieppel 1979), or the direction it moves relative to the food that is being processed in the animal’s mouth, depends on its position relative to the jaw hinge (D’Amore 2009). For a more efficient bite, the apex of a tooth needs to contact the food first, focusing the force onto a smaller area for puncturing the food (D’Amore 2009). The curved teeth would also help forcing food back into the throat of tyrannosaurids, especially when considering the inertial feeding behavior proposed by Snively and Russell (2007) for tyrannosaurids.

Indeed, the curvature of a *Tyrannosaurus* tooth roughly matches the circular arcs of radius equal to the distance from the tooth tip to the craniomandibular joint (Molnar 1998). Additionally, D’Amore (2009) suggests that the apex of a tooth indicates the direction in which a tooth must move when initially contacting the substrate. A “line of action” (Rieppel 1979) is then drawn on the anterior margin of the tooth, based on the orientation of the apex. The area opposite to the line of action may not contact the substrate and is defined by D’Amore (2009) as “dead space” (Fig. I.2.). D’Amore (2009) demonstrated that the height of the position where anterior denticulation terminates correlates with the posterior curving of the tooth. Consequently, the height of the dead space correlates to the extent of anterior denticulation.

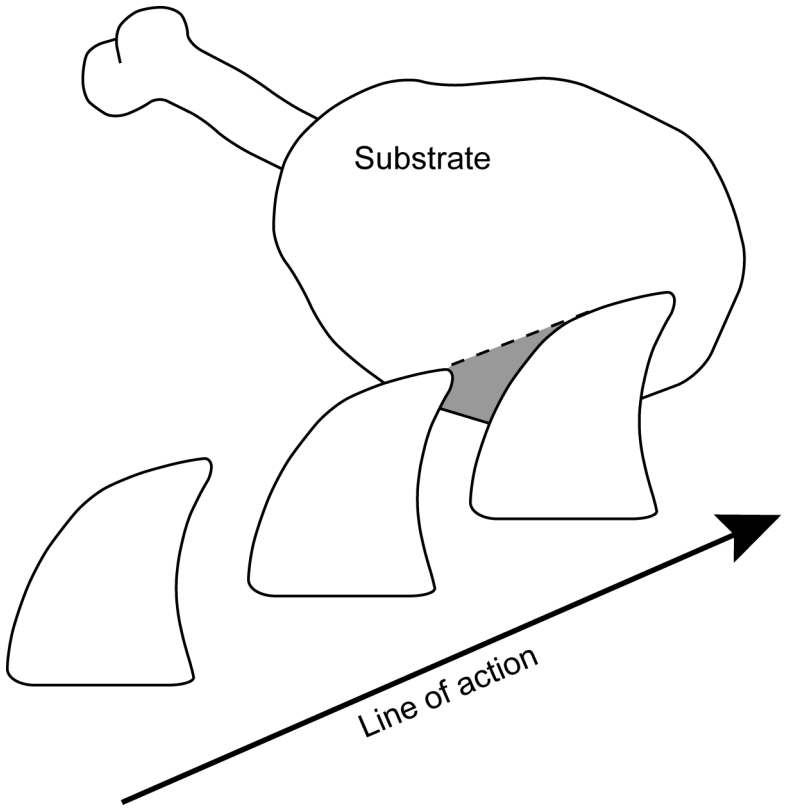

Fig. I.2. Diagram representing the interaction between teeth and substrate, after Rieppel (1979) and D'Amore (2009). The line of action determines the direction the apex of the tooth is moving (towards the substrate). Opposite to the motion of the tooth, a "dead space" forms (gray area).

Mechanical models made of metal have been used to simulate tyrannosaurid bites (Abler 1992) and test the performance of teeth. Erickson et al. (1996) estimated bite forces for *Tyrannosaurus rex* based on tooth marks left on bones. But little is known about how the tooth itself responds to such stresses and how the different morphologies found within one specimen react to various situations involved in biting motions. Mazzetta et al. (2004) performed stress tests on a *Giganotosaurus* tooth. They used a three dimensional model generated by a CT scanner and simulated forces in four different directions. In that experiment, the authors were able to estimate the amount of force tolerated by that tooth and inferred the type of prey that *Giganotosaurus* would have preferred.

Although a detailed study on theropod tooth and serration morphology was done by Currie et al. (1990), with indications of general carinae positioning, the details on angles and variations of carinae along the tooth rows in each taxon have only been superficially addressed (Samman et al. 2005; Smith 2005). Because the front of the snout of tyrannosaurids is wider (U-shaped rather than V-shaped) than in most theropods, the anterior carinae of the anterior teeth have shifted to the posterior surfaces, so that the cross sections of those teeth are D-shaped (Currie et al. 1990). A similar condition is observed in another small theropod, *Troodon*, in which the cross section of anterior teeth is triangular (Currie et al. 1990). On more posterior teeth, the carinae gradually shift in position, until they attain an angle of approximately 180° degrees between

them. Smith (2005) analyzed the dentition of a single theropod taxon, *Tyrannosaurus rex*, in a detailed morphometric study. Some of the measurements include angles for the crown curvature based on photographs, but none define the position changes of the carinae along the tooth rows. In that study, Smith (2005) pointed out the *en echelon* placement (diagonal alignment) of teeth in *Tyrannosaurus*, which produces a wider cut, and promotes a more efficient grip for anterior, incisor-like teeth. This tooth placement is also likely to influence carinae positioning in the teeth of this taxon.

Smith et al. (2005) published a study on theropod tooth morphology in which an emphasis is given to easily repeatable measurements that will aid the identification of isolated crowns commonly found in the field. The techniques described in the study are valuable tools for identification purposes but no functional inferences were made to supplement the morphometrics.

To develop an understanding of tooth function and biomechanics, this project is divided into five parts. The first one (Chapter 2) deals with the development of carinae in theropod dinosaurs and the varanid lizards *Varanus komodoensis* and *Varanus rudicollis*. This project is based on the descriptions of thin sections of theropod teeth and histological sections of varanid teeth and jaws. The second project (Chapter 3) is a comparison of 3D models of *Albertosaurus sarcophagus* and *Tyrannosaurus rex* teeth. These models were analyzed through finite element analyses (FEA) and

the degree of heterodonty in these taxa is compared. The third project (Chapter 4) is an analysis of the variation in carinae positioning in *Albertosaurus, Daspletosaurus, Gorgosaurus, Tarbosaurus,* and *Tyrannosaurus*. The positions of carinae and other tooth proportions were measured in all taxa, and multivariate analyses were used to compare them. The fourth project (Chapter 5) is a study of enamel microstructures found in theropods, in the varanid lizard *Varanus komodoensis* and the mosasaurid *Platecarpus.* The biomechanics of these microstructures with some functional inferences are described. This project tests stress levels on 3-D models representing the enamel microstructures, through FEA. The fifth project (Chapter 6) represents a case study of a herbivorous taxon, *Stegosaurus stenops*, which has denticulate teeth; functional inferences are made based on a 3-D model with FEA analyses similar to the ones in Chapter 3.

The main goal of this thesis is to determine why and how carinae (and denticles) develop in such a variety of different taxa. There are multiple hypotheses tested in each chapter. However, the main hypotheses in this thesis are: 1. Carinal and denticle development are similar in a variety of taxa and are therefore an adaptive convergence; and 2. Carinal positions, along with other measurable variables in tooth morphometrics influence tooth function, its biomechanics, and make heterodonty quantifiable.

The first hypothesis is tested in Chapter 2, in which details about tooth and especially carinal and denticle development are described for two varanid lizards and some theropod dinosaurs. The analysis of histological sections and SEM images helped to identify the differences and similarities between the development of these structures in the dentition of such distantly related taxa.

The second hypothesis is tested in Chapters 3 to 6. Chapter 3 describes the degree of heterodonty found in the tyrannosaurids *Albertosaurus* and *Tyrannosaurus* based on tooth crown proportions and root lengths. Chapter 4 is an analysis of the changes in the angles measured between anterior and posterior carinae along the tooth rows of five tyrannosaurid taxa (*Albertosaurus*, *Daspletosaurus*, *Gorgosaurus*, *Tarbosaurus*, and *Tyrannosaurus*). This chapter also compares other tooth measurements obtained from *in situ* teeth only and estimates the potential for such morphometric studies to help quantify heterodonty among different tyrannosaurid taxa. In Chapter 5 the enamel microstructures in isolated teeth of a troodontid, a tyrannosaurid, a varanid lizard, and two mosasaurids are compared. 3-D models representing these structures are tested biomechanically, through Finite Element Analyses. Each microstructure is then analyzed from a functional point of view, taking into consideration the feeding habits of each group tested. Chapter 6 draws a comparison of some of the techniques applied in the previous chapters into a herbivorous taxon, *Stegosaurus*. This homodont taxon has teeth

ornamented with denticles and ridges and some biomechanical and functional inferences are made based on 3-D models tested with Finite Element Analyses.

The significance of this thesis lies in the better understanding of how much behavioral information can be obtained from studying reptile teeth in more detail, even in taxa that have previously been considered to have rather homogenous dentition (Dong et al. 1975; Bonaparte and Novas 1985). Additionally, the enamel microstructures of mosasaurid and varanid lizard teeth are described for the first time, as well as *Varanus komodoensis* and *Varanus rudicollis* tooth crown histology. Finally, the study of carinal development in teeth is an initial step to understand the evolution of such a widespread solution for carnivory. Mammals have been shown to have developed a great variety of tooth morphologies and a highly successful configuration in their prismatic enamel. Although reptile dentition has been neglected or ignored by scientists for decades, in more recent research the increasing potential for studies in reptile teeth has been demonstrated. This thesis introduces new research techniques that can be applied to a variety of taxa in the future and reinforces the variety of adaptations and morphological diversity found in reptile teeth. All it takes is a closer look, and high-end computer software.

References

Abler, W. L. 1992. The serrated teeth of tyrannosaurid dinosaurs, and biting structures in other animals. Paleobiology, **18**(2): 161–183.

Baszio, S. 1997*a*. Investigations of Canadian dinosaurs: Palaeoecology of dinosaurs throughout the Late Cretaceous of south Alberta, Canada. Courier Forschungsinstitut Senckenberg, **196**: 1–31.

Baszio, S. 1997*b*. Investigations of Canadian dinosaurs: systematic palaeontology of isolated dinosaur teeth from the Latest Cretaceous of south Alberta, Canada. Courier Forschungsinstitut Senckenberg, **196**: 33–77.

Beatty, B.L., and Heckert, A.B. 2009. A large archosauriform tooth with multiple supernumerary carinae from the Upper Triassic of New Mexico (USA), with comments on carina development and anomalies in the Archosauria. Historical Biology, **21**(1): 57–65.

Bell, P.R., and Currie, P.J. 2009. A tyrannosaur jaw bitten by a confamilial: scavenging or fatal agonism? Lethaia, **43**: 278–281.

Bonaparte, J.F., and Novas, F.E. 1985. *Abelisaurus comahuensis*, n. gen., n. sp. Carnosauria del Cretacico tardio de Patagonia. Ameghiniana, **21**: 259–265.

Brusatte, S.L., Benson, R.B.J., Carr, T.D., Williamson, T.E., and Sereno, P.C. 2007. The systematic utility of theropod enamel wrinkles. Journal of Vertebrate Paleontology, **24**: 1052–1056.

Buffetaut, E., Dauphin, Y., Jaeger, J.J., Martin, M., Mazin, J.M., and Tong, H. 1986. Prismatic dental enamel in theropod dinosaurs. Naturwissenschaften, **73**: 326–327.

Caldwell, M.W., Budney, L.A., and Lamoureux, D.O. 2003. Histology of tooth attachment tissues in the Late Cretaceous mosasaurid *Platecarpus*. Journal of Vertebrate Paleontology, **23**(3): 622–630.

Candeiro, C.R., and Tanke, D.H. A pathological Late Cretaceous carcharodontosaurid tooth from Minas Gerais, Brazil. Bulletin of Geosciences, **83**(3): 351–354.

Carlson, S.J. 1990. Vertebrate dental structures. *In*: Skeletal biomineralization: patterns, processes and evolutionary trends, vol. 1. *Edited by*: J.G. Carter (ed.). New York: Van Nostrand Reinhold. pp. 534 – 556.

Carpenter, K., Russell, D., Baird, D., and Denton, R. 1997. Redescription of the holotype of *Dryptosaurus aquilunguis* (Dinosauria: Theropoda) from the Upper Cretaceous of New Jersey. Journal of Vertebrate Paleontology, **17**: 561–573.

Cifelli, R.L. 2001. Early mammalian radiations. Journal of Paleontology, **75**(6): 1214–1226.

Clemens, W.A. 1997. Characterization of enamel microstructure terminology and applications in systematic analyses. *In*: Tooth enamel microstructure. *Edited by*: W.v. Koeningsvald and P.M. Sander. Rotterdam: A. A. Balkema. pp. 85–112.

Clementz, M.T., Hoppe, K.A., and Koch, P.L. 2003. A paleoecological paradox: the habitat and dietary preferences of the extinct tethythere *Desmostylus*, inferred from stable isotope analysis. Paleobiology, **29**(4): 506–519.

Clementz, M.T., Holroyd, P.A., and Koch, P.L. 2008. Identifying aquatic habits of herbivorous mammals through stable isotope analysis. PALAIOS, **23**: 574–585.

Currie, P.J., and Coy, C. 2008. *In* Vertebrate Microfossil Assemblages: their role in palaeoecology and palaeobiogeography. *Edited by* Sankey, J.T., and Baszio, S. (eds.). Indiana University Press, Bloomington. pp. 159–165.

Currie, P.J., Rigby, J.K. Jr., and Sloan, R.E. 1990. Theropod teeth from the Judith River Formation of Southern Alberta, Canada. *In*: Dinosaur Systematics: Approaches and Perspectives. *Edited by* Carpenter, K. and P. J. Currie (eds.). Cambridge University Press. pp. 107–125

D'Amore, D.C. 2009. A functional explanation for denticulation in theropod teeth. The Anatomical Record, **292**: 1297–1314.

Dieckwisch, T.G.H., Berman, B.J., Anderton, X., Gurinsky, B., Ortega, A.J., Satchell, P.G., Williams, M., Arumugham, C., Luan, X., McIntosh, J.E., Yamane, A., Carlson, D.S., Sire, J.-Y., and Shuler, C.F. 2002. Membranes, minerals, and proteins of developing vertebrate enamel. Microscopy research and technique, **59**: 373–395.

Dong, Z., Zhang, Y., Li, X., and Zhou, S. 1975. A new carnosaur from Yongchuan County, Sichuan Province. Kexue Tongbao (Science Newsletter), **23**: 302–304.

Eberth, D.A., and Currie, P.J. 2005. Vertebrate taphonomy and taphonomic modes. *In* Dinosaur Provincial Park: A spectacular ancient ecosystem revealed. *Edited by* P.J. Currie and E.B. Koppelhus. Indiana University Press. pp. 453–477.

Edmund, A.G. 1960. Tooth replacement phenomena in the lower vertebrates. The Royal Ontario Museum, Life Sciences Division, Contributions No. **52**: 1–190.

Edmund, A.G. 1962. Sequence and rate of tooth replacement in the Crocodilia. The Royal Ontario Museum, Life Sciences Division, Contributions No. **56**: 1–42.

Edmund, A.G. 1969. Dentition. *In* Biology of the Reptilia – Volume 1, Morphology A. *Edited by* C. Gans, A.d'A. Bellairs, and T.S. Parsons. Academic Press, London, UK. pp. 117–200.

Erickson, G.M. 1995. Split carinae on tyrannosaurid teeth and implications of their development. Journal of Vertebrate Paleontology, **15**(2): 268–274.

Erickson, G.M. 1996. Daily deposition of dentine in juvenile *Alligator* and assessment of tooth replacement rates using incremental line counts. Journal of Morphology, **228**: 189 –194.

Erickson, G.M., Van Kirk, S.D., Su, J., Levenston, M.E., Caler, W.E., and Carter, D.E. 1996. Bite-force estimation for *Tyrannosaurus rex* from tooth-marked bones. Nature, **382**:706–708.

Farlow, J.O., Brinkman, D.L., Abler, W.L., and Currie, P.J. 1991. Size, shape and serration density of theropod dinosaur lateral teeth. Modern Geology **16**: 161–198.

Feranec, R.S. 2003. Stable isotopes, hypsodonty, and the paleodiet of *Hemiauchenia* (Mammalia: Camelidae): a morphological specialization creating ecological generalization. Paleobiology, **29**(2): 230–242.

Fincham, A.G., Luo, W., Moradian-Oldak, J. Paine, M.L., Snead, M.L., and Zeichner-David, M. 2000. Enamel biomineralization: the assembly and

disassembly of the protein extracellular organic matrix. *In* Development, function and evolution of teeth. *Edited by* M.F. Teaford, M.M. Smith, and M.W.J. Ferguson (eds.). Cambridge University Press, Cambridge. pp. 37–61.

Fiorillo, A.R., and Gangloff, R.A. 2000. Theropod teeth from the Prince Creek Formation (Upper Cretaceous) of Northern Alaska, with speculations on Arctic dinosaur paleoecology. Journal of Vertebrate Paleontology, **20**(4): 675–682.

Frazzetta, T.H. 1988. The mechanics of cutting and the form of shark teeth (Chondrichthyes, Elasmobranchii). Zoomorphology, **108**: 93–107.

Freeman, P.W., and Lemen, C. 2006. Puncturing ability of idealized canine teeth: edged and non-edged shanks. Journal of Zoology, **269**: 51 – 56.

Fricke, H. C., Hencecroth, J., and Hoerner, M. E. 2011. Lowland – upland migration of sauropod dinosaurs during the Late Jurassic epoch. Nature (letter), doi:10.1038/nature10570. Published online 26 October 2011.

Gayet, M., Jégu, M., Bocquentin, J., and Negri, F.R. 2003. New characoids from the Upper Cretaceous and Paleocene of Bolivia and the Mio-Pliocene of Brazil: phylogenetic position and paleobiogeographic implications. Journal of Vertebrate Paleontology, **23**(1): 28–46.

Hahn, G., Sigogneau-Russell, D., and Wouters, G. 1989. New data on Theroteinidae – their relations with Paulchoffatiidae and Haramiyidae. Geologica et Paleontologica, **23**: 205–215.

Harris, M.P., Hasso, S.M., Ferguson, M.W.J., and Fallon, J.F. 2006. The development of archosaurian first-generation teeth in a chicken mutant. Current Biology, **16**: 371–377.

Holtz, T.R., Jr. 2004. Tyrannosauroidea. *In* The Dinosauria. *Edited by* D.B. Weishampel, P. Dodson, and H. Osmólska (eds.). University of California Press, USA. pp. 111–136.

Hungerbühler, A. 2000. Heterodonty in the European phytosaur *Nicrosaurus kapffi* and its implications for the taxonomic utility and functional morphology of phytosaur dentitions. Journal of Vertebrate Paleontology, **20**(1): 31–48.

Hutt, S., Naish, D.W., Martill D.M., Barker, M.J., and Newbery, P. 2001. A preliminary account of a new tyrannosaurid theropod from the Wessex Formation (Early Cretaceous) of southern England. Cretaceous Research, **22**: 227–242.

Hwang, S.H. 2005. Phylogenetic patterns of enamel microstructure in dinosaur teeth. Journal of Morphology, **266**: 208–240.

Kermack, K.A., Kermack, D.M., Lees, P.M., and Mills, J.R. E. 1998. New multituberculate-like teeth from the Middle Jurassic of England. Acta Paleontologica Polonica, **43**(4): 581–606.

Kieser, J.A., Klapsidis, C. Law, L., and Marion, M. 1993. Heterodonty and patterns of tooth replacement in *Crocodylus niloticus*. Journal of Morphology, **218**: 195–201.

Koeningswald, W.V., and Clemens, W.A. 1992. Levels of complexity in the microstructure of mammalian enamel and their application in studies of systematics. Scanning microscopy, **6**: 195–218.

Koeningswald, W.V., and Sander, P.M. 1997. Glossary of terms used for enamel microstructure. *In* Tooth enamel microstructure. *Edited by* W.V. Koeningswald, and P.M. Sander (eds.). A.A. Balkema, Rotterdam. pp. 267–280.

Kolodny, Y., Luz, B., Sander, M., and Clemens, W.A. 1996. Dinosaur bones: fossils or pseudomorphs? The pitfalls of physiology reconstruction from apatitic fossils. Palaeogeography, Palaeoclimatology, Palaeoecology, **126**: 161–171.

Larson, D.W. 2008. Diversity and variation of theropod dinosaur teeth from the uppermost Santonian Milk River Formation (Upper Cretaceous), Alberta; a quantitative method supporting identification of the oldest

dinosaur tooth assemblage in Canada. Canadian Journal of Earth Sciences, **45**(12): 1455–1468.

Lester, K.S., and Koeningswald, W.V. 1989. Crystallite orientation discontinuities and the evolution of mammalian enamel – or, when is a prism? Scanning microscopy, **3**: 645–663.

Longrich, N. R. 2008. Small theropod teeth from the Lance Formation of Wyoming, USA. *In* Vertebrate microfossil assemblages: their role in paleoecology and paleogeography. *Edited by* J.T. Sankey and S. Baszio (eds.). Indiana University Press, Bloomington, IN. pp. 135–158.

Longrich, N. R., Horner, J. R., Erickson, G. M., and Currie, P. J. 2010. Cannibalism in *Tyrannosaurus rex*. PLoS ONE, **5**(10): e13419. doi:10.1371/journal.pone.0013419

Lucas, P.W. 2004. Dental functional morphology: how teeth work. University Press, Cambridge, UK. 355 pp.

Luo, Z.-X., Cifelli, R.L., and Kielan-Jaworowska, Z. 2001. Dual origin of tribosphenic mammals. Nature, **409**: 53–57.

Luo, Z.-X., Ji, Q., and Yuan, C.-X. 2007. Convergent dental adaptations in pseudo-tribosphenic and tribosphenic mammals. Nature, **450**: 93–97.

Mazzetta, G.V., Blanco, R.E., and Cisilino, A.P. 2004. Modelizacion con elementos finitos de un diente referido al genero *Giganotosaurus* Coria

y Salgado, 1995 (Theropoda: Carcharodontosauridae). *Ameghiniana* **41(4)**: 619–626.

McKenna, M. C. 1975. Toward a phylogenetic classification of the Mammalia. *In* Phylogeny of the primates. *Edited by* W.P., Luckett, and F.S. Szalazay. Plenum, New York. pp 55–95.

Molnar, R.E. 1998. Mechanical factors in the design of the skull of *Tyrannosaurus rex* (Osborn, 1905). *In* GAIA 15: Aspects of theropod paleobiology. *Edited by* B.P. Pérez-Moreno, T. Holtz, J.L. Sanz, and J.J. Mortalla. Museu Nacional de História Natural, Lisbon, Portugal. pp. 193–218.

Nambiar, P., Brown, K.A., and Bridges, T.E. 1996. Forensic implications of the variation in morphology of marginal serrations on the teeth of the Great White Shark. Journal of Forensic Odontostomatology, **14**(1): 2–8.

van Nievelt, A.F.H., and Smith, K.K. 2005. Tooth eruption in *Monodelphis domestica* and its significance for phylogeny and natural history. Journal of Mammalogy, **86**(2): 333–341.

Nyberg, K.G., Ciampaglio, C.N., and Wray, G. A. 2006. Tracing the ancestry of the great white shark, *Carcharodon carcharias*, using morphometric analyses of fossil teeth. Journal of Vertebrate Paleontology, **26**(4): 806–814.

Peyer, B. 1968. Comparative odontology. The University of Chicago Press, Chicago, USA. 347 pp.

Poole, D.F. 1956 The structure of the teeth of some mammal-like reptiles. Quarterly Journal of Microscopical Science, **97**: 303–312.

Purdy, R.W., and Francis, M.P. 2007. Ontogenetic development of teeth in *Lamna nasus* (Bonnaterre, 1758) (Chondrichthyes: Lamnidae) and its implications for the study of fossil shark teeth. Journal of Vertebrate Paleontology, **27**(4): 798–810.

Reichel, M. 2010. The heterodonty of *Albertosaurus sarcophagus* and *Tyrannosaurus rex*: biomechanical implications inferred through 3-D models. Canadian Journal of Earth Sciences, **47**: 1253–1261.

Renesto, S., and Vecchia, F.M.D. 2000. The unusual dentition and feeding habits of the prolacertiform reptile *Langobardisaurus* (Late Triassic, northern Italy). Journal of Vertebrate Paleontology, **20**(3): 622–627.

Renvoisé, E., Evans, A.R., Jebrane, A., Labruère, C., Laffont, R., and Montuire, S. 2009. Evolution of mammal tooth patterns: new insights from a developmental prediction model. Evolution, **63**(5): 1327–1340.

Rieppel, O. 1979. A functional interpretation of varanid dentition (Reptilia, Lacertilia, Varanidae). Gegenbaurs Morphologisches Jahrbuch, Leipzig, **125**: 797–817.

Samman, T. Powell, G.L., Currie, P.J., and Hills, L.V. 2005. Morphometry of the teeth of western North American tyrannosaurids and its applicability to quantitative classification. Acta Palaeontologica Polonica, **50**(4): 757–776.

Sander, P. M. 1997. Non-mammalian synapsid enamel and the origin of mammalian enamel prisms: the bottom-up perspective. *In* Koenigswald, W.v. and Sander, P. M. (eds) Tooth enamel microstructure. Balkema, Rotterdam, Netherlands. Pp. 41–62.

Sander, P.M. 1999. The microstructure of reptilian tooth enamel: terminology, function, and phylogeny. München Geowissenschaften Abhandlungen (Reihe A), **38**: 1–102.

Sander, P. M. 2000. Prismless enamel in amniotes: terminology, function, and evolution. *In* Development, function and evolution of teeth. *Edited by* M.F. Teaford, M.M. Smith, and M.W.J. Ferguson. Cambridge University Press, Cambridge, UK, pp. 92–106.

Sankey, J.T. 2001. Late Campanian southern dinosaurs, Aguja Formation, Big Bend, Texas. Journal of Paleontology, **75**(1): 208–215.

Sankey, J.T. 2008*a*. Vertebrate paleoecology from microsites, Talley Mountain, Upper Aguja Formation, (Late Cretaceous), Big Bend National Park, Texas, USA. *In* Vertebrate microfossil assemblages: their role in paleoecology and paleobiogeography. *Edited by* J.T.

Sankey and S. Baszio. Indiana University Press, Bloomington, Ind., pp. 61–77.

Sankey, J.T. 2008*b*. Diversity of Latest Cretaceous (late Maastrichtian) small theropods and birds: teeth from the Lance and Hell Creek formations, USA. *In* Vertebrate microfossil assemblages: their role in paleoecology and paleobiogeography. *Edited by* J.T. Sankey and S. Baszio. Indiana University Press, Bloomington, Ind., pp. 117–137.

Sankey, J.T., Brinkman, D.B., Guenthier, M., and Currie, P.J. 2002. Small theropod and bird teeth from the Late Cretaceous (Late Campanian) Judith River Group, Alberta. Journal of Paleontology, **76**(4): 751–763.

Sansom, I.J., Smith, M.P., Armstrong, H.A., and Smith, M.M. 1992. Presence of the earliest vertebrate hard tissues in conodonts. Science, **256**: 1308–1311.

Schubert, B.W., and Unguar, P.S. 2005. Wear facets and enamel spalling in tyrannosaurid dinosaurs. Acta Palaeontologica Polonica, **50**: 93–99.

Sereno, P.C., and Brusatte, S.L. 2008. Basal abelisaurid and carcharodontosaurid theropods from the Lower Cretaceous Elrhaz Formation of Niger. Acta Palaeontologica Polonica, **53**(1): 15–46.

Shimada, K. 2005. Phylogeny of lamniform sharks (Chondrichthyes: Elasmobranchii) and the contribution of dental characters to lamniform systematics. Paleontological Research, **9**(1): 55–72.

Shintani, S., Kobata, M., Toyosawa, S., and Ooshima, T. 2006. Expression of ameloblastin during enamel formation in a crocodile. Journal of Experimental Zoology (Molecular and Developmental Evolution), **306B**: 126–133.

Sigogneau-Russell, D. 1983. Nouveaux taxons de Mammiféres rhétiens. Acta Paleontologica Polonica, **28**: 233 – 249.

Smith, J.B. 2005. Heterodonty in *Tyrannosaurus rex*: implications for the taxonomic and systematic utility of theropod dentitions. Journal of Vertebrate Paleontology, **25**: 865–887.

Smith, J.B., and Dodson, P. 2003. A proposal for a standard terminology of anatomical notation and orientation in fossil vertebrate dentitions. Journal of Vertebrate Paleontology, **23**(1): 1–12.

Smith, J.B., Vann, D.R., and Dodson, P. 2005. Dental morphology and variation in theropod dinosaurs: implications for the taxonomic identification of isolated teeth. The Anatomical Record Part A, **285**(A): 699–736.

Smith, M.M. 1989. Distribution and variation in enamel structure in the oral teeth of sarcopterygians: its significance for the evolution of a protoprismatic enamel. Historical Biology, **3**: 97–126

Smith, M.M. 1992. Microstructure and evolution of enamel amongst osteichthyan fishes and early tetrapods. *In* Structure, function, and evolution of teeth. *Edited by* P. Smith, and E. Tchernov (eds.). Freund Publishing House, Ltd., London and Tel Aviv. pp. 73–101.

Smith, M.M., and Sansom, I. J. 2000. Evolutionary origins of dentine in the fossil record of early vertebrates: diversity, development and function. *In* Development, function and evolution of teeth. *Edited by* M.F. Teaford, M.M. Smith, and M.W.J. Ferguson. Cambridge University Press, Cambridge. pp. 65–81.

Snively, E., and Russell, A. P. 2007. Craniocervical feeding dynamics of *Tyrannosaurus rex*. Paleobiology, **33**: 610–638.

Stokosa, K. 2005. Enamel microstructure variation within the Theropoda. *In* The carnivorous dinosaurs. *Edited by* K. Carpenter. Indiana University Press, Bloomington, IN. pp. 163–178.

Straight, W.H., Barrick, R.E., and Eberth, D.A. 2004. Reflections of surface water, seasonality, and climate in stable Oxygen isotopes from tyrannosaurid tooth enamel. Palaeogeography, Palaeoclimatology, Palaeoecology, **206**: 239–256.

Szalay, F. S. 1994. Evolutionary history of the marsupials and an analysis of Osteological characters. Cambridge University Press, Cambridge, 481p.

Tanke, D.H., and Currie, P.J. 2000. Head-biting in theropods: paleopathological evidence. *In* GAIA 15: Aspects of theropod paleobiology. *Edited by* B.P. Pérez-Moreno, T. Holtz, J. L. Sanz, and J. J. Mortalla. Museu Nacional de História Natural, Lisbon, Portugal. pp. 167–184.

Thomas, K.J.S., and Carlson, S.J. 2004. Microscale $\delta^{18}O$ and $\delta^{13}C$ isotopic analysis of an ontogenetic series of the hadrosaurid dinosaur *Edmontosaurus*: implications for Physiology and ecology. Palaeogeography, Palaeoclimatology, Palaeoecology, **206**: 257–287.

Westergaard, B., and Ferguson, M.W.J. 1990. Development of the dentition in *Alligator mississippiensis*: upper jaw dental and craniofacial development in embryos, hatchlings, and young juveniles, with a comparison to lower jaw development. The American Journal of Anatomy, **187:** 393–421.

Wood, C.B., and Stern, D.N. 1997. The earliest prisms in mammalian and reptilian enamel. *In* Tooth enamel microstructure. *Edited by* Koenigswald, W.V. and Sander, P. M. (eds). Balkema, Rotterdam, Netherlands. pp. 63–84.

Xu, X., Norell, M.A., Kuang, X., Wang, X., Zhao, Q., and Jia, C. 2004. Basal tyrannosaurids from China and evidence for protofeathers in tyrannosaurids. Nature, **431**: 680–684.

Xu X., Clark, J.M., Forster, C. A., Norell, M.A., Erickson, G.M., Eberth, D.A., Jia, C., and Zhao, Q. 2006. A basal tyrannosauroid dinosaur from the Late Jurassic of China. Nature, **439** (7077): 715–718.

Zazzo, A., Bocherens, H., Brunet, M., Beauvilain, A., Billiou, D., Mackaye, H.T., Vignaud, P., and Mariotti, A. 2000. Herbivore paleodiet and paleoenvironmental changes in Chad during the Pliocene using stable isotope ratios of tooth enamel carbonate. Paleobiology, **26**(2): 294–309.

Chapter 2

The development of tooth carinae in the extant lizards *Varanus rudicollis* and *Varanus komodoensis*, and theropods of the Late Cretaceous of Alberta and Saskatchewan.

Introduction

The similarity between the dentition of varanid lizards and theropod dinosaurs has been recognized for a number of years (Farlow et al. 1991; Abler 1992). This is due to the fact that some varanid lizards, such as *Varanus komodoensis* (Fig. II.1) and *Varanus salvator* have serrations on the cutting edges of their teeth, similarly to those of most theropod dinosaurs.

Studies of tooth development in reptiles (Bullet 1942; Edmund 1962a, 1962b,1969; Peyer, 1968; Westergaard and Ferguson 1990) generally do not deal with the development of carinae, although there are a few exceptions (Erickson 1995; Beatty and Heckert 2009). The tooth development process has similar basic stages to those seen in mammals. Histogenesis takes place at the boundary between ectoderm and mesoderm. The enamel originates from the ectoderm, and increases outward. The dentine originates from the mesoderm, and increases inward (Peyer 1968). The final shape of the tooth is determined at the bell stage, when the odontoblasts and ameloblasts differentiate at the interface of the

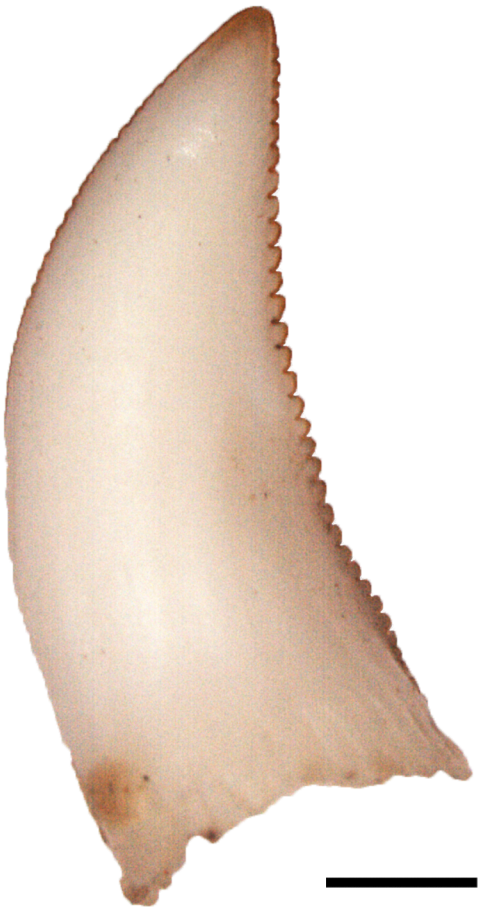

Fig. II.1. Lateral tooth of *Varanus komodoensis* (UALVP 53481) with denticulate carinae. Scale bar = 2 mm. Anterior edge to the left.

mesenchyme (which originates from the mesoderm) and the epithelium (which originates from the ectoderm), and deposit the dentine and enamel matrices, respectively (Thesleff 2003).

The processes of carinal and denticular development in varanid lizards and theropod dinosaurs are still not fully understood. Sander (2000) analyzed the enamel microstructures of various amniote taxa, but stated that usually only denticles along the cutting edges of reptilian teeth develop at the enamel-dentine junction. This is clearly seen in histological sections (Fig. II.2). Some taxa have multiple enamel structures that do not extend into the dentine layer, such as the fine 'ribs' of the enamel surface of an extant crocodile tooth described by Peyer (1968). A *Tyrannosaurus rex* tooth (SMNH 2523.8) collected in Saskatchewan shows another interesting feature (Fig. II.3), which is the presence of discontinuities in the dentine deposition in the deep layers of dentine near the pulp cavity. These discontinuities have the same shape as the denticles seen on the surface of the tooth, and will be referred to as "denticle shadows", because they mirror the denticulate carinae of the tooth. This specimen shows that in some cases, denticles can develop in even deeper levels than what was described by Sander (2000).

The taxa analyzed in this study have polyphyodonty (high tooth replacement rates that continue throughout their lives), which facilitates tooth development studies, because there are multiple stages observed at

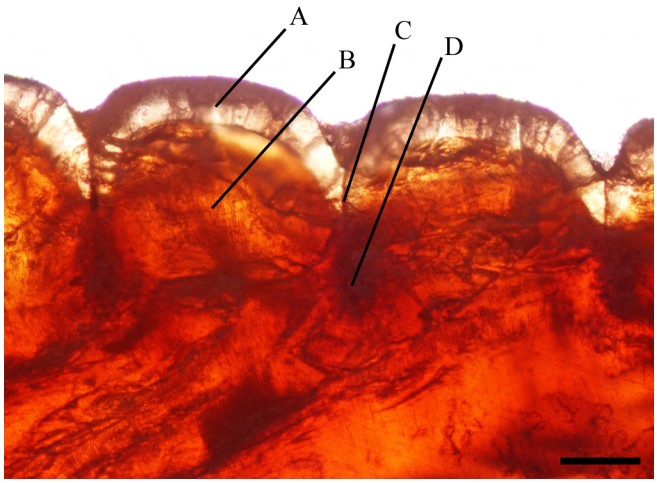

Fig. II.2. Photomicrograph of a tyrannosaurid tooth section (UALVP 53364) featuring the posterior carina with well-developed denticles. (A) Enamel, (B) dentinal tubules, (C) diaphyseal channel, (D) ampulla. Scale bar = 100 μm. Apical to the left.

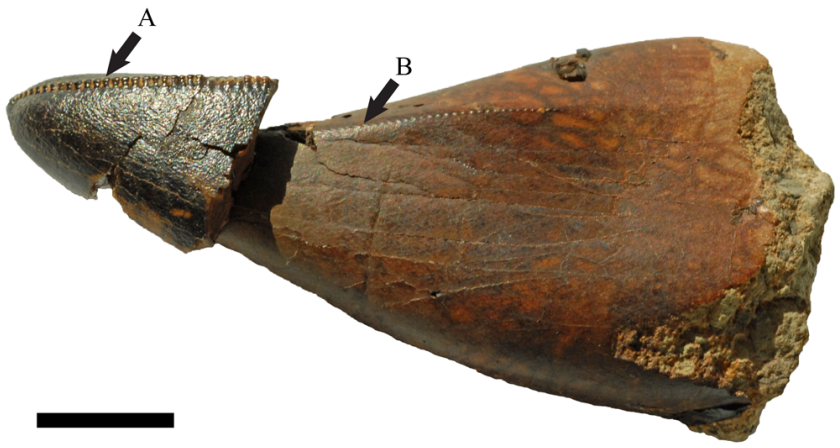

Fig. II.3. Anterolabial view of a left premaxillary *Tyrannosaurus rex* (SMNH 2523.8) tooth, featuring (A) denticulate carinae, and (B) “denticle shadows”. Scale bar = 10 mm.

different levels in each tooth family. Polyphyodonty also explains the abundance of theropod teeth in the fossil record.

The presence of denticulate carinae and polyphyodonty in teeth of the distantly related taxa representing the Lepidosauromorpha (varanid lizards) and Archosauromorpha (theropod dinosaurs) offers great potential for a comparative analysis of their tooth morphology (Fig. II.4). Detailed studies of the tooth histology of *Caiman sclerops* and *Iguana iguana* by Edmund (1969) also demonstrated numerous similarities between tooth development in these two groups.

The objective of this study is to describe with detail how carinae and denticles form in reptile teeth. The hypothesis tested is that carinal formation is similar in pleurodont (lizards) and thecodont reptiles (including theropods and crocodilians), and is therefore an adaptive convergence that evolved separately in different groups of animals.

Materials and methods

The University of Calgary Museum of Zoology provided the *Varanus rudicollis* alcohol-preserved specimen. The left lower jaw of the specimen (UALVP 53485) was dissected and sectioned in three planes: labiolingual, anteroposterior, and dorsoventral.

Prior to sectioning, the varanid teeth were decalcified with a fast commercial decalcifier (RDO®), which is largely composed of hydrochloric

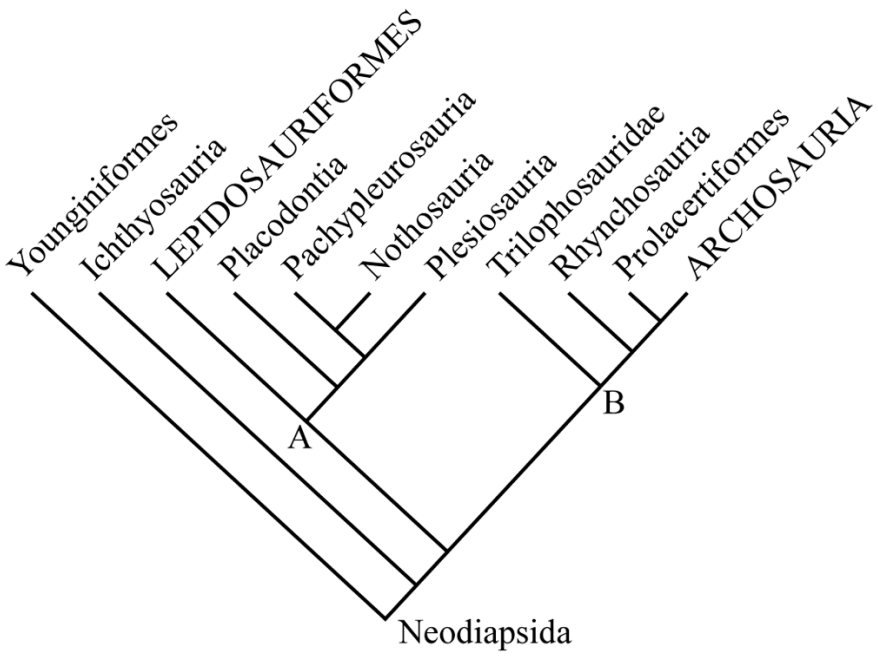

Fig. II.4. Cladogram showing the relationships of the major diapsid groups, including the Archosauromorpha and Lepidosauromorpha analyzed in this study, based on the work of Benton (2005). (A) Lepidosauromorpha, (B) Archosauromorpha. Lepidosauriformes includes varanid lizards described here, and Archosauria includes theropods described.

acid. They were then embedded in paraffin wax and sectioned (Fig. II.5) with a microtome. The 7µm sections were stained with Masson's trichrome stain. The *Varanus komodoensis* specimens consist of isolated shed crowns (UALVP 53481) donated by the Toronto Zoo. Small theropods, such as *Dromaeosaurus* (UALVP 53359), *Saurornitholestes* (UALVP 53365), and *Troodon* (UALVP 53358) are represented by isolated shed crowns collected in Dinosaur Provincial Park (Dinosaur Park Formation). Thin sections of *Varanus komodoensis* and the small theropods were prepared at the Thin Section Laboratory in the Department of Earth and Atmospheric Sciences at the University of Alberta. The specimens were mounted onto petrographic slides and sectioned with a microtome, but not stained. Some of them were polished to allow further analysis in a scanning electron microscope (SEM). The SEM analyses were done using a JEOL 6301F field emission SEM at the SEM Lab in the Earth and Atmospheric Sciences Department at the University of Alberta. The samples were coated with carbon prior to being analyzed.

The isolated tyrannosaurid teeth (UALVP 53352 and UALVP 53364) were also collected in Dinosaur Provincial Park, Dinosaur Park Formation. They were embedded in EpoThin® Epoxy Resin. After the resin had set, the specimens were glued onto petrographic slides and sectioned with a microtome. The sections were polished using sand paper with grits ranging from 220 to 600. Additionally, the petrographic slide TMP 98.68.85

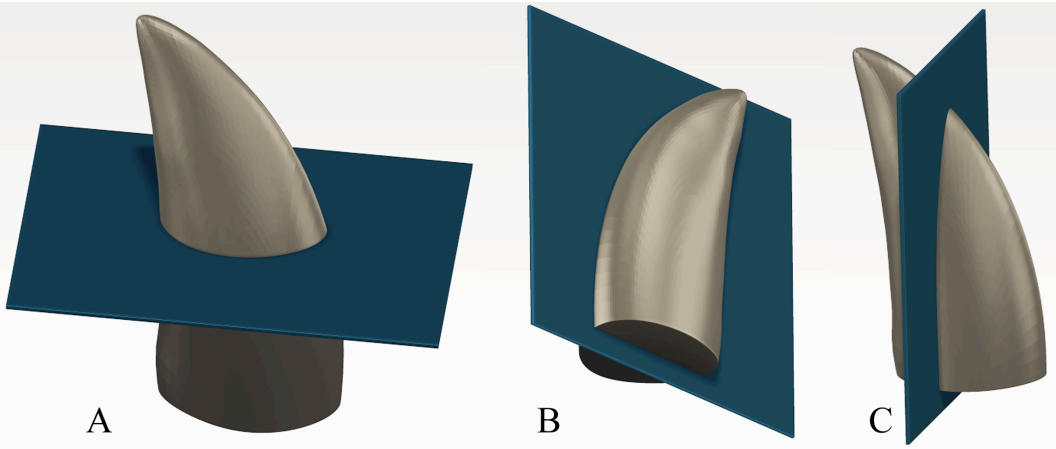

Fig. II.5. Diagram showing the planes of section for the histological sections described. (A) horizontal cross-section, (B) vertical labiolingual section, (C) vertical anteroposterior section.

of a lateral unidentified tyrannosaurid tooth was photographed for this study. A *Tyrannosaurus rex* specimen (SMNH 2523.8, Fig. II.3) from the Frenchman Formation in the Frenchman River valley, southwestern Saskatchewan (Tokaryk and Bryant 2004) was not sectioned but only photographed. This specimen shows macroscopic evidence of “denticle shadows” in the dentine layer of a premaxillary tooth.

Results

The sections of the *Varanus rudicollis* teeth show a range of stages in tooth development. It is possible to identify patterns in both erupted and unerupted teeth. The lack of serrations in this taxon compromises some of the comparisons with theropods, but carinal development was observed in most specimens studied. The *Varanus rudicollis* tooth sections were separated into three categories: A) vertical labiolingual sections; B) vertical anteroposterior sections; and C) horizontal cross-sections (Fig. II.5). Enamel thicknesses in germ teeth range from less than 10 μm to about 20 μm. It was not possible to obtain accurate measurements from erupted teeth because, in most cases, the enamel was dissolved during the decalcification process. It is also difficult to determine from the histological sections if there are any signs of wear on the *Varanus rudicollis* teeth.

The vertical labiolingual sections of *Varanus rudicollis* teeth provide little information about carinal development, because it is difficult to

identify in this view where these structures start or end, partially due to the lack of serrations. The dentine layer near the tooth attachment site (at which point it is called plicidentine) forms lamellae, which anastomose to form a honeycomb-like surface that helps attach the tooth to the jaw (Maxwell et al. 2011). The interface between crown and root will not be detailed here, and has been described elsewhere (Maxwell et al. 2011). Some of the unerupted crowns have enamel layers that were not affected by the decalcification process as much as the exposed crowns of the erupted teeth. Labiolingual sections shows the enamel-dentine junction, but are of limited value for studies on non-serrated carinae.

The vertical anteroposterior sections of *Varanus rudicollis* teeth include some unerupted teeth (Fig. II.6). The enamel covers about three quarters of the maximum apicobasal length of the dentine. The dentinal tubules (microscopic channels that extend from the enamel-dentine junction to the pulp cavity and are filled with fluid and cellular structures) are clearly visible. The pulp cavity is about 100 μm wide at the base of the crown in the first dentary tooth. In each of the first few lateral teeth, the pulp cavity is smaller than that of the most anterior dentary tooth, and the enamel still extends as far as three quarters of the apicobasal length of the dentine. The dentine layer is still not fully mineralized (at this stage it is called predentine) in some of the teeth and its structure looks like a mesh of cellular structures (Fig. II.7).

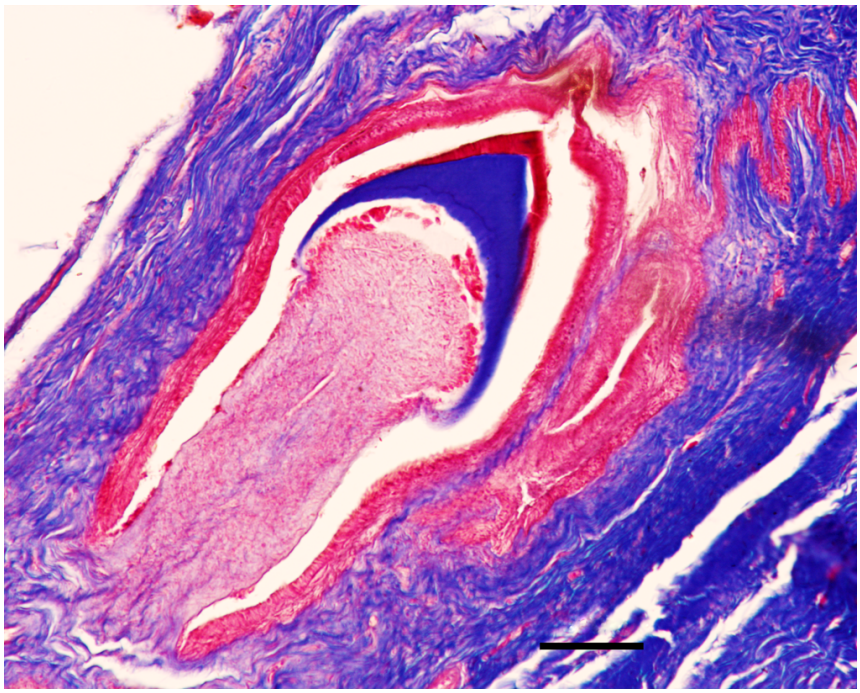

Fig. II.6. Vertical anteroposterior section of an unerupted tooth of *V. rudicollis* (UALVP 53485). Scale bar = 50 μm.

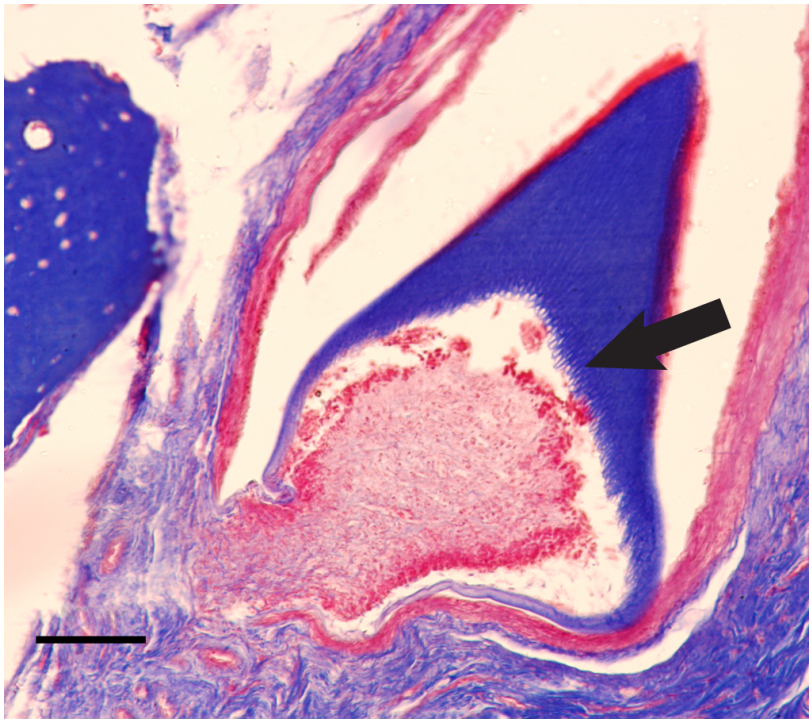

Fig. II.7. Vertical anteroposterior section of an unerupted tooth of *V. rudicollis* (UALVP 53485) featuring predentine (arrow). Scale bar = 50 µm.

The horizontal cross-sections of *Varanus rudicollis* teeth do not have any signs of structures mirroring the carinae near the pulp cavity (or any structure analogous to the “denticle shadows” observed in SMNH 2523.8) in either erupted or unerupted crowns. The dentine layer has a higher concentration of odontoblasts and predentine near the anterior margin of the pulp cavity (Fig. II.8), indicating that the anterior portion of the dentine in these teeth takes longer to mineralize than the posterior portion. This has been verified in all sectioned erupted crowns. There is a trend of concentrating a large number of anteroposteriorly oriented dentinal tubules near the posterior carinae of erupted crowns (Fig. II.9), which is not observed near the anterior carina. Posterior carinae in *Varanus rudicollis* extend further basally than anterior carinae, as observed in theropod teeth. In unerupted crowns, shorter dentinal tubules can be found throughout the dentine and do not seem to be more concentrated in any particular area (Fig. II.10). Odontoblasts and predentine are found near the pulp cavities of unerupted crowns, and at this stage dentine deposition and mineralization seem to be equal on all sides of the tooth.

The cross-sections of *Varanus komodoensis* teeth show concentrations of anteroposteriorly oriented dentinal tubules near the posterior carinae (Fig. II.11), similarly to *Varanus rudicollis.* Some of the dentinal tubules are filled with a dark substance, probably originated from the soil from which the teeth have been collected. In some specimens, the

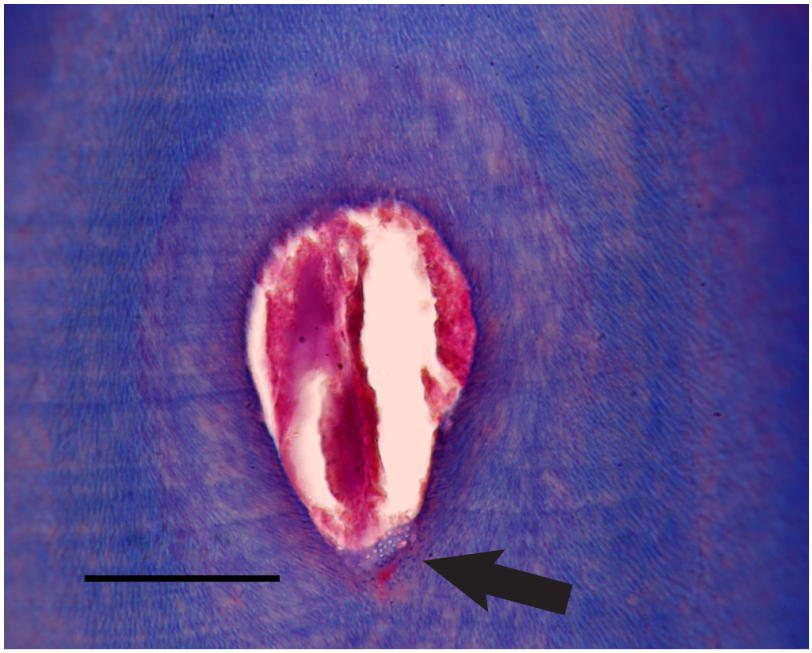

Fig. II.8. Horizontal cross-section of an erupted crown of *V. rudicollis* with predentine on the anterior margin of the pulp cavity (arrow). Scale bar = 50 μm. Lingual to the left.

Fig. II.9. Horizontal cross-section of an erupted *V. rudicollis* (UALVP 53485) crown featuring a concentration of dentinal tubules oriented anteroposteriorly near the posterior carina (arrow). Scale bar = 50 μm. Lingual to the left

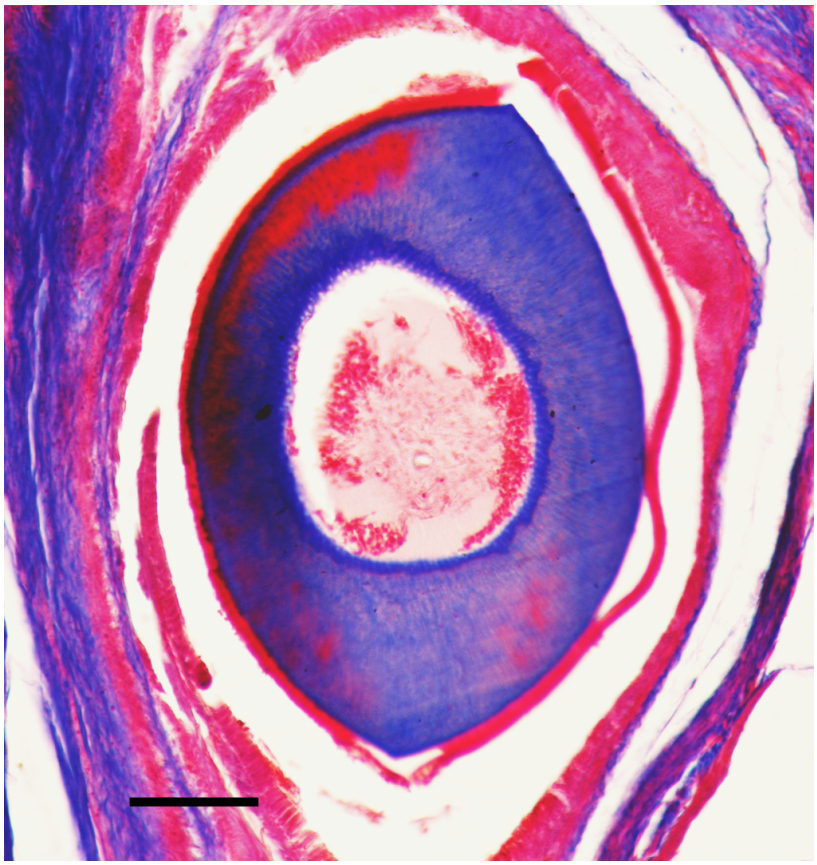

Fig. II.10. Horizontal cross-section of an unerupted *V. rudicollis* tooth (UALVP 53485) showing the even distribution of dentinal tubules at this stage. Scale bar = 50 μm.

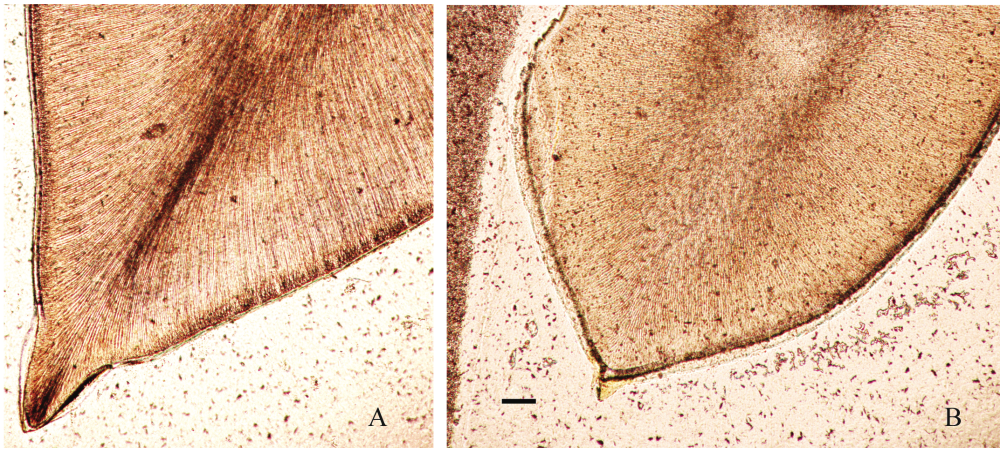

Fig. II.11. Horizontal cross-sections of a *V. komodoensis* tooth (UALVP 53481) showing a concentration of dentinal tubules oriented anteroposteriorly near the posterior carina (A), whereas the anterior carina lacks this feature (B). Scale bar = 50 μm.

pulp cavities were filled with dark soil and the surfaces of the teeth were also heavily soiled. The enamel thicknesses range from 10 to 15 μm. There are no signs of “denticle shadows” near the pulp cavity region.

Tyrannosaurid tooth crowns have clearly defined boundaries between the enamel and dentine layers in all tooth sections. The quality of preservation allows the observation of some of the basic features of relevance to this study. The enamel layer thickness ranges from about 50 to 100 μm in most specimens. No signs of “denticle shadows” are visible near the pulp cavity in the specimens that were sectioned. A premaxillary tooth of *Tyrannosaurus rex* (SMNH 2523.8) (Fig. II.3), however, has “denticle shadows” near the pulp cavity. This is visible because of the matrix-filled pulp cavity, which shows impressions of the “denticle shadows” preserved in the internal walls of the tooth.

Some worn surfaces (usually the carinae) of the sectioned tyrannosaurid teeth show exposed dentine on the outer surface of the tooth. The dentinal tubules tend to be more concentrated around posterior carinae in lateral teeth (Fig. II.12). The pulp cavities in these teeth show the higher concentration of anteroposteriorly oriented dentinal tubules in the posterior half of the tooth. However, in premaxillary teeth, these dentinal tubules are equally distributed in the dentine, and the area around the pulp cavity shows this clearly (Fig. II.13). The tubules are more visible in fossils (compared with fresh varanid specimens), because the dentinal tubules often become filled with darker colored minerals during the

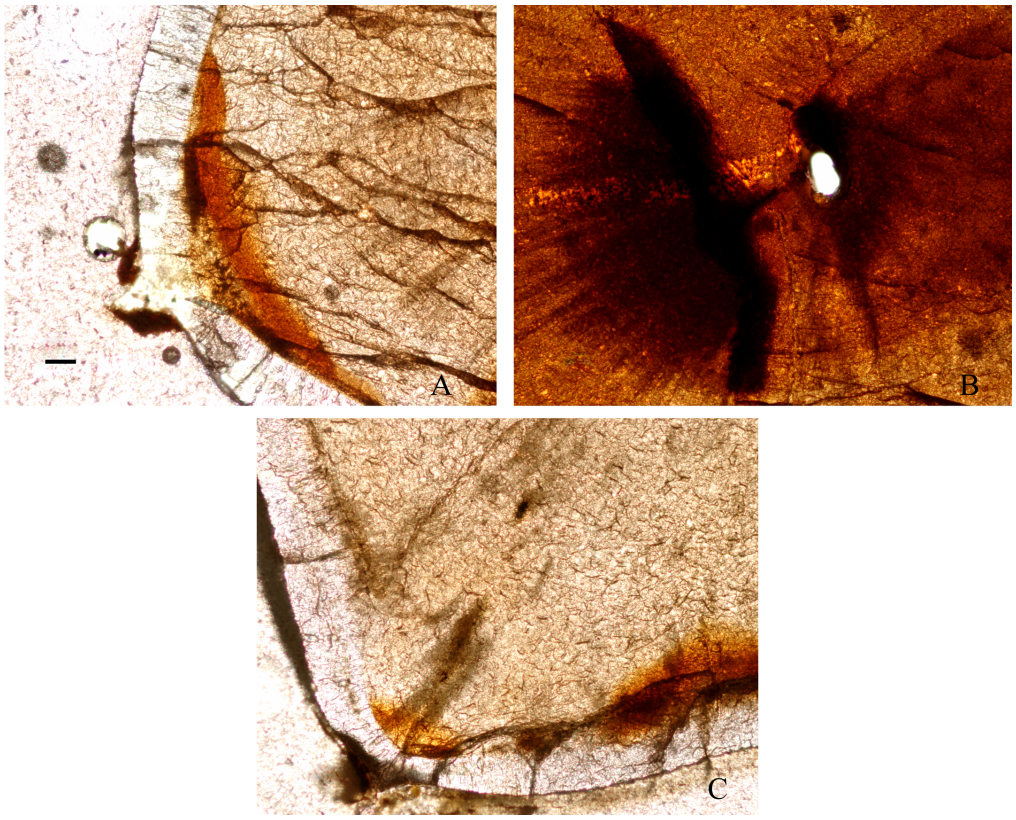

Fig. II.12. Horizontal cross-sections of a lateral tyrannosaurid tooth (TMP 98.68.85) showing a concentration of anteroposteriorly oriented dentinal tubules near the posterior carina (A). The area near the pulp cavity also shows anteroposteriorly oriented dentinal tubules on the posterior half of the tooth (B). The area near the anterior carina lacks anteroposteriorly oriented dentinal tubules (C). Scale bar = 50 μm.

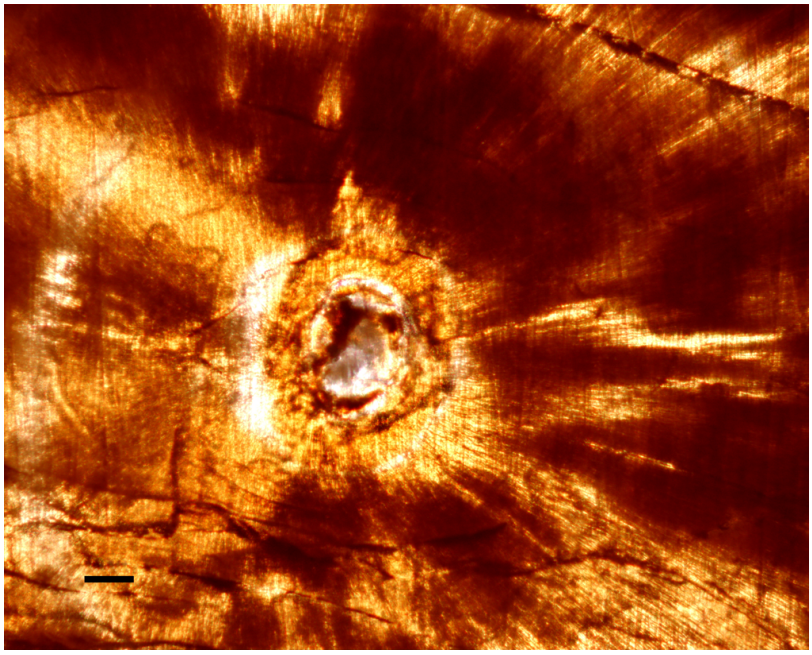

Fig. II.13. Horizontal cross-section of a tyrannosaurid premaxillary tooth (UALVP 53352) showing the pulp cavity surrounded by dentinal tubules in all directions. Scale bar = 50 μm. Lingual to the right.

fossilization process. All the sectioned tyrannosaurid teeth are isolated shed teeth, and therefore no predentine was observed, because it only occurs in teeth that are not fully mature.

The sections of teeth of *Dromaeosaurus*, *Troodon* and *Saurornitholestes* (Figs. II.14–II.16) also show concentrations of dentinal tubules near the denticles. The darker coloration near the denticles also indicates the presence of minerals acquired post-mortem. The enamel thicknesses in these taxa vary from 10 to 20 μm. The dentine incremental lines of von Ebner are clearly visible in the *Troodon* tooth section and are distorted near the denticles, conforming to the shapes of the denticles (Fig. II.15).

The vertical labiolingual sections of series of denticles of theropods (Figs. II.2, II.14–II.16) and *Varanus komodoensis* (Fig. II.17) show detailed configurations of enamel between denticles. In theropod taxa, a slot extends perpendicular to the plane of wear, providing mechanical support to the denticles, by interrupting the propagation of cracks in apico-basal direction. This slot has been referred to by Abler (1992), as a diaphyseal channel terminating in an ampulla that has multiple cracks in its centre. Some of these cracks might have been created or enlarged post-mortem; however, it is possible that these cracks were caused by stresses on the denticles during feeding. These structures are not observed between the denticles of the *Troodon* specimen described here, probably because the

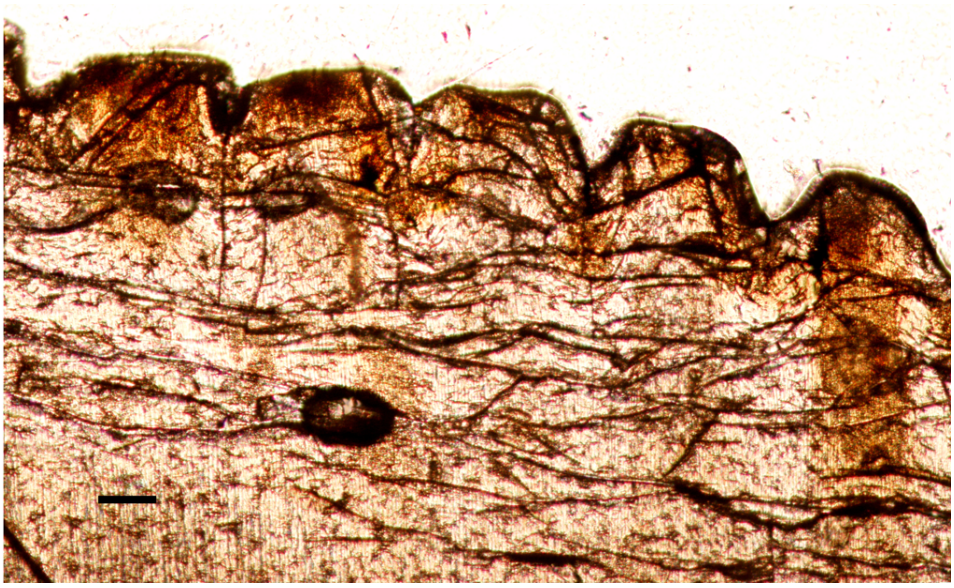

Fig. II.14. Vertical labiolingual section of a *Dromaeosaurus* tooth (UALVP 53359) showing denticles on the posterior carina. Scale bar = 50 μm. Apical to the left.

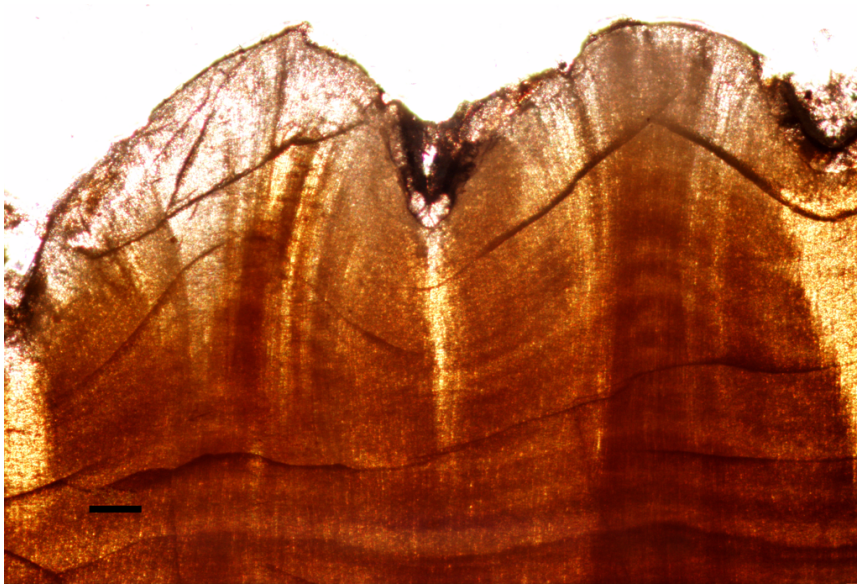

Fig. II.15. Vertical labiolingual section of a *Troodon* tooth (UALVP 53358) showing denticles on the posterior carina. Scale bar = 50 μm. Apical to the left.

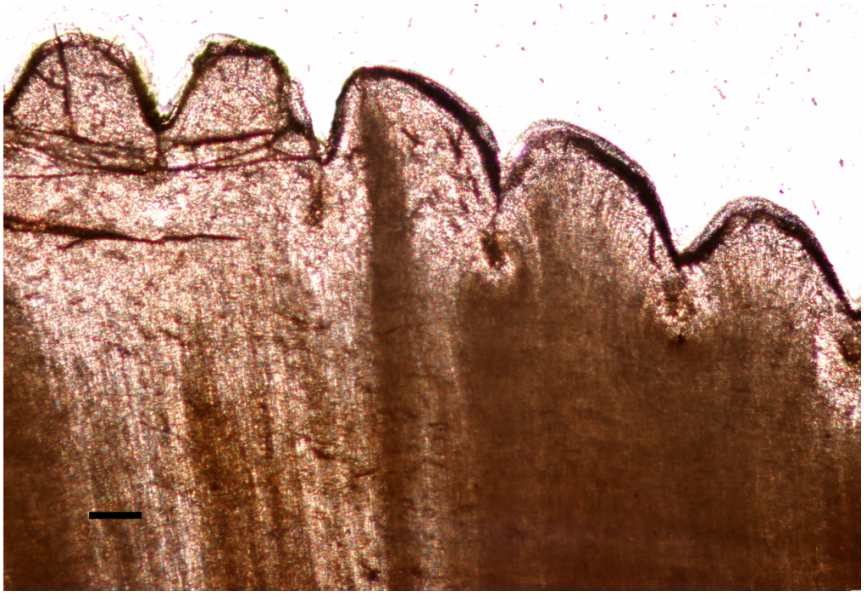

Fig. II.16. Vertical labiolingual section of a *Saurornitholestes* tooth (UALVP 53365) showing denticles on the posterior carina. Scale bar = 50 μm. Apical to the left.

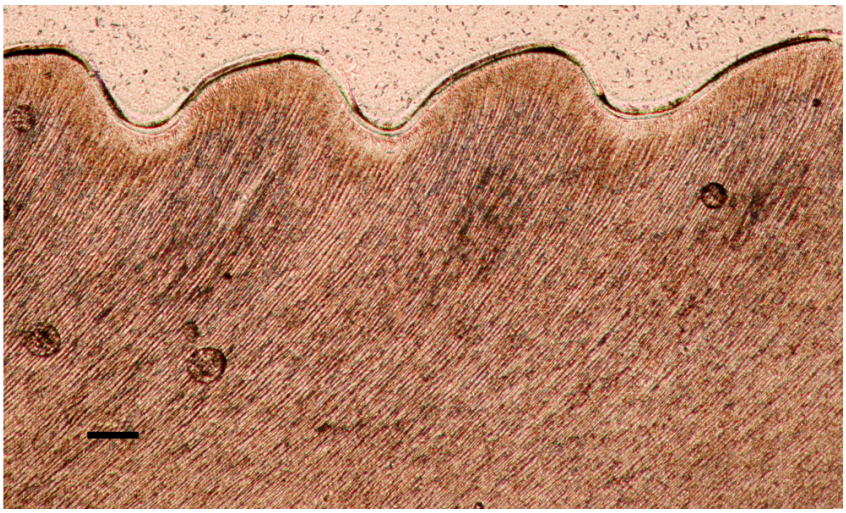

Fig. II.17. Vertical labiolingual section of a *V. komodoensis* tooth (UALVP 53481) showing denticles on the posterior carina. Scale bar = 50 μm. Apical to the right.

section was parallel to them. The presence of diaphyseal channels and ampullae between denticles of *Troodon* has been documented by Currie et al. (1990).

A vertical labiolingual section of the denticles in *Varanus komodoensis* (Fig. II.17) indicates that there is no diaphyseal channel or an ampulla. This is also confirmed by an SEM analysis (Fig. II.18). The denticles observed in *Varanus komodoensis* are morphologically similar in size and shape to the most apical denticles of *Dromaeosaurus* (Fig. II.19) and to the most basal denticles of *Saurornitholestes* (Fig. II.20). However, even these denticles in theropod taxa still have diaphyseal channels. Interestingly, a serrated bird tooth (TMP 89.103.25) described by Currie and Coy (2008) lacks diaphyseal channels and ampullae between its denticles.

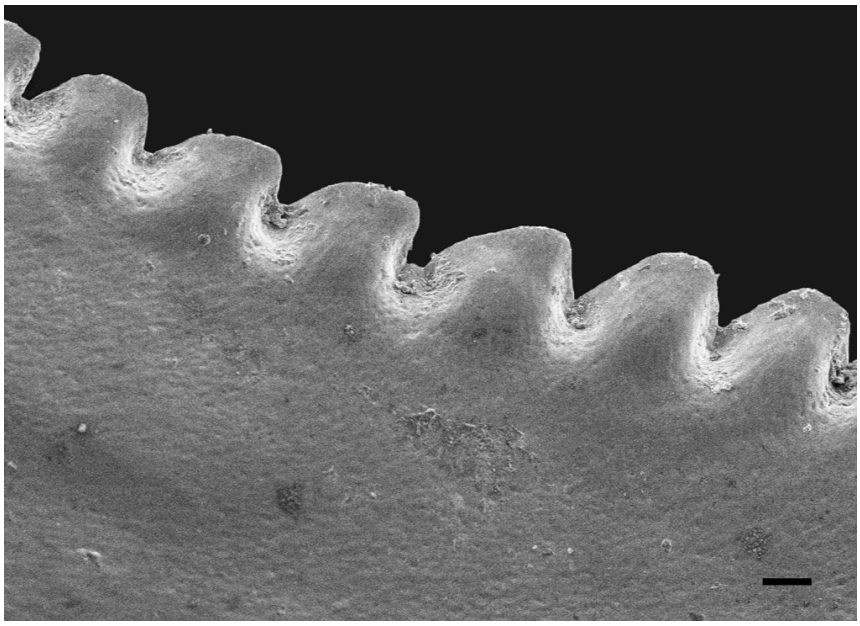

Fig. II.18. SEM micrograph of a *V. komodoensis* tooth (UALVP 53481) showing the surface detail of the denticles and the lack of diaphyseal channels or ampullae in this taxon. Scale bar = 100 μm. Apical to the right.

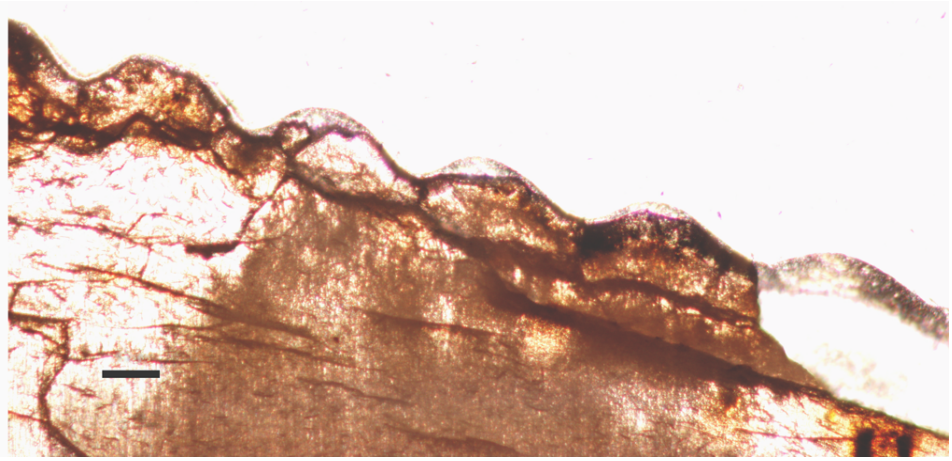

Fig. II.19. Posterior apical denticles of *Dromaeosaurus* (UALVP 53359). Scale bar = 50 μm. Apical to the left.

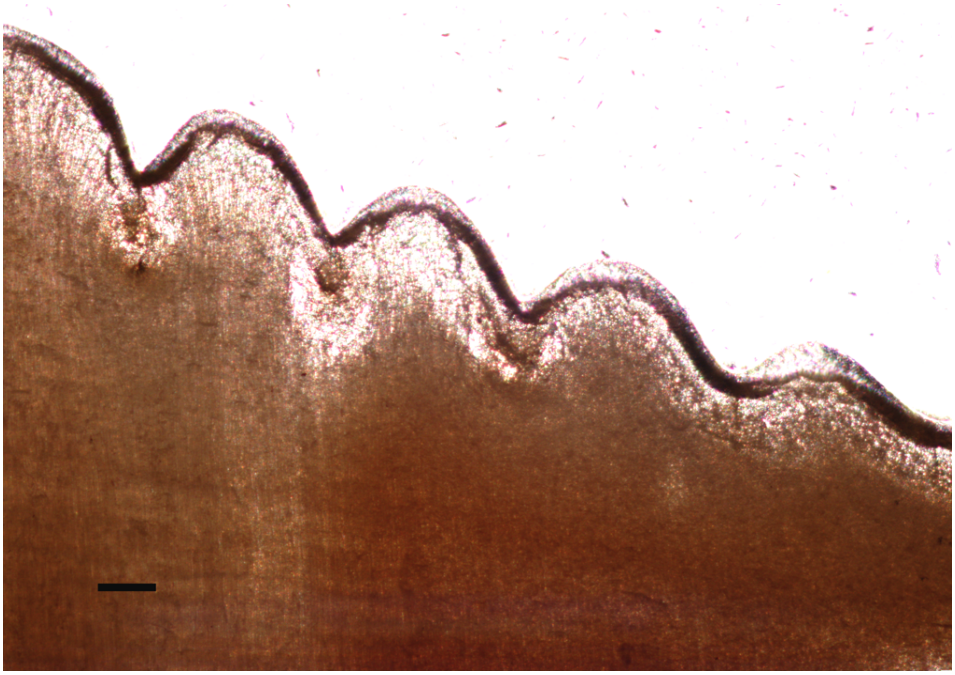

Fig. II.20. Posterior basal denticles of *Saurornitholestes* (UALVP 53365). Scale bar = 50 μm. Apical to the left.

Discussion and conclusions

Sander (1997) showed that carinae on the outer enamel surface of some reptiles are features of the enamel only and do not extend deeper than the enamel-dentine junction. Later on, Sander (2000) observed that serrations along the cutting edge of other reptile teeth do indeed extend internally into and across the enamel-dentine junction. In the same paper, Sander relates the thickness of the enamel to the formation of carinae solely by the enamel layer, arguing that there would be an upper limit for carinal size to prevent it from having an influence on the enamel-dentine junction. He does not establish what that upper limit is, and it is evident from the observations of this project that the carinae seem to influence the enamel-dentine junction in both *Varanus* (with an enamel thickness of about 10 μm) and all theropods described here (with an enamel thickness ranging from 10 to about 56 μm in tyrannosaurids). The data show that carinal formation starts before enamel precipitation, at the dentinogenesis stage of tooth formation, in accordance with what was suggested by Beatty and Heckert (2009) for crowns with supernumerary carinae. The inner surface of the basal membrane possibly influences the development of the morphology of carinae, because odontoblasts begin to secrete the organic matrix that will form the dentine along that surface. Enamel deposition takes place after the dentine is formed (Peyer, 1968), and therefore conforms to, in this case, the morphology dictated by the dentine. This study demonstrates that the presence of carinae is not a

feature dependent on enamel thickness, but is determined during early stages of tooth development for *Varanus komodoensis, Varanus rudicollis*, and theropod dinosaurs. The presence of “denticle shadows” in the pulp cavity of a *Tyrannosaurus rex* (SMNH 2523.8) tooth suggests that denticle development affects even deeper layers of dentine. It seems that these “denticle shadows” are the result of the internal structure of the denticles in most theropod teeth, which have radices and growth distortions in the dentine incremental lines surrounding the denticles. Indeed, *Varanus komodoensis*, does not have radices or local growth distortions in the dentine layer near the denticles, and consequently, no “denticle shadows”. It seems that even though denticles appear in early stages of tooth development, radices and other internal structures in denticles seem to be associated with more specialized teeth. Denticles in *Varanus komodoensis* are more irregular in size and proportions than in theropods.

Even though there are no sections of early developing stages of the teeth of theropods described here, their morphology at the enamel-dentine junction demonstrates that carinal development and tooth shape in reptiles is of considerable adaptive value for these groups. The presence of similar structures in teeth of other major vertebrate lineages, such as birds (Currie and Coy 2008), mammals (like *Arctocyon ferox* and *Oxyaena forcipata* [M. Reichel, personal observations of AMNH 4209 and AMNH 2456]), and various fish (especially sharks), indicates a strong selective pressure for the development of denticulate carinae in groups with teeth adapted for

carnivory. This suggests convergent evolution, as also suggested by Sander (1997), for enamel surface morphology in reptiles.

There is a trend for long dentinal tubules to be present near the posterior carinae of erupted crowns (Figs. II.9, II.11, II.12) in varanid lizards and at least some theropods. As previously mentioned, dentinal tubules are microscopic channels filled with fluid and cellular structures, which may also transport nutrients and minerals to the external layers of the tooth. This suggests a higher transport of material for the posterior carinae, which are generally more robust in theropod teeth, as well as in *Varanus*. The higher transport of material to the posterior carina could also explain the larger denticles observed (Figs. II.11, II.12).

Differential growth of the dentine layer is indicated by a higher concentration of odontoblasts and predentine near the anterior margin of the pulp cavity in cross sections of each *Varanus rudicollis* tooth. This shows that dentine mineralization takes longer in the anterior portion of the crown, which could be due to the larger size of the anterior half of the tooth (noted by the posterior placement of the pulp cavity in Fig. 9). Therefore, the dentine takes longer to mineralize in the anterior portion, because it is being deposited for a longer time than in the posterior portion, causing the curvature of teeth. If that is the case, a larger extent of this lag in dentine mineralization is expected for more curved teeth. The extent of this lag is currently unknown, and timed analyses of varanid tooth

development would help determine if the anterior portion of the tooth crown mineralizes hours or days later than the posterior one.

The increased size of the posterior carina in all taxa suggests that posterior carinae endure high amounts of stress, especially when the teeth are employed in feeding mechanics such as the hold and pull-feeding technique, in which the animal secures its pray with its limbs and pulls on the carcass by employing its neck muscles. This behavior has been described by Snively and Russell (2007*a*, *b*) for tyrannosaurids and also by Moreno et al. (2008) for *Varanus komodoensis*. High amounts of biomechanical stress have also been observed in lateral teeth of tyrannosaurids in an anteroposterior direction (Reichel 2010), which is the direction in which the carinae are employed the most. The differences in dentine on anterior and posterior carinae are only visible in late developmental stages. Just before eruption, *Varanus rudicollis* teeth have predentine on anterior portions of some sections. In already erupted (and even shed) crowns, the dentinal tubules are more concentrated near the posterior carina in both varanid species, which is also the case in most of the theropod teeth described. The differential growth of teeth only in late developmental stages is consistent with the stage when they also acquire their final shape. In early stages of development, teeth have an overall cone shape and the dentine is equally distributed in the crown (including dentinal tubules).

There are some similarities in the carinae of *Varanus* and theropods, such as the concentration of dentinal tubules in the posterior carina. However, in theropods this concentration may occur in both carinae (in tyrannosaurid premaxillary teeth), whereas in *Varanus* it occurs mainly in the posterior carina. The pattern of dentinal tubule concentration seen in tyrannosaurid premaxillary teeth could be related to the unique biomechanics associated to these teeth (Reichel 2010). If tyrannosaurids were indeed using the hold and pull-feeding behavior, it would make sense that both carinae would be reinforced in premaxillary teeth, because they are both posterior in position. The premaxillary teeth in *Varanus komodoensis* have similar morphologies to the ones in tyrannosaurids, and histological sections help to verify this point. Additionally, *Varanus komodoensis* teeth have denticles that are less developed than in theropods. Although the teeth and denticles develop to similar sizes as those observed in theropods like *Saurornitholestes*, their level of complexity is not the same. The denticles in *Varanus komodoensis* do not have ampullae, which are present between most fully developed theropod denticles.

Therefore, this study suggests that some of the basic elements in carinal development, such as the dentinal tubule arrangement and the reinforced posterior carina are common to theropods and varanid lizards, as stated by the hypothesis. However, at the denticular level, there are still differences. The theropod teeth that have diaphyseal channels between

denticles have a more complex enamel arrangement than *Varanus komodoensis*, in which the enamel layer is more uniform, and does not show any features that differentiate denticulate and smooth areas of the tooth.

It is still not possible to answer which factors determine the development of denticles in carinate teeth. Size has been suggested as having a major role in determining it (Currie and Coy 2008), and it is definitely true for the small sample size analyzed here (in which *Varanus rudicollis* has the smallest teeth and non-denticulate carinae). However, a more detailed study on presence versus absence of denticles in teeth of various taxa with carinate teeth would be of great help to verify the existence of a size threshold for denticle development.

References

Abler, W. L. 1992. The serrated teeth of tyrannosaurid dinosaurs, and biting structures in other animals. Paleobiology, **18**(2): 161 – 183.

Beatty, B.L., and Heckert, A.B. 2009. A large archosauriform tooth with multiple supernumerary carinae from the Upper Triassic of New Mexico (USA), with comments on carina development and anomalies in the Archosauria. Historical Biology, **21**(1): 57–65.

Benton, M.J. 2005. Vertebrate Palaeontology. Blackwell Publishing, Oxford, UK. 455 pp.

Bullet, P. 1942. Beiträge zur Kenntnis des Gebisses von *Varanus salvator* Laur. Viertesjahresschrift der Naturforschenden Gesellschaft in Zürich, **87**: 139–192.

Currie, P.J., Rigby, J.K. Jr., and Sloan, R.E. 1990. Theropod teeth from the Judith River Formation of Southern Alberta, Canada. *In*: Dinosaur Systematics: Approaches and Perspectives. *Edited by* Carpenter, K. and P. J. Currie (eds.). Cambridge University Press. pp. 107–125.

Currie, P.J., and Coy, C. 2008. *In*: Sankey, J.T., and Baszio, S. (eds.). Vertebrate Microfossil Assemblages: their role in palaeoecology and palaeobiogeography. Indiana University Press, Bloomington, IN. 296 pp.

Edmund, A.G. 1962a. Tooth replacement phenomena in the lower vertebrates. The Royal Ontario Museum, Life Sciences Division, Contributions No. **52**: 1–190.

Edmund, A.G. 1962b. Sequence and rate of tooth replacement in the Crocodilia. The Royal Ontario Museum, Life Sciences Division, Contributions No. **56**: 1–42.

Edmund, A.G. 1969. Dentition. *In* Biology of the Reptilia – Volume 1, Morphology A. *Edited by* C. Gans, A.d'A. Bellairs, and T.S. Parsons. Academic Press, London, UK. pp. 117 – 200.

Erickson, G.M. 1995. Split carinae on tyrannosaurid teeth and implications of their development. Journal of Vertebrate Paleontology, **15**(2): 268–274.

Farlow, J.O., Brinkman, D.L., Abler, W.L., and Currie, P.J. 1991. Size, shape and serration density of theropod dinosaur lateral teeth. Modern Geology **16**: 161–198.

Moreno, K., Wroe, S., Clausen, P., McHenry, C., D'Amore, D.C., Rayfield, E., and Cunningham, E. 2008. Cranial performance in the Komodo dragon (*Varanus komodoensis*) as revealed by high-resolution 3-D finite element analysis. Journal of Anatomy, **212**: 736–746.

Peyer, B. 1968. Comparative odontology. The University of Chicago Press, Chicago, USA. 347 pp.

Reichel, M. 2010. The heterodonty of *Albertosaurus sarcophagus* and *Tyrannosaurus rex*: biomechanical implications inferred through 3-D models. Canadian Journal of Earth Sciences, **47**: 1253–1261.

Sander, P. M. 1997. Non-mammalian synapsid enamel and the origin of mammalian enamel prisms: the bottom-up perspective. *In* Koenigswald, W.v. and Sander, P. M. (eds) Tooth enamel microstructure. Balkema, Rotterdam, Netherlands. Pp. 41–62.

Sander, P. M. 2000. Prismless enamel in amniotes: terminology, function, and evolution. *In* Development, function and evolution of teeth. *Edited by* M.F. Teaford, M.M. Smith, and M.W.J. Ferguson. Cambridge University Press, Cambridge, UK, pp. 92–106.

Snively, E., and Russell, A. P. 2007*a*. Craniocervical feeding dynamics of *Tyrannosaurus rex*. Paleobiology, **33**: 610–638.

Snively, E., and Russell, A. P. 2007*b*. Functional morphology of the neck musculature in the Tyrannosauridae (Dinosauria, Theropoda) as determined via a hierarchical inferential approach. Zoological Journal of the Linnean Society, **151**(4): 759–808.

Thesleff, I. 2003. Epithelial-mesenchymal signaling regulating tooth morphogenesis. Journal of Cell Science, **116**(9): 1647–1648.

Tokaryk, T., and H. N. Bryant 2004. The Fauna from the *Tyrannosaurus rex* excavation, Frenchman Formation (Late Maastrichtian),

Saskatchewan. *In*: Summary of Investigations 2004, Volume 1, Saskatchewan Geological Survey, Sask. Industry Resources.

Westergaard, B., and Ferguson, M.W.J. 1990. Development of the dentition in *Alligator mississippiensis*: upper jaw dental and craniofacial development in embryos, hatchlings, and young juveniles, with a comparison to lower jaw development. The American Journal of Anatomy, **187:** 393–421.

Chapter 3

The heterodonty of *Albertosaurus sarcophagus* and *Tyrannosaurus rex*: biomechanical implications inferred through 3-D models[1]

Introduction

Tyrannosaurid teeth have been simplistically referred to as dull smooth blades (Abler 1992). They function by concentrating large forces onto small areas. Tyrannosaurids did indeed have high bite forces, estimated as being up to 13,400N (Erickson et al. 1996). Additionally, these bite forces were often applied to bone (Erickson et al. 1996) or teeth, especially during feeding (Erickson et al. 1996; Molnar 1998) and intra-specific face-biting (Tanke and Currie 2000), and this frequently resulted in worn or broken tips. Nevertheless, the wear patterns observed in tyrannosaurid teeth usually do not indicate tooth-to-tooth contact inside the mouth (Molnar 1998).

---

[1] A version of this chapter has been published. Reichel, M. 2010. The heterodonty of *Albertosaurus sarcophagus* and *Tyrannosaurus rex*: biomechanical implications inferred through 3-D models. Canadian Journal of Earth Sciences, **47**: 1253–1261.

Tyrannosaurid heterodonty is well documented (Currie et al. 1990; Molnar 1998; Smith 2005) and their teeth can generally be grouped into at least three classes (Smith 2005). This variation in tooth morphology suggests that there are different functions for each region in the mouth. The anterior portion of the jaws of a tyrannosaurid has teeth that are slightly curved posteriorly and have characteristic D-shaped cross sections. Robust, curved and tall teeth characterize the middle portion of the jaws. Finally, the posterior region of the jaws has small, strongly curved and labiolingually compressed teeth.

The jaw position of a tooth in a tyrannosaurid, therefore, dictates the curvature of the tooth. This is because the “line of action” of a tooth (Rieppel 1979), or the direction it moves relative to the food that is being processed in the animal’s mouth, depends on its position relative to the jaw hinge (D’Amore 2009). For a more efficient bite, the apex of a tooth needs to contact the food first, focusing the force onto a smaller area for puncturing the food (D’Amore 2009).

Mechanical models made of metal have been used to simulate tyrannosaurid bites (Abler 1992) and test the performance of teeth. But little is known about how the tooth itself responds to such stresses and how the different morphologies found within one specimen react to various situations involved in biting motions. Mazzetta et al. (2004) performed stress analyses on a tooth of *Giganotosaurus carolinii*. They used a three

dimensional model generated by a CT scanner and simulated forces in four different directions. In that experiment, the authors were able to estimate the amount of force tolerated by that tooth and inferred the type of prey that *Giganotosaurus* would have preferred.

However, *Giganotosaurus* does not feature the same variation on tooth morphology as seen in tyrannosaurids. According to Smith (2005), *Tyrannosaurus* appears to have a higher degree of heterodonty than *Albertosaurus*. Some differences in the skull proportions of these taxa could influence the degree of morphological variation in their teeth. The snout of *Albertosaurus* is more elongated and narrower than in *Tyrannosaurus* and the maxillary teeth of *Tyrannosaurus* are larger relative to the skull than those of *Albertosaurus*, so that *Tyrannosaurus* has been referred to as a “saber-toothed dinosaur” (Molnar and Farlow 1990). Farlow et al. (1991) analyzed various theropod teeth, and their statistical analyses also showed that some maxillary teeth of *Tyrannosaurus* are indeed disproportionately tall. However, even though this significant difference in tooth proportions between *Albertosaurus* and *Tyrannosaurus* has been noticed, little has been inferred regarding the functional aspects of teeth and consequences to feeding behavior differences between them, as well as how their heterodonty differs. The two taxa studied in this project show therefore a great potential for exploring these differences between two large sized predators from the Late Cretaceous of North America, which usually end up having their

feeding behaviors generalized to the family level (Farlow et al. 1991, Abler 1992). Form and function inferences can be made from the dentition, and there is a significantly large amount of specimens available for such studies.

In this project, three-dimensional models of teeth from *Albertosaurus sarcophagus* and *Tyrannosaurus rex* are compared. These models were based on six tooth specimens of *Albertosaurus*, and six casts of a *Tyrannosaurus* specimen ("Stan", BHI 3033) from the Black Hills Institute. The taxa chosen for this study represent two groups of tyrannosaurids: the albertosaurines (*Albertosaurus*) and tyrannosaurines (*Tyrannosaurus*). The comparison between these groups adds a functional aspect to the analyses, in addition to the study of biomechanical differences that occur in the dentition within these taxa. This study combines detailed morphological and Finite Element analyses to examine the effects of heterodonty on tyrannosaurid tooth function, and how the heterodonty is affected by the distinct tooth proportions observed in these two groups of tyrannosaurids. The influence of different sized roots is also analyzed in the models that represent specimens with this structure preserved. These analyses will test the hypothesis that distinct patterns of heterodonty occur in *Tyrannosaurus* and *Albertosaurus* so that different tooth functions are observed for specific tooth positions, and that consequently the root/crown proportions in the teeth of these two groups are different.

Materials and Methods

The models were based on a total of twelve isolated tooth specimens (Table III.1). The *Albertosaurus sarcophagus* specimens from the Royal Tyrrell Museum of Palaeontology were collected from the *Albertosaurus* bonebed (TMP locality L2204) in the Horseshoe Canyon Formation in Dry Island Buffalo Jump Provincial Park, Alberta (Fig. III.1). The *Tyrannosaurus rex* models were based on casts of the specimen BHI 3033 ("Stan") from the Black Hills Institute (Fig. III.2).

Most specimens were CT-scanned with an I-Cat Classic scanner at the Dentistry/Pharmacy Centre at the University of Alberta. The cone-beam CT-scans were taken with a 0.4mm voxel size. The models were transferred to the software Mimics© v.12.11, in which a 3D mesh compatible with Finite Element analyses (FEA) was created. Some of the specimens were too large for the CT-scanner used in this project and were therefore digitized using a MicroScribe® MX System that samples multiple points on the surface of a three-dimensional object. This system allows the collection of point clouds using the Immersion® Corporation MicroScribe® Utility Software 5.0.0.2. The point clouds are then transferred to the software Rhinoceros® v.4.0, which converts them into 3D meshes that can be used for FEA. The FEA for all models were done with Strand7© v.7.2.3.

Table III.1. List of specimens used for building the 3D models.

Specimen Number	Taxon	Institution	Jaw Position	Data Acquisition
TMP 2001.45.28	*Albertosaurus sarcophagus*	Royal Tyrrell Museum of Palaeontology, AB	Premaxillary	CT-scanner
TMP 1999.50.67	*Albertosaurus sarcophagus*	Royal Tyrrell Museum of Palaeontology, AB	Left mid-maxillary	CT-scanner
TMP 2004.56.19	*Albertosaurus sarcophagus*	Royal Tyrrell Museum of Palaeontology, AB	Right posterior maxillary	CT-scanner
TMP 1998.63.11	*Albertosaurus sarcophagus*	Royal Tyrrell Museum of Palaeontology, AB	Left anterior dentary	CT-scanner
TMP 1999.50.86	*Albertosaurus sarcophagus*	Royal Tyrrell Museum of Palaeontology, AB	Left mid-dentary	MicroScribe® Digitizer
TMP 1999.50.158	*Albertosaurus*	Royal Tyrrell Museum	Left posterior dentary	CT-scanner

	sarcophagus	of Palaeontology, AB		
UALVP 48586.21	*Tyrannosaurus rex*	University of Alberta, AB	Right premaxillary 1	CT-scanner
UALVP 48586.9	*Tyrannosaurus rex*	University of Alberta, AB	Right maxillary 7	MicroScribe® Digitizer
UALVP 48586.17	*Tyrannosaurus rex*	University of Alberta, AB	Left maxillary 11	CT-scanner
UALVP 48586.29	*Tyrannosaurus rex*	University of Alberta, AB	Right dentary 1	MicroScribe® Digitizer
UALVP 48586.2	*Tyrannosaurus rex*	University of Alberta, AB	Right dentary 6	MicroScribe® Digitizer
UALVP 48586.30	*Tyrannosaurus rex*	University of Alberta, AB	Left dentary 13	CT-scanner

Note: specimens from the University of Alberta are casts of BHI 3033 (“Stan”) from the Black Hills Institute, South Dakota.

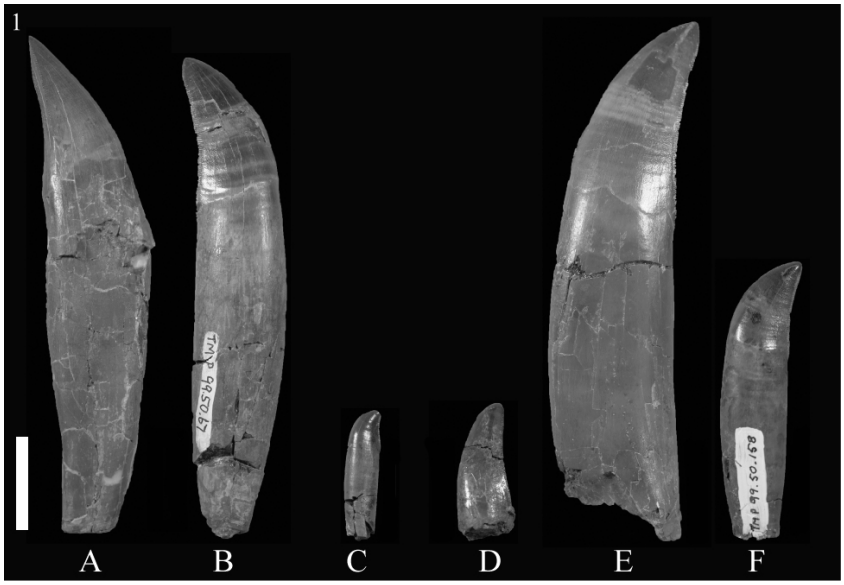

Fig. III.1. *Albertosaurus sarcophagus* specimens used for the construction of 3D models. (A) a premaxillary tooth (TMP 2001.45.28). (B) A mid-maxillary tooth (TMP 1999.50.67). (C) A posterior maxillary tooth (TMP 2004.56.19). (D) An anterior dentary tooth (TMP 1998.63.11). (E) A mid-dentary tooth (TMP 1999.50.86). (F) A posterior dentary tooth (TMP 1999.50.158). All specimens in labial view. Scale bar = 20 mm.

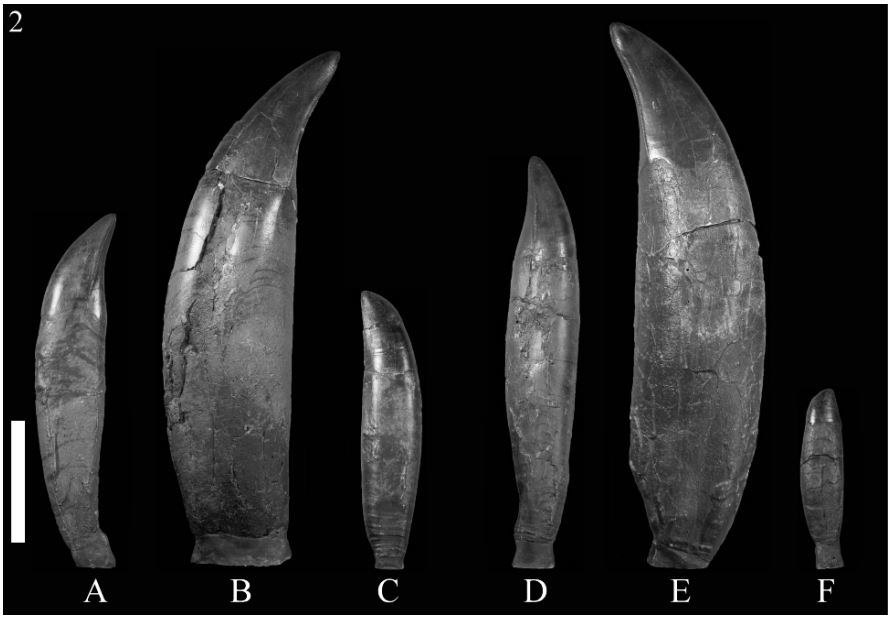

Fig. III.2. *Tyrannosaurus rex* specimens used for the construction of 3D models. (A) Right premaxillary 1 (UALVP 48582.21). (B) Right maxillary 7 (UALVP 48586.9). (C) Left maxillary 11 (UALVP 48586.17). (D) Right dentary 1 (UALVP 48586.29). (E) Right dentary 6 (UALVP 48586.2). (F) Left dentary 13 (UALVP 48586.30). All specimens in labial view. Scale bar = 50mm.

Bite-force estimates were made for *Albertosaurus* and *Tyrannosaurus* using the method used by McHenry (2009) for *Kronosaurus queenslandicus*. The measurements were taken from the skulls of the specimens TMP 81.10.1 (*Albertosaurus*) and BHI 3033 (*Tyrannosaurus*). The cross-sectional area of bite muscles through the subtemporal fenestra was estimated as 260.2 cm^2 for *Albertosaurus*, and as 772.6 cm^2 for *Tyrannosaurus*. The jaw proportions necessary for calculating forces at the different tooth positions include the "in lever" (distance from the jaw articulation to the center of the jaw muscle insertions) and the "out lever" (distance from the centre of jaw muscle insertions to specific positions along the tooth row). The angle between the muscle line of pull and the dentary bone was estimated to be approximately 45°. Based on these measurements, the bite force calculations were done as follows. The concentric specific tension (as a muscle shortens) is conservatively equivalent to 20N per square centimeter (Bamman et al. 2000; Snively and Russell 2007*a*), in muscles with simple fiber architecture. This specific tension multiplied by the cross sectional area gives the muscle force (F_y). The total vertical force (F_{in}) applied by the temporal muscles to its point of attachment (in this case, to the jaw) is given by the following formula:

$F_{in} = sin \propto . F_y$ (in which $\propto = 45°$, the muscle's angle of pull relative to the vertical).

The overall line of pull for each of the temporal muscles is in the same sagittal plane as its insertion on the mandible, so medial or lateral components of the force were judged to be insignificant for calculating the F_{in}.

After F_{in} is known, it is possible to calculate the bite forces for each part of the jaw using the following formula:

$l_{in} \cdot F_{in} = l_{out} \cdot F_{out}$ (in which l_{in} and l_{out} are, respectively, the "in lever" and the "out lever", measured previously in centimeters, and F_{in} and F_{out} are, respectively, the concentric force applied by the muscle to its point of attachment and the bite force at specific point of the jaw).

Four material and structural performance properties dictate how a 3D object will react to the forces applied to it. The elastic or Young's Modulus is a ratio of stress to strain and is thus a measure of stiffness. The Young's Modulus value used in the analyses is 2.5 e10 Pascals (Pa), and is based on the value measured in human teeth (Kinney et al. 1996). Poisson's Ratio (transverse versus axial strain) describes how a structure deforms perpendicularly to the direction of force, by bulging transversely under compression and thinning under tension. The Poisson's ratio used in the analyses is 0.31, which is the same as in human teeth (Rees and Jacobsen 1997). The density - 2100 kilograms per cubic meter (Kg/m^3) – assigned to the models is also that of human dentine (Johansson et al. 1945). The choice of dentine material properties for the model reflects the predominance of that material in theropod teeth. These teeth have a

characteristically thin layer of enamel (Stokosa 2005), and the influence of this thin layer with different material properties on tooth mechanics can be tested at a later stage.

The models were kept the same size as the specimens, so that scale effects could also be considered. The bite forces calculated for *Albertosaurus* and *Tyrannosaurus* were applied to the tips of the models according to their position in the jaws. The forces were applied at a 45° angle, as a vector of the X and Y axes (Fig. III.3). The X axis represents the anteroposterior axis of the tooth, Y represents apicobasal, and Z represents labiolingual. All models had their roots restrained, simulating the ligaments present in the jaws. One exception is the *Albertosaurus* anterior dentary tooth specimen (TMP 1998.63.11), which had no root preserved, and the model was therefore restrained at its base.

The results were viewed with the Tresca yield criterion, which indicates how close a given material is to failure. This yield criterion, also known as maximum shear-stress criterion, approaches objects in such a way that instead of showing how tension and compression are gotten from certain stresses, it shows how forces pull or push at right angles to each other, causing shear. In that case, materials will fail whenever their molecules slide past each other (also known as “slip” in engineering). This concept is widely used in material mechanics, especially for shear-related phenomena in ductile metals, and more information about how it is

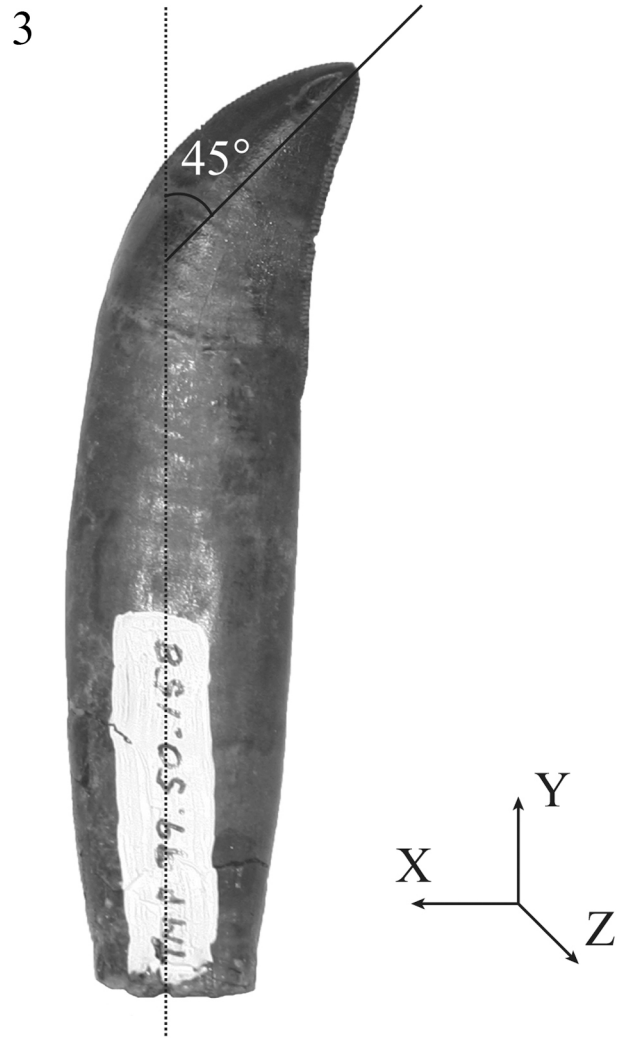

Fig. III.3. Forces applied to all 3D models. The solid line indicates the direction in which the calculated forces were applied, at 45° to the normal line (dashed) of the tooth. The axes are also shown, and are the same for all models.

calculated is detailed elsewhere (Boresi and Schmidt 2003). The stress values in this analysis therefore indicate shear, and the scale in all models was set to an upper level of 300 Megapascals (MPa), which is the yielding point for dentine (Currey 2002). Higher shear stresses would suggest failure of the material.

The specimens with roots each had the total tooth height and root height measured. These measurements were then used to calculate the proportion of the root size in relation to the total tooth size in each specimen. A *t*-statistic test was done to compare the root proportions between *Albertosaurus* and *Tyrannosaurus*. The critical value (*p*) was calculated with an α=0.05. The null hypothesis (Ho) for the test is that there is no significant difference between the root proportions in *Albertosaurus* and *Tyrannosaurus*.

Results

The estimated bite forces for an adult specimen of *Albertosaurus* were 1,536N for the anterior teeth, 2,143N for the middle teeth, and 3,413N for the posterior teeth. For an adult *Tyrannosaurus*, the bite forces were estimated at 5,880N (anterior teeth), 8,178N (middle teeth), and 13,876N (posterior teeth).

The resulting Tresca stresses after the calculated forces were applied to the 3D models are shown on Figs. III.4 and III.5. The scale maxima are set to 300 MPa, the yielding stress of dentine (Currey 2002). Some of the models show stresses superior to that and any off-scale values are shown in the models as white areas.

Tooth measurements and shear stresses for all models are given in Table III.2. The maximum stresses were measured along the XY plane. Shear stresses were also measured along the Z axis so that the labiolingual width of each tooth could be taken into consideration. A ratio between the stresses measured in the XY plane and Z axis was calculated. Higher ratios indicate higher stresses along the anteroposterior and apicobasal axes (usually a combination of both, because of the 45° angle of the force applied to the models), as opposed to labiolingual stresses.

The root proportions and the stress ratios for XY/Z are plotted on a graph in Fig. III.6. The graph shows that the roots of *Albertosaurus* teeth are generally shorter than in *Tyrannosaurus*, but that the shear stress along the X and Y axes are highest for the mid-maxillary and mid-dentary teeth of *Albertosaurus*.

A pattern can be observed for both *Albertosaurus* and *Tyrannosaurus* regarding the distribution of shear stresses in the maxillary teeth. Both taxa show the highest XY/Z stress ratios in the mid-maxillary

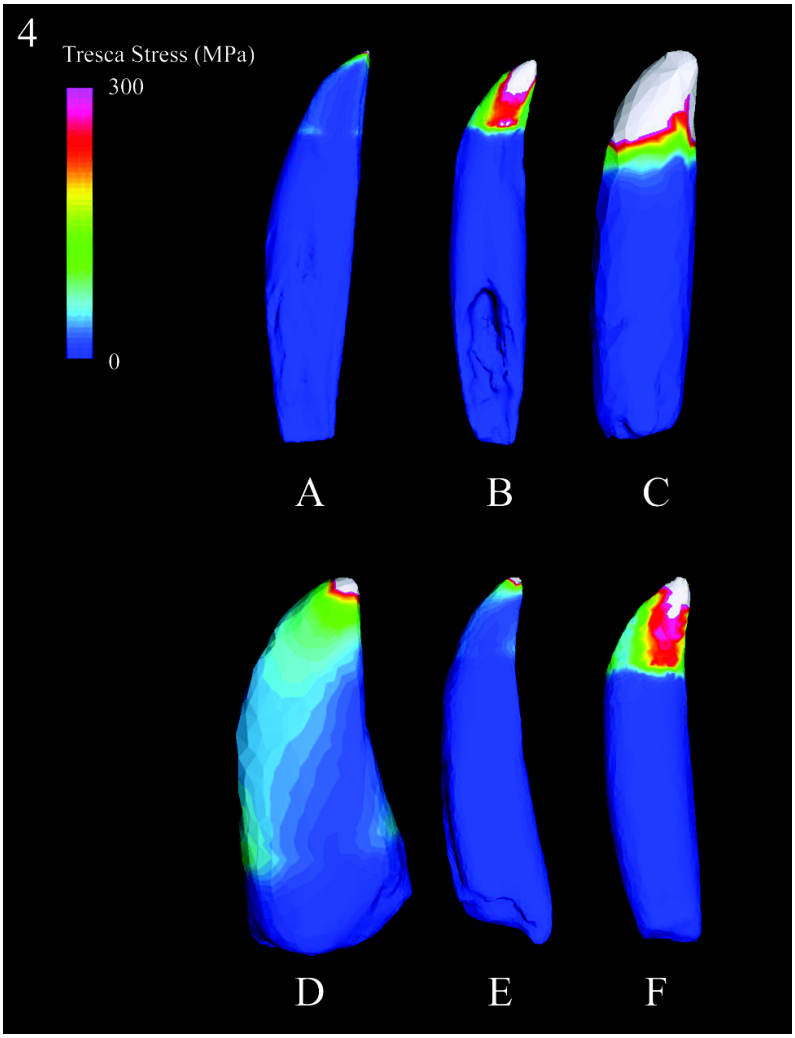

Fig. III.4. Finite Element analyses of tooth models from *Albertosaurus sarcophagus*. (A) Premaxillary tooth. (B) Mid-maxillary tooth. (C) Posterior maxillary tooth .(D) anterior dentary tooth. (E) Mid-dentary tooth. (F) Posterior dentary tooth. Models are not in scale. Stresses are shown with Tresca yield criterion.

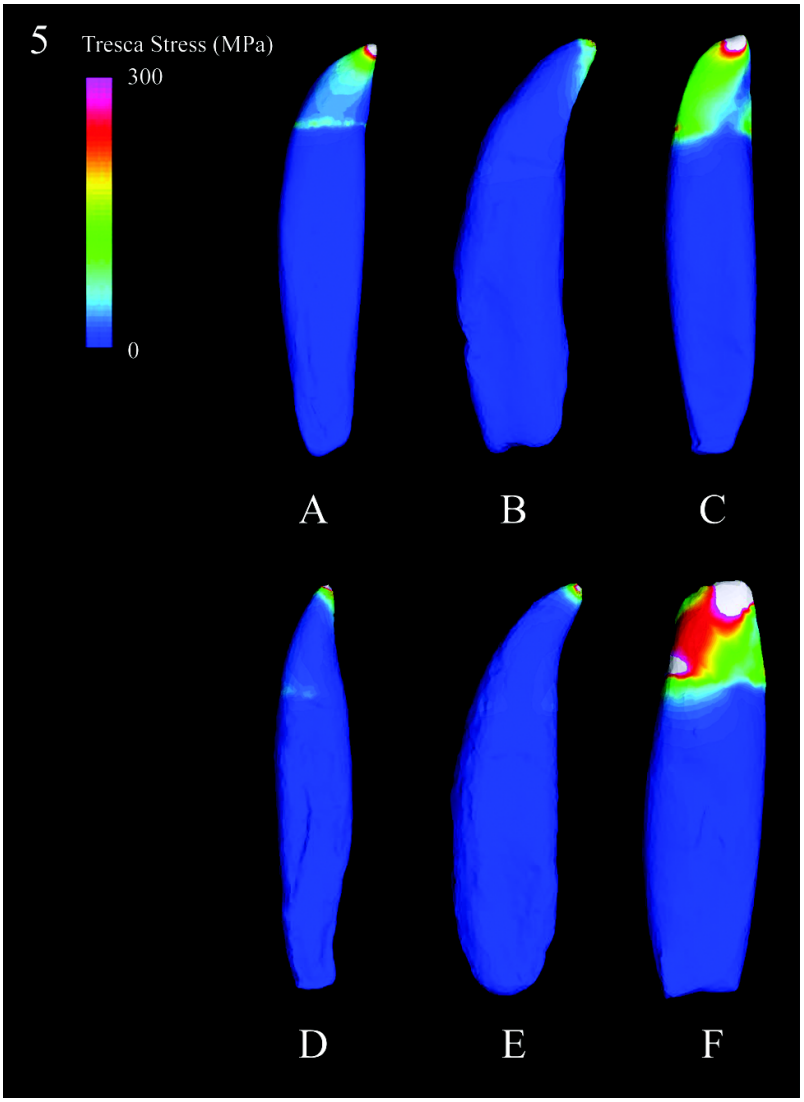

Fig. III.5. Finite Element analyses of tooth models from *Tyrannosaurus rex*. (A) premaxillary tooth. (B) Mid-maxillary tooth. (C) Posterior maxillary tooth. (D) anterior dentary tooth. (E) Mid-dentary tooth. (F) Posterior dentary tooth. Models are not in scale. Stresses are shown with Tresca yield criterion.

Table III.2. Root height and Tresca stresses measurements in *Albertosaurus* and *Tyrannosaurus.*

Taxon	Tooth position	Root length (mm)	Total tooth length (mm)	Percentage of root	Maximum shear stress along XY plane (MPa)	Maximum shear stress along Z axis (MPa)	Ratio XY/ Z stress
Albertosaurus	Premaxillary	79	106.3	0.74	3918.3	1994	1.96
Albertosaurus	Mid-maxillary	66	103.2	0.64	4342.3	868.3	5.00
Albertosaurus	Posterior maxillary	19.5	28.6	0.68	11293.3	7462.7	1.51
Albertosaurus	Anterior dentary	?	?	?	4436.2	1901.9	2.33
Albertosaurus	Mid-dentary	66	103.2	0.64	858.1	132.8	6.46
Albertosaurus	Posterior	39	60	0.65	3292.9	1099.5	2.99

	dentary						
Tyrannosaurus	Premaxillary	102	135	0.75	24485.6	12415.6	1.97
Tyrannosaurus	Mid-maxillary	135	195	0.69	1401.2	553.7	2.53
Tyrannosaurus	Posterior maxillary	74	105	0.7	331773.8	161715	2.05
Tyrannosaurus	Anterior dentary	115	154	0.75	1152.1	335	3.44
Tyrannosaurus	Mid-dentary	145	209	0.69	557.9	237	2.35
Tyrannosaurus	Posterior dentary	42	64	0.66	41036.7	12315	3.33

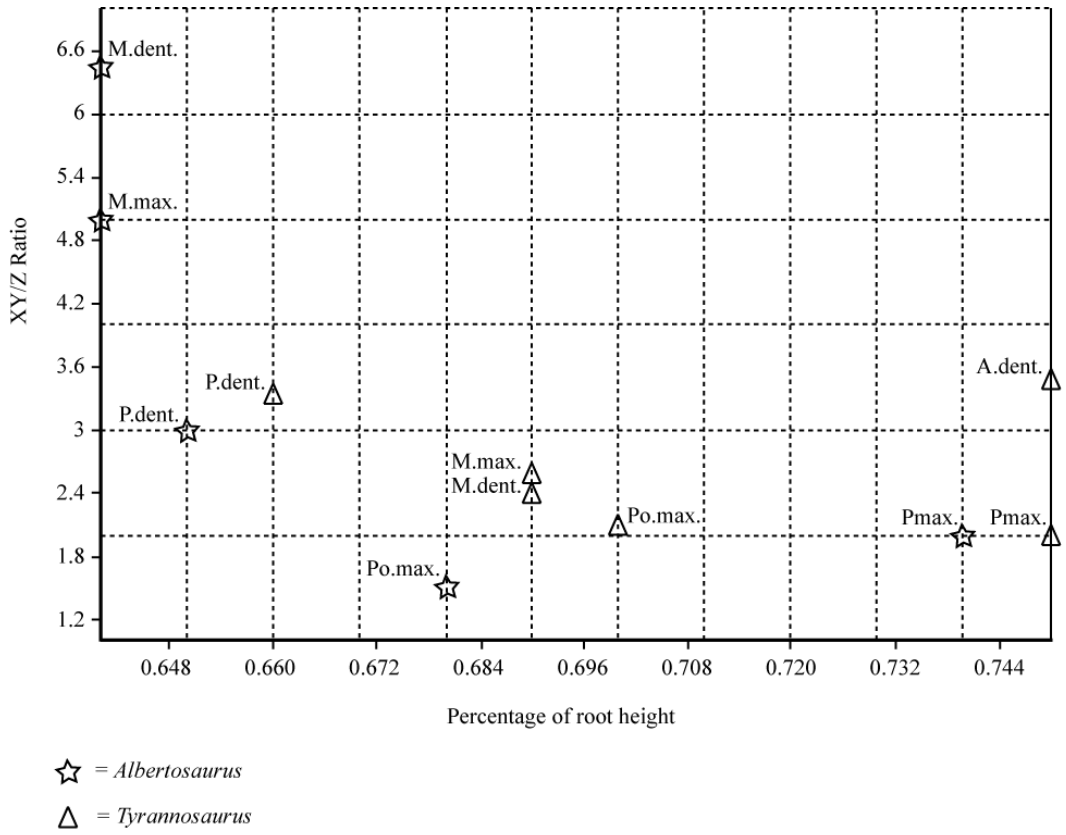

Fig. III.6. Graph showing the measurements of the root percentages of the teeth (X axis of the graph), and the ratio of Tresca stresses measured along the XY plane versus the Z axis of all models (Y axis of the graph). *A.dent.*, anterior dentary tooth; *M.dent.*, mid-dentary tooth; *M.max.*, mid-maxillary tooth; *P.dent.*, posterior dentary tooth; *Pmax.*, premaxillary tooth; *Po.max.*, posterior maxillary tooth.

teeth, followed by the premaxillary and posterior maxillary teeth (the last two show little stress ratio differences).

In the dentary teeth, however, *Albertosaurus* and *Tyrannosaurus* teeth behave differently. Even though the anterior dentary tooth for *Albertosaurus* is not shown (Fig. III.6) because the root length is unknown, the XY/Z stress ratio was still measured on the crown (Table III.2). The ratios for *Albertosaurus* are highest in the mid dentary teeth, while for *Tyrannosaurus* the same ratios are highest in the anterior dentary and posterior dentary teeth.

The distribution of root proportions in *Albertosaurus* and *Tyrannosaurus* is also different. Although both taxa have the relatively tallest roots in their premaxillary teeth (and in the case of *Tyrannosaurus* also in the anterior dentary tooth) followed by the posterior maxillary teeth, the next tallest roots differ in these taxa. For *Albertosaurus* the third tallest root is the one in the posterior dentary, and the shortest roots are found in the mid-maxillary and mid-dentary, which have both the same root/crown proportions. For *Tyrannosaurus*, the third tallest roots are the ones in the mid-maxillary and mid-dentary (also with equal root/crown proportions), and the relatively shortest root is found in the posterior dentary tooth.

A *t*-test was done to compare all the root height percentages of *Albertosaurus* and *Tyrannosaurus*. There is no significant difference between the average root height proportions in these two groups, which

does not allow the rejection of the null hypothesis. However, although both taxa have similar overall root proportions, the differences in the way these proportions are distributed along the tooth positions are still informative and allow for some biomechanical interpretations.

Discussion and conclusions

The bite forces estimated for *Tyrannosaurus* in this project are comparable to the values obtained by Erickson et al. (1996). Whereas the methods in this paper include skull and jaw proportions, Erickson et al. (1996) calculated the bite forces for this taxon based on bite marks found in bones. The bite forces for *Albertosaurus* have not been previously estimated and additional calculations using the same methods by Erickson et al. (1996) would test the results obtained here.

The *Albertosaurus* specimens used in the analyses in this paper pose a problem regarding the application of bite forces onto them. The forces were estimated based on an adult specimen. Some of the tooth specimens are of sizes expected for adults (for example TMP 1999.50.86), but others are more likely to have belonged to juveniles (for example TMP 2004.56.19). This becomes evident (Fig. III.4) where some of the models show large off-scale areas (representing failure of the material, due to exceedingly large shear stresses caused by large forces).

Because of the problems related to different sizes of teeth in the sample (as also noted by Buckley et al., this volume), the use of proportions was preferred over the use of absolute values for the comparative analyses. When dividing the stress values measured along the XY plane by the stress value measured along the Z axis, the resulting proportion is less dependant on how big or how small the tooth is, even though the proportions of the teeth could also play a roll in stress distribution. Nevertheless, it makes comparisons between taxa with significant size differences more informative. The same logic is applied to the root measurements. It is obvious that the absolute values for root height in *Tyrannosaurus* are larger than these of *Albertosaurus*, but the objective of this study is to compare the proportions of teeth in order to test the influence of root height in tooth biomechanics. This will help to better understand the heterodonty observed in these taxa, and how their tooth morphologies differ, as opposed to how their absolute sizes differ.

Another reason for material failure could be the angle that the forces were applied. In this study, all models had the forces applied in a 45º angle (as shown in Fig. III.3), but this angle caused high enough stresses along the XY plane in some models to cause the material to fail even in the anterior portion of the tooth, near the base (Fig. III.5), in the case of the posterior dentary tooth of *Tyrannosaurus*. This suggests that different tooth positions have different biting angles, and that the distance from the jaw hinges influences tooth shape, as also observed by D'Amore

(2009). Additional studies on tooth wear would help to learn more details about biting angles and forces used in the different regions of the jaws.

The 3D models used in this study helped visualizing two things: how shear stress is distributed in tyrannosaurid teeth along the different jaw positions, and how different root heights are distributed along the jaw. The Tresca stresses measured along the XY plane were the highest in all models. Some shear stress was also observed along the Z axis. The results showed similar patterns for *Albertosaurus* and *Tyrannosaurus* in the maxillary teeth, but opposite patterns for shear stress in the dentary teeth of *Tyrannosaurus*.

In *Albertosaurus*, the highest shear stresses along the XY plane in the mid-maxillary teeth indicate that these teeth are more efficient than premaxillary and posterior maxillary teeth in avoiding labiolingual (Z) shear. Most of the stress is deflected to the anteroposterior/apicobasal (XY) plane on the mid-maxillary teeth. The premaxillary and posterior maxillary teeth, however, were more efficient at sustaining forces along the XY plane, because some of the stress is deflected to the Z axis. In summary, mid-maxillary teeth in *Albertosaurus* are suited to endure labiolingual stresses, whereas premaxillary and posterior maxillary teeth in that taxon are capable of resisting higher anteroposterior/apicobasal stresses. The same pattern is observed in the dentary teeth of *Albertosaurus*, and the upper jaw of *Tyrannosaurus*. It is important to point

out, however, that caution should be used when interpreting the results for the anterior dentary tooth of *Albertosaurus*. This specimen did not have the root preserved and therefore the model had to be restrained at the base of the crown. Nevertheless, the general stress distribution on that model is still informative, and the stress values obtained are similar to the ones obtained for the premaxillary tooth in *Albertosaurus*. An additional model with the root preserved would reinforce this analysis.

For the dentary teeth in *Tyrannosaurus*, the exact opposite of what is described for *Albertosaurus* is observed: the mid-dentary models can endure high anteroposterior/apicobasal stresses, whereas anterior and posterior dentary teeth are more suited to resist labiolingual stresses.

In addition the root proportion distribution among different tooth positions in *Albertosaurus* and *Tyrannosaurus* is also distinct in these two genera. Whereas *Albertosaurus* has the relatively shortest roots in the mid-maxillary and mid-dentary teeth, *Tyrannosaurus* has the relatively shortest roots in the posterior dentary teeth. These results suggest a shift in high mechanical stress points (associated with longer roots) in the lower jaws of these taxa to a more anterior position in *Tyrannosaurus*.

As mentioned earlier, tyrannosaurid dinosaurs are characterized by teeth that are slightly curved posteriorly and have characteristic D-shaped cross sections in the anterior portion of their jaws; robust, curved and tall teeth in the middle portion of the jaws; and small, strongly curved and

labiolingually compressed teeth in the posterior region of the jaws. Based on the analyses done here, the upper and lower jaws of *Albertosaurus* have anterior teeth suited for pulling on prey, in order to remove large pieces of meat. The middle teeth could be employed when capturing struggling prey, or during feeding if lateral movements of the jaws are required. The posterior teeth are located at the position of the jaw capable of maximum bite force, and that force could be employed in securing food firmly and pulling, in a “grab and hold” fashion in which the teeth and jaw bones act like a clamp, rather than for crushing bones or other tough materials. The same pattern is observed in the upper jaws of *Tyrannosaurus*.

When the lower jaw of *Tyrannosaurus* is analyzed, a different pattern is identified. The anterior and posterior teeth are compatible with lateral movements of the jaw during feeding, whereas the mid-dentary teeth seem more suited for pulling on carcasses. Craniocervical feeding dynamics in tyrannosaurids suggest powerful lateral movements during feeding (Snively and Russell 2007*a*, 2007*b*), consistent with large lateral semicircular canals (Witmer and Ridgely 2009).

The increased bending resistance observed in both taxa would facilitate behaviors such as holding struggling prey or rapid head movements to remove large pieces of meat from carcasses. Tyrannosaur tooth resistance to lateral bending has also been suggested by Farlow et

al. (1991), and Snively et al. (2006). The differences in stress distribution in the upper and lower jaws of *Tyrannosaurus* show that heterodonty developed differently in this taxon when compared to *Albertosaurus*, in concordance to the hypothesis, because the strongest axes of dentary teeth are distributed differently in these taxa.

When taking into consideration that *Tyrannosaurus* has an overbite (E. Snively, personal communication, 2010), causing the anterior dentary teeth to align with the first few maxillary teeth (as opposed to the premaxillary teeth), this difference in heterodonty seems to compensate for different jaw proportions in these two taxa. The fact that in *Albertosaurus* the anterior dentary teeth are somewhat aligned with the premaxillary teeth suggests that in *Tyrannosaurus* the function of the dentary teeth shifted a few tooth positions to compensate for that disparity. The tooth mechanics therefore seems similarly regionalized in both taxa, even though the heterodonty and tooth function is distributed differently when considering tooth position alone.

It is important to note, however, that the variety of wear facets occurring in shed and *in situ* teeth (personal observation) indicates that although some teeth are stronger in one axis than the other, they were probably still employed in different ways than the optimal ways predicted in this analysis. A more detailed description of wear patterns for both

Albertosaurus and *Tyrannosaurus* would be a valuable tool to compare the results obtained in this study.

The new techniques introduced here show potential for further dentition comparisons of closely related taxa, and for understanding the forms and functions of simple structures. Tyrannosaurid teeth indeed had potential for performing different functions in different regions of the jaws, as suggested by some authors (Currie et al. 1990; Molnar 1998; Smith 2005).

References

Abler, W.B. 1992. The serrated teeth of tyrannosaurid dinosaurs, and biting structures in other animals. Paleobiology, **18**(2): 161–183.

Bamman, M. W., Newcomer, B. R., Larson-Meyer, D., Weisner, R. L., and Hunter, G. R. 2000. Evaluation of the strength-size relation *in vivo* using various muscle size indices. Medicine and Science in Sports and Exercise, **32**: 1307–1313.

Boresi, A. P., and Schmidt, R. J. 2003. Advanced mechanics of materials. John Wiley & Sons, Inc., N.J.

Buckley, L.G., Larson, D.W., Reichel, M., and Samman, T. 2010. Tooth and consequences: quantifying variation of teeth within a single population of *Albertosaurus sarcophagus* (Theropoda: Tyrannosauridae) from the Horseshoe Canyon Formation (Upper Cretaceous: Lower Maastrichtian) and implications for identifying isolated tyrannosaurid teeth in Maastrichtian-aged deposits. Canadian Journal of Earth Sciences, **45**: 1227–1251.

Currey, J.D. 2002. Bones: structure and mechanics. Princeton University Press, N.J.

Currie, P.J., Rigby, J.K. Jr., and Sloan, R.E. 1990. Theropod teeth from the Judith River Formation of Southern Alberta, Canada. *In*: Dinosaur Systematics: Approaches and Perspectives. *Edited by* Carpenter, K. and P. J. Currie (eds.). Cambridge University Press. pp. 107–125.

D'Amore, D.C. 2009. A functional explanation for denticulation in theropod teeth. The Anatomical Record, **292**: 1297–1314.

Erickson, G.M. 1995. Split carinae on tyrannosaurid teeth and implications of their development. Journal of Vertebrate Paleontology, **15**(2): 268–274.

Erickson, G.M., Van Kirk, S.D., Su, J., Levenston, M.E., Caler, W.E., and Carter, D.E. 1996. Bite-force estimation for *Tyrannosaurus rex* from tooth-marked bones. Nature, **382**:706–708.

Farlow, J.O., Brinkman, D.L., Abler, W.L., and Currie, P.J. 1991. Size, shape and serration density of theropod dinosaur lateral teeth. Modern Geology **16**: 161–198.

Johansson, E.G., Falkenheim, M., and Hodge, H.C. 1945. The adsorption of phosphates by enamel, dentin, and bone - I. Adsorption time studied by means of the radioactive isotope. Journal of Biological Chemistry, **159**: 129–134.

Kinney, J.H., Balooch, M., Marshall, S.J., Marshall, G.W. Jr., and Weihs, T.P. 1996. Hardness and Young's Modulus of human peritubular and intertubular dentine. Archives of Oral Biology, **41**(1): 9–13.

Mazzetta, G.V., Blanco, R.E., and Cisilino, A.P. 2004. Modelizacion con elementos finitos de un diente referido al genero *Giganotosaurus* Coria y Salgado, 1995 (Theropoda: Carcharodontosauridae). *Ameghiniana* **41(4)**: 619 – 626.

McHenry, C. R. 2009. Devourer of gods: the paleoecology of the Cretaceous pliosaur *Kronosaurus queenslandicus*. Unpublished Ph. D. dissertation, Department of Earth Sciences, University of Newcastle, Newcastle, N.S.W., Australia.

Molnar, R.E. 1998. Mechanical factors in the design of the skull of *Tyrannosaurus rex* (Osborn, 1905). *In* GAIA 15: Aspects of theropod paleobiology. *Edited by* B.P. Pérez-Moreno, T. Holtz, J.L. Sanz, and J.J. Mortalla. Museu Nacional de História Natural, Lisbon, Portugal. pp. 193–218.

Molnar, R.E., and Farlow, J.O. 1990. Carnosaur paleobiology. *In* The Dinosauria. *Edited by* D.B. Weishampel, P. Dodson, and H. Osmolska. University of California Press, USA. pp. 210–224.

Rees, J.S., and Jacobsen, P.H. 1997. Elastic modulus of the periodontal ligament. Biomaterials, **18**: 995–999.

Rieppel, O. 1979. A functional interpretation of varanid dentition (Reptilia, Lacertilia, Varanidae). Gegenbaurs Morphologisches Jahrbuch, Leipzig, **125**: 797–817.

Smith, J.B. 2005. Heterodonty in *Tyrannosaurus rex*: implications for the taxonomic and systematic utility of theropod dentitions. Journal of Vertebrate Paleontology, **25**(4): 865–887.

Snively, E., and Russell, A. P. 2007*a*. Craniocervical feeding dynamics of *Tyrannosaurus rex*. Paleobiology, **33**: 610–638.

Snively, E., and Russell, A. P. 2007*b*. Functional morphology of the neck musculature in the Tyrannosauridae (Dinosauria, Theropoda) as determined via a hierarchical inferential approach. Zoological Journal of the Linnean Society, **151**(4): 759–808.

Snively, E., Henderson, D.M., and Phillips, D.S. 2006. Fused and vaulted nasals of tyrannosaurid dinosaurs: Implications for cranial strength and feeding mechanics. Acta Palaeontologica Polonica, **51**: 435–454.

Stokosa, K. 2005. Enamel microstructure variation within the Theropoda. *In* The carnivorous dinosaurs. *Edited by* K. Carpenter. Indiana University Press, Bloomington, IN. pp. 163–178.

Tanke, D.H., and Currie, P.J. 2000. Head-biting in theropods: paleopathological evidence. *In* GAIA 15: Aspects of theropod paleobiology. *Edited by* B.P. Pérez-Moreno, T. Holtz, J. L. Sanz, and J. J. Mortalla. Museu Nacional de História Natural, Lisbon, Portugal. pp. 167–184.

Witmer, L.M., and Ridgely, R.C. 2009. New insights into the brain, braincase, and ear region of tyrannosaurs (Dinosauria, Theropoda), with implications for sensory organization and behavior. The Anatomical Record, **292**: 1266 –1296.

Chapter 4

The variation of angles between anterior and posterior carinae of tyrannosaurid teeth[1]

Introduction

Tyrannosaurid teeth have been extensively studied for their function (Abler 1992; Smith 2005; D'Amore 2009), taxonomy (Currie et al. 1990; Sankey 2001; Sankey et al 2002; Samman et al. 2005), and palaeoecological distribution (Sankey 2001; Sankey et al 2002). Farlow et al. (1991) standardized tooth measurements and analyses for theropods, including tyrannosaurids. The trend was followed by numerous other authors (Brinkman 1990, 2008; Fiorillo and Currie 1994; Baszio 1997; Fiorillo and Gangloff 2000; Sankey 2001; Sankey et al. 2002; Smith and Dodson 2003; Smith 2005, 2007; Larson 2008; Sankey 2008*a,* 2008*b*; Buckley 2009*a*, 2009*b*; Buckley et al. 2010; Larson 2009), contributing significantly to the development of a more complete dataset of theropod tooth measurements and analyses.

However, studies of carinal variation along the tooth rows of theropods have been superficial and limited to a few papers (Molnar 1998; D'Amore 2009). Carinae are keels on the posterior and anterior edges of a

[1] A version of this chapter has been accepted for publication. Reichel, M. The variation of angles between anterior and posterior carinae of tyrannosaurid teeth. Canadian Journal of Earth Sciences.

tooth, often with denticles along most of their length, that occur in a great number of theropod taxa, including all tyrannosaurids.

Carinae can be variable in number (Erickson 1995; Beatty 2009), size, number and density of denticles (Buckley et al. 2010; Currie et al. 1990; Sankey 2001; Samman et al. 2005; Larson 2008), and of course, morphology. Additionally, in tyrannosaurids, they are placed on the anterior and posterior cutting edges of a tooth, so that it is possible to measure an angle between them, when looking at a transverse section of a tooth (Fig. IV.1). The angles between anterior and posterior carinae on tyrannosaurid teeth vary along the tooth row, in a manner that smaller angles (when measured from the lingual side of the tooth) occur on the most anterior teeth, and the angles increase progressively in posterior dentition. It is currently not known how much the patterns of carinal angles vary in different tyrannosaurid taxa, how the angles between carinae are related to other tooth measurements, and if this is a valid character for taxonomic or functional analyses.

It is, however, hard to interpret variations in carinal angles, because a static reference point has to be established first. The curvature in a tooth of a tyrannosaurid makes it difficult to effectively measure the angle between carinae in various teeth in a consistent manner. Here, a new method is introduced to overcome this problem through the use of a three-dimensional tool that allows the creation of reference points in space and that plots the carinal positions onto a two-dimensional plane of a cross-

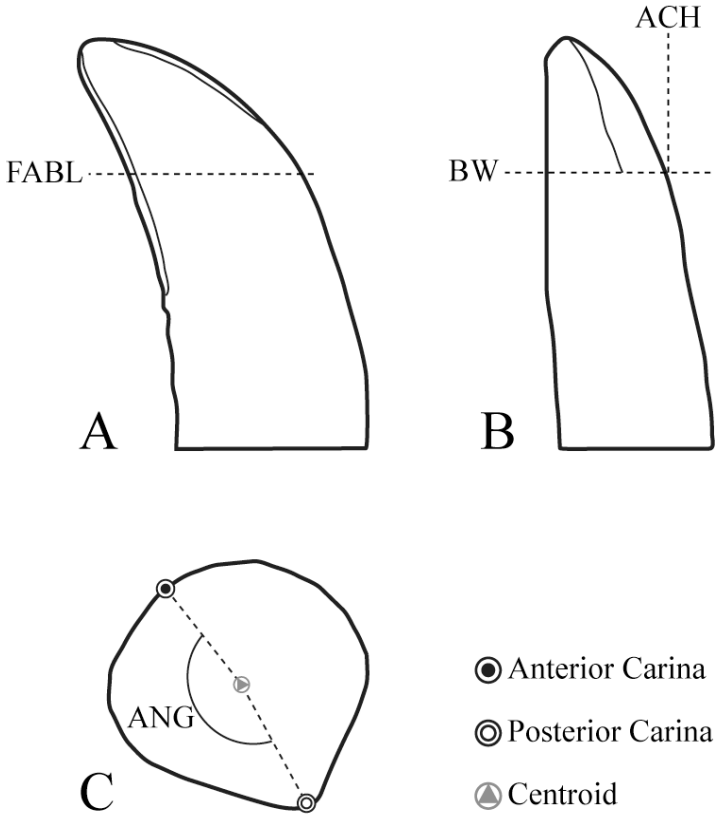

Fig. IV.1. Diagram showing measurements taken for this study. (A) Lateral view of a tooth, indicating fore-aft basal length (FABL) taken at the base of the anterior carina. (B) Anterior view of a tooth, showing basal width (BW) and anterior carina height (ACH), also measured from the base of the anterior carina. (C) Outline of a tooth, traced with the aid of a Microscribe® digitizer, showing the angle between anterior and posterior carinae (ANG), using the centroid of the "tooth slice" as a reference point.

section of each tooth. The centroid of each cross-section can be used as a reference point to make the measurements consistent amongst different tooth positions in different taxa.

The objective of this is to document and analyze variation in angles between carinae of tyrannosaurid taxa. Because the angles vary along the tooth row, comparisons were made within datasets of one specimen and between different specimens. Only data from *in situ* teeth (or with known jaw position) were used, because the jaw position information plays an essential role in the analysis. Multivariate analysis was used for making comparisons, and to determine the amount of variation within the tooth population. The hypotheses tested here are that 1) angles between carinae contribute significantly to variations in tooth measurement datasets, 2) angles between carinae vary among different tyrannosaurid taxa, and 3) the variation in angles between carinae is related to tooth function.

Materials and methods

Five genera of tyrannosaurids were analyzed (Appendix IV.1). The *Tyrannosaurus* measurements were obtained from TMP 1981.006.0001 (“Black Beauty”) and from casts of teeth of “Stan” (BHI-3033). *Tarbosaurus* measurements were taken from specimens PIN 551-1, PIN 551-3, PIN 551-91, PIN 551-2 and from upper and lower left jaws of

UALVP 47949 (casts of *Tarbosaurus*). Additionally, measurements of *Albertosaurus*, *Daspletosaurus*, and *Gorgosaurus* were taken from various specimens at the collections in the Royal Tyrrell Museum of Palaeontology. The present sample size is a representation of important taxonomic groups and is adequate as an initial step to demonstrate the applicability of the methods described. The future inclusion of additional specimens will help to further verify the results obtained in this preliminary analysis.

There is no standardized nomenclature for zyphodont teeth (Sweetman 2004), and therefore the nomenclature used here is modified from what was proposed by Smith and Dodson (2003): anterior, equivalent to 'mesial', towards the premaxillary region; posterior, equivalent to 'distal', towards the tail; lingual, towards the tongue; labial, towards the lips; apical, towards the tip of the tooth; basal, towards the base of the tooth, where it meets the host bone.

Only measurements from *in situ* teeth were considered for this analysis. The measurements used are based on what previous authors have employed in morphometric studies (Currie et al. 1990; Samman et al. 2005; Smith 2007; Buckley et al. 2010), and the way they were taken is shown in Figure IV.1. In some cases, some of the measurements could not be taken because of wear or post-mortem damage, and the positions in the table were filled in by a question mark.

The tool used to measure the angles between carinae was a Microscribe® digitizer. To keep the data consistent, it was necessary to measure that angle at an equivalent height in each tooth, in this case the most basal point of the anterior carina. At that level, the digitizer was used to trace the perimeter of the crown (Fig. IV.1). This generated a two-dimensional projection of that "slice" of the tooth. The outline of the "tooth slice" shows clearly where the anterior and posterior carinae are located (Fig. IV.1). The next step was to determine the centroids of these slices, which was done using ImageJ®. A line was traced from each carina to the centroid and the angle between these lines was then measured for each tooth. The angles were entered in the dataset in degrees, and they were not log-transformed. Multivariate analyses of the data were also run with the angles converted to radians, and the results obtained did not differ. Therefore, the preferred method was to express angles in degrees, because they are more intuitive for presenting the results.

Multivariate analysis of the measurements was done using Paleontological Statistics (PAST), version 2.06 (Hammer et al. 2001). These analyses described the amount of variation in the tooth population. All the data collected (except for carinal angles, and FABL/BW proportions) were $\log_{10}$ transformed to minimize size-biased results. In order to determine how much each measured variable contributed to the total variation in the dataset, Principal Component Analyses (PCA) were done. PCA ordinance plots project three-dimensional plots of specimens

into two dimensions, and sometimes reveal discrete groupings. PCA substitutes missing data using column average substitution (Hammer and Harper 2006), which reduces problems related to smaller sample sizes often seen when dealing with paleontological analyses. PCAs were run using the "correlation" setting to reduce the size-related differences between $\log_{10}$ transformed values and those measured in degrees, such as carinal angles, similarly to Buckley et al. (2010).

Another important step was to determine if the amount of variation found in the dataset is enough to separate the population of teeth into different groups. This is necessary to verify the taxonomic value of the different tooth measurements. One method used to verify taxonomic value of measurements is Discriminant Analysis (DA). DAs project multivariate datasets down to one dimension, maximizing separation between two predetermined groups. A 90% or greater separation between two groups is sufficient support for the presence of two taxonomically distinct morphotypes (Hammer and Harper 2006). These analyses were done between all possible pairs of the studied tyrannosaurid groups to verify if the measurements used here show potential for genus differentiation.

Additionally, Canonical Variates Analyses (CVAs) were used in cases where three or more groups were being analyzed at the same time, so that the data could be displayed on a two-dimensional plot. Additionally, Multivariate Analyses of Variance (MANOVA) were run in order to test whether several samples have significantly different means. The Wilks'

lambda statistic was used to quantify the variation between the datasets of different groups. Wilks' lambda values closer to one indicate poor separation between groups and values closer to zero indicate a good separation. CVAs were used to verify the separation between the datasets of genera studied, as well as the separation between the datasets of each area of the jaws within each genus. Missing data were supported by column average substitution (Hammer and Harper 2006).

In order to test the significance of the results of the DAs and CVAs, the Hotelling's t^2 was done on all analyses. The value of the calculated *p*(same) indicates whether a result is statistically significant at $p < 0.05$.

Results

The principal component analysis showed that 55.3% of the variance in the dataset, when comparing the measurements taken from all specimens included in this analysis, is attributable to principal component 1 (PC1, Fig. IV.2). In PCA, PC1 is normally related to size variation, even in $\log_{10}$ transformed data (Hammer and Harper 2006). Principal component 2 (PC2) is responsible for 35.5% of the variation in the dataset and shows variations in carinae angles and the FABL/BW ratio. Smaller teeth have relatively higher FABL/BW ratios, meaning that smaller teeth in the sample tend to be more labiolingually compressed. The variations in angles between carinae are not strongly related to tooth size, according to

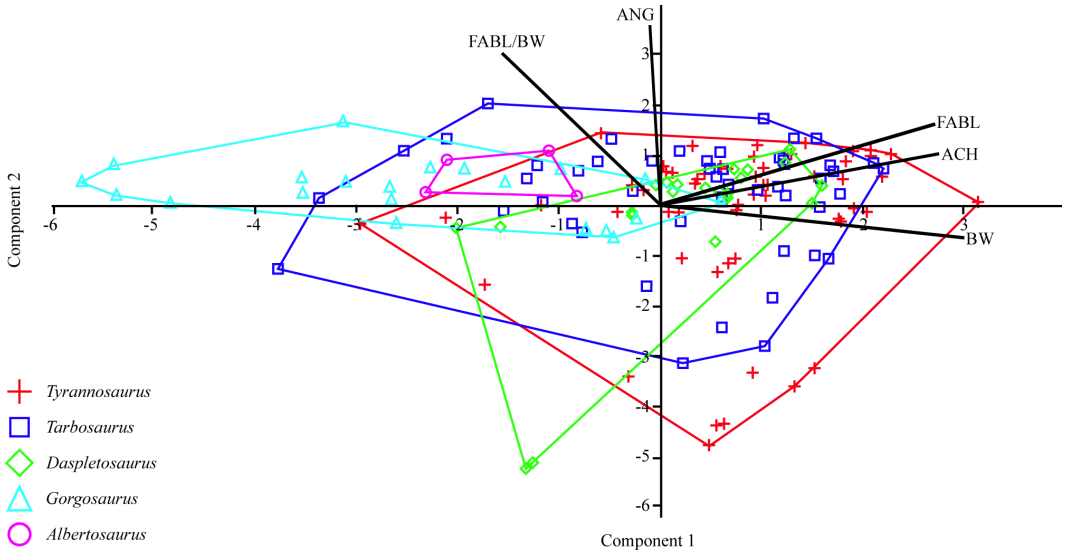

Fig. IV.2. Principal component analysis plot PC1 (size) and PC2 (angle between carinae – fore-aft basal length and basal width proportion) comparing tooth measurements of *Albertosaurus*, *Daspletosaurus*, *Gorgosaurus*, *Tarbosaurus*, and *Tyrannosaurus*. Variance vectors show the relative amount of variation each variable contributes to the data set. Abbreviations as in the morphometric abbreviations section.

the ordinance plot (Fig. IV.2), which contributes to a significant amount of the variation found in the dataset.

When excluding PC1 (size) from the analysis, the ordinance plot shows that some of the tyrannosaurid groups cluster (Fig. IV.3), with a significant amount of overlap. The ordinance plot in Figure IV.3 shows that teeth in *Tarbosaurus* have the greatest range in the FABL/BW proportion, in that they range from the anteroposteriorly shortest and labiolingually widest teeth to the anteroposteriorly longest and labiolingually narrowest ones in the dataset.

When plotting a graph (Fig. IV.4) of the tooth position in the X-axis versus the angle between carinae on the Y-axis, it becomes clear that the angle variation occurs in a similar manner in all tyrannosaurids. The main difference between taxa occurs in the premaxillary teeth. Although there is not a significant separation between different tyrannosaurid groups, there are clear patterns for different tooth positions. This shows that the measurement of carinal angles has great potential for identifying tooth positions in isolated tyrannosaurid teeth.

The discriminant analyses determined the amount of separation between the groups of tooth measurements obtained from each tyrannosaurid group. Most pairings showed values from 70 to 90% of correctly classified tooth measurements, indicating a fair separation between them. The values for Hotelling's t^2 are summarized on Table IV.1.

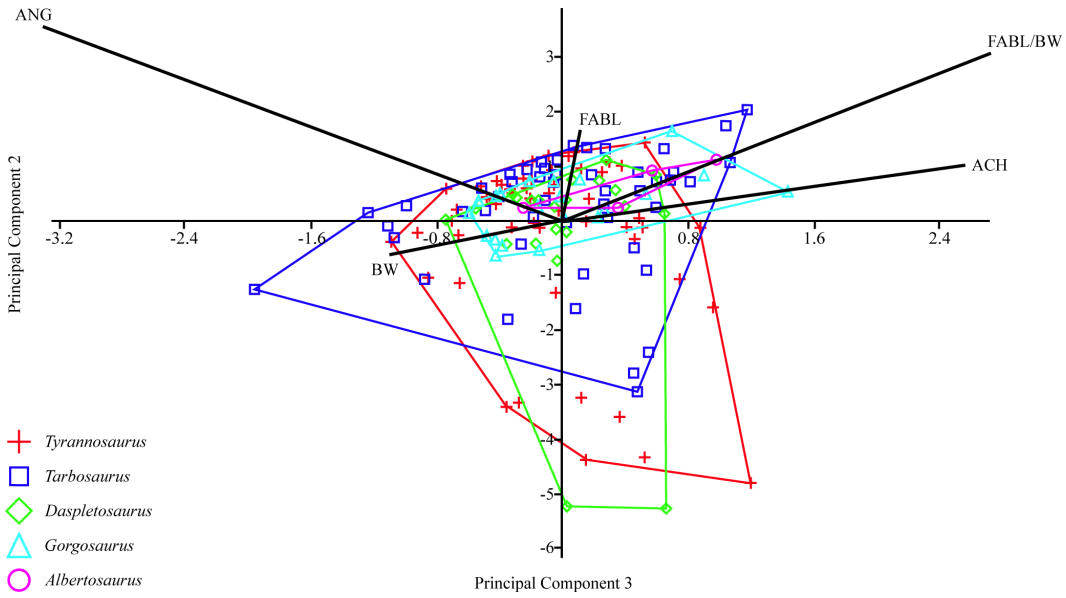

Fig. IV.3. Principal component analysis plot showing PC2 and PC3. The comparison between tooth measurements of *Albertosaurus*, *Daspletosaurus*, *Gorgosaurus*, *Tarbosaurus*, and *Tyrannosaurus* suggests a significant amount of the variance in the dataset is attributed to size, as shown by the data overlap between different taxa. Abbreviations as in the morphometric abbreviations section.

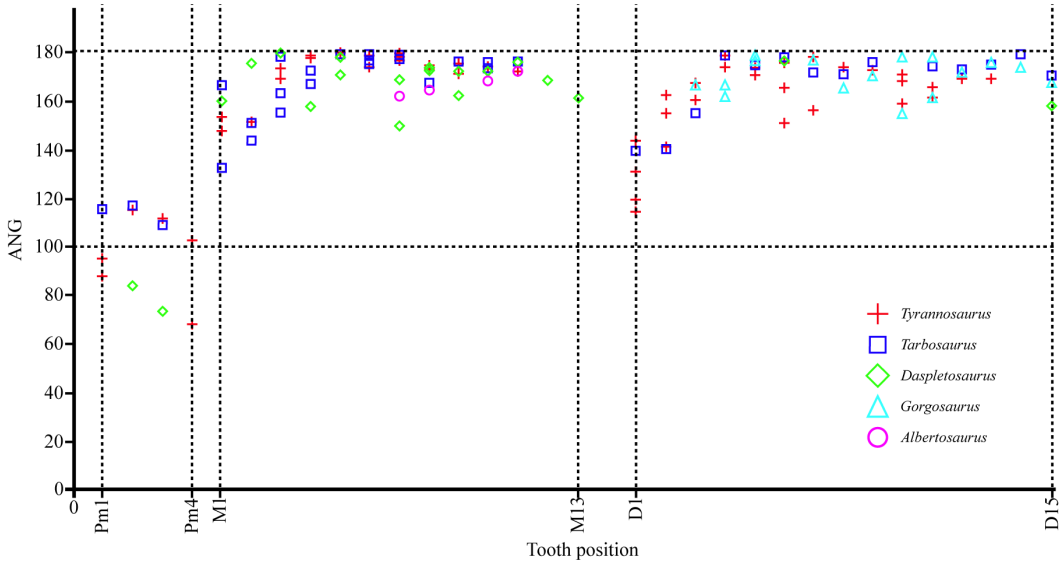

Fig. IV.4. Graph showing the angles measured between carinae for different tooth positions. Similar patterns are seen between different taxa. *D*, dentary teeth; *M*, maxillary teeth; *Pm*, premaxillary teeth.

Table IV.1: Discriminant analyses (DA) results for comparisons among *Albertosaurus*, *Daspletosaurus*, *Gorgosaurus*, *Tarbosaurus*, and *Tyrannosaurus*. tooth measurements.

Groups compared	Percent correctly classified	Hotelling's t^2: p (same) at $p < 0.05$
Albertosaurus vs. *Gorgosaurus*	76%	0.4
Daspletosaurus vs. *Albertosaurus*	92.3%	0.002
Daspletosaurus vs. *Gorgosaurus*	86.05%	2.2×10^{-6}
Tarbosaurus vs. *Albertosaurus*	85.19%	0.06
Tarbosaurus vs. *Daspletosaurus*	77.78%	6.2×10^{-4}
Tarbosaurus vs. *Gorgosaurus*	81.69%	9.9×10^{-8}
Tyrannosaurus vs. *Albertosaurus*	91.53%	5.3×10^{-14}
Tyrannosaurus vs. *Daspletosaurus*	67.53%	7.3×10^{-15}
Tyrannosaurus vs. *Gorgosaurus*	89.47%	1.9×10^{-17}

There were some exceptions that did not fall into this range. The comparison between *Daspletosaurus* and *Albertosaurus* showed 92.3% of teeth correctly classified (Hotelling's t^2: p [same]= 0.002 indicates a significant difference between groups at $p < 0.05$). Additionally, the comparison between *Tyrannosaurus* and *Albertosaurus* showed 91.53% of teeth correctly classified (the Hotelling's t^2: p [same]= 5.3×10^{-14} indicates that there is a significant difference between these groups at $p < 0.05$). The lowest percentages of correctly classified teeth result from comparing *Tyrannosaurus* and *Tarbosaurus*, (55.24% of teeth correctly classified), and *Tyrannosaurus* and *Daspletosaurus* (67.53% of teeth correctly classified). Although showing the lowest percentages of correctly classified teeth, the difference found between those groups was statistically significant in both comparisons at $p < 0.05$.

Only two of the comparisons resulted in separations between groups that were not statistically significant at $p < 0.05$. The first one is the comparison between *Tarbosaurus* and *Albertosaurus*, in which 85.19% of the teeth were correctly classified (Hotelling's t^2: p [same]= 0.06). The second one is the comparison between *Albertosaurus* and *Gorgosaurus*, with 76% of teeth correctly classified (Hotelling's t^2: p [same]= 0.4).

The CVA plot with all datasets combined (Fig. IV.5) shows overlapping areas between taxa. However, the Wilk's lambda of 0.359 indicates that there is some degree of separation between the groups. The

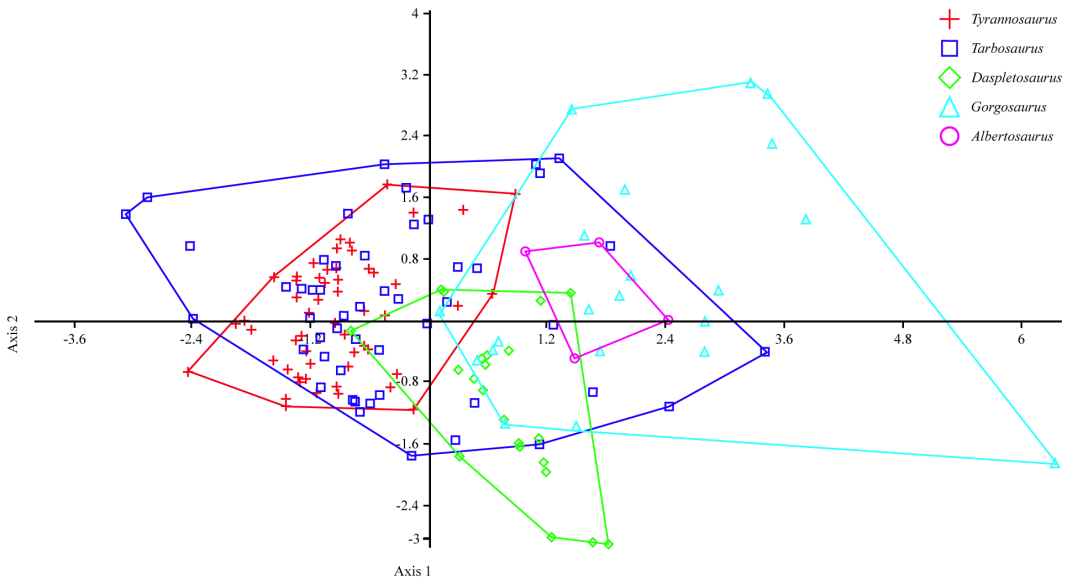

Fig. IV.5. Canonical variance analysis plots comparing teeth of *Albertosaurus*, *Daspletosaurus*, *Gorgosaurus*, *Tarbosaurus*, and *Tyrannosaurus*. The plot shows that the teeth of these taxa are morphologically similar, due to the overlap in the data.

Hotelling's pairwise tests for this CVA were similar to the DA results, and will not be discussed here.

The CVAs for each taxon reveal information on how different tooth families cluster for different tyrannosaurids. *Tyrannosaurus* teeth show separation of the dataset into four main clusters (Fig. IV.6). The Wilk's lambda of 0.02 indicates good separation between them. The first cluster is composed of premaxillary teeth, and the Hotelling's pairwise test indicates that the difference between premaxillary teeth and any other tooth family is statistically significant at $p < 0.05$. The second cluster is composed of anterior maxillary teeth (first and second) and anterior dentary teeth (from first to third). Besides being clustered together on the plot, the Hotelling's pairwise test indicated that there is no significant difference between these two tooth families at $p < 0.05$, but they are significantly different from all the other tooth families. The third cluster is composed of posterior dentary teeth (from fourth to thirteenth). Although this cluster shares a few nodes with the posterior maxillary tooth family, the Hotelling's pairwise test indicates that the differences between the posterior dentary teeth and any other tooth family is statistically significant at $p < 0.05$. The fourth cluster is composed of posterior maxillary teeth (from third to eleventh). Although a few of the posterior maxillary tooth nodes are shared with the third cluster, the Hotelling's pairwise test indicates that the posterior maxillary teeth are significantly different from

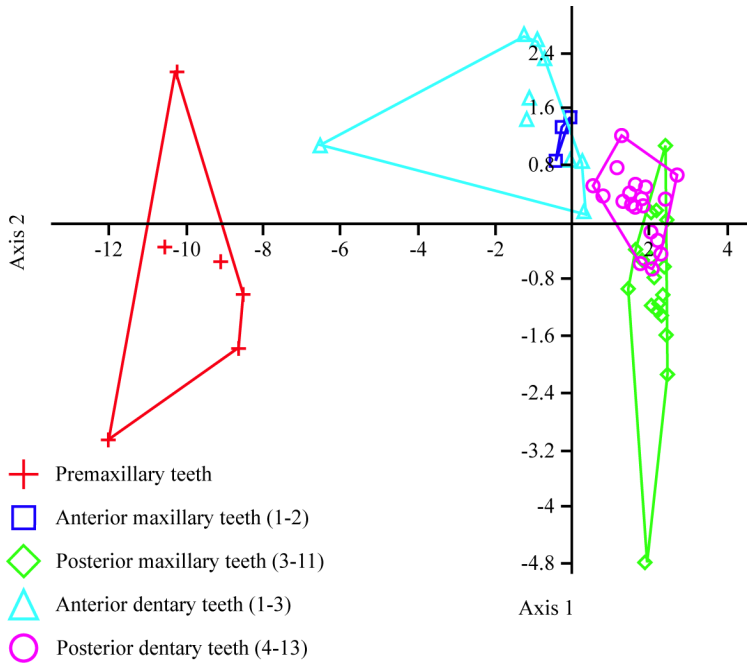

Fig. IV.6. Canonical variance analysis plots comparing tooth families of *Tyrannosaurus*. The plot shows good separation between premaxillary teeth, anterior maxillary and dentary teeth, and posterior maxillary and dentary teeth.

any of the other tooth families at $p < 0.05$. The variation in size and shape of maxillary teeth in *Tyrannosaurus* is evident in lateral view (Fig. IV.7). However, the crown view of mid-maxillary and posterior maxillary teeth (Fig. IV.8) reveals that although there is a significant variation in size, the angles measured between anterior and posterior carinae are virtually the same.

For *Tarbosaurus*, the CVA shows five main clusters (Fig. IV.9). The Wilks' lambda of 0.05 indicates good separation between these groups. The three first clusters represent the most anterior teeth. One is composed of premaxillary teeth; the second of the first and second maxillary teeth, and the third is composed of the first through third dentary teeth. Although these three tooth families cluster separately on the CVA plot, the Hotelling's pairwise test reveals that there is no significant difference between the premaxillary and anterior maxillary teeth at $p < 0.05$. In addition to that, the same test indicates that there is no significant difference between anterior dentary and anterior maxillary teeth, as well as a "failed" result when comparing anterior dentary to premaxillary teeth. The fourth cluster is represented by posterior maxillary teeth (from third to eleventh), and although it shows some overlap with the posterior dentary cluster, the Hotelling's pairwise test indicates that there is a significant difference between this cluster and all the other ones at $p < 0.05$. The fifth cluster is composed of posterior dentary teeth (from fourth to fifteenth),

Fig. IV.7. Lateral view of the maxilla of *Tyrannosaurus* (TMP 1981.006.0001). Photograph is a courtesy of T. Miyashita. Scale bar = 150 mm.

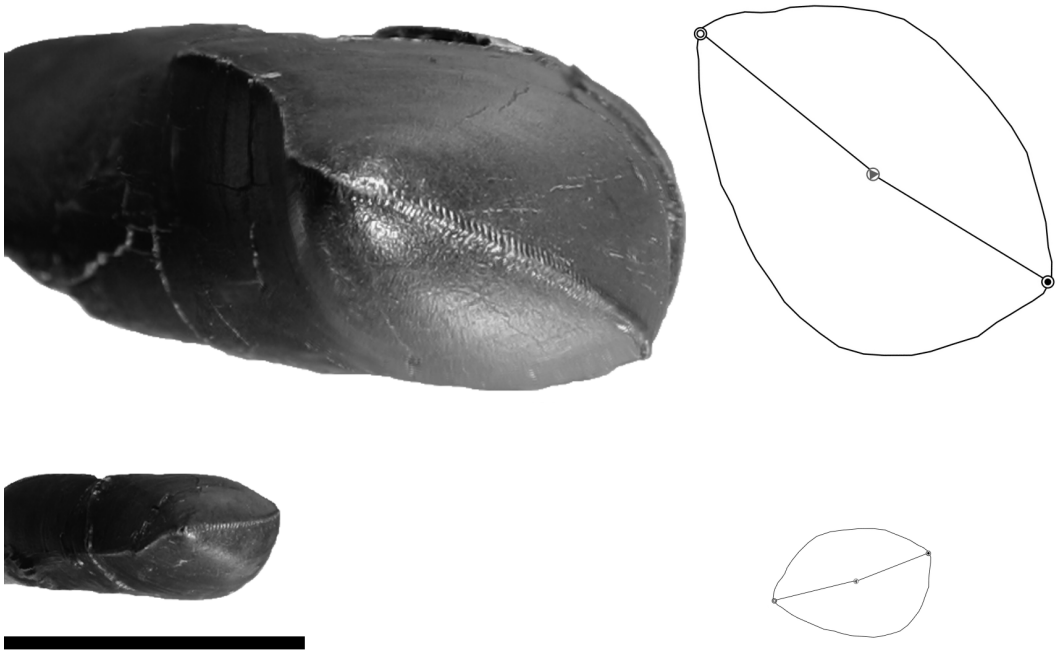

Fig. IV.8. Crown view of a *Tyrannosaurus* seventh right maxillary tooth (UALVP 48586.9) (top), and eleventh left maxillary tooth (UALVP 48586.17) (bottom), with their respective outlines (on the right) obtained through digitizing. Scale bar = 50 mm.

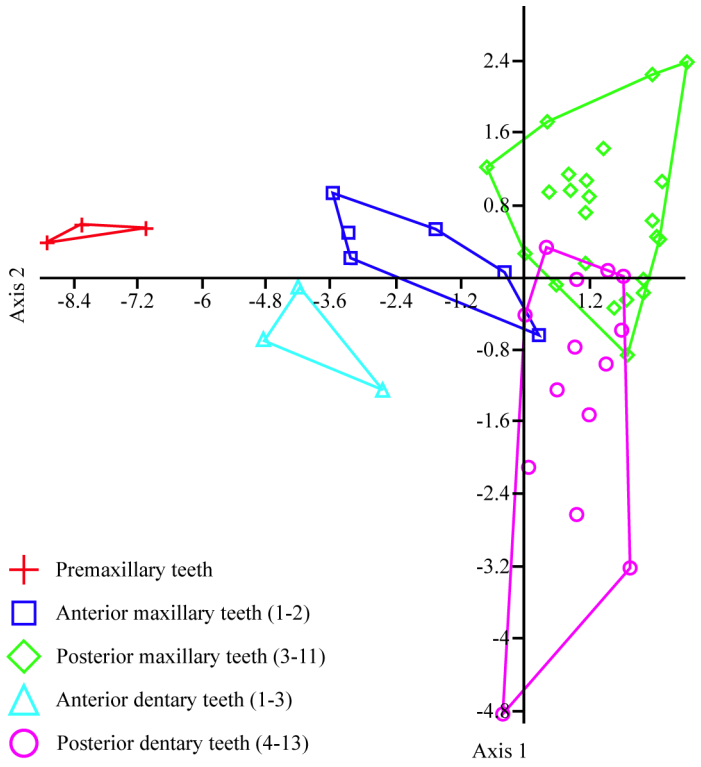

Fig. IV.9. Canonical variance analysis plots comparing tooth families of *Tarbosaurus*. The plot shows good separation between premaxillary, anterior maxillary, posterior maxillary, anterior dentary, and posterior dentary teeth.

and it overlaps slightly with the anterior maxillary and posterior maxillary clusters. The Hotelling's pairwise test indicates a significant difference between this cluster and all other clusters at $p < 0.05$.

The CVA with *Daspletosaurus* teeth (Fig. IV.10) shows only two main clusters: one with premaxillary teeth and another with the remaining maxillary and dentary teeth. The Wilks' lambda of 0.01 indicates good separation between these clusters, and a DA (because only two groups are being compared here) indicates that the separation between premaxillary teeth and the remaining tooth families (with 100% of teeth correctly classified) is statistically significant at $p < 0.05$. Indeed, the maxillary teeth of *Daspletosaurus* show the uniformity of tooth sizes found in this taxon (Fig. IV.11).

For *Gorgosaurus*, only dentary data was used, and the CVA plot (Fig. IV.12) shows three clusters that overlap somewhat. There is a good separation between the most anterior dentary teeth (up to number four) and the most posterior ones (from ten to thirteen). These two clusters also revealed a statistically significant difference observed at $p < 0.05$ when using the Hotelling's pairwise test. Not enough *in situ* data was available to do a similar analysis for *Albertosaurus* teeth.

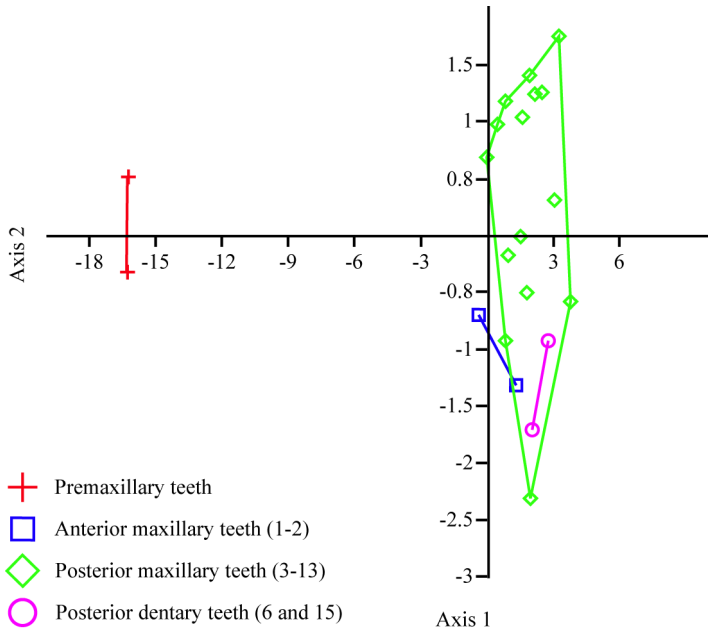

Fig. IV.10. Canonical variance analysis plots comparing tooth families of *Daspletosaurus*. The plot shows good separation between the premaxillary and all remaining teeth.

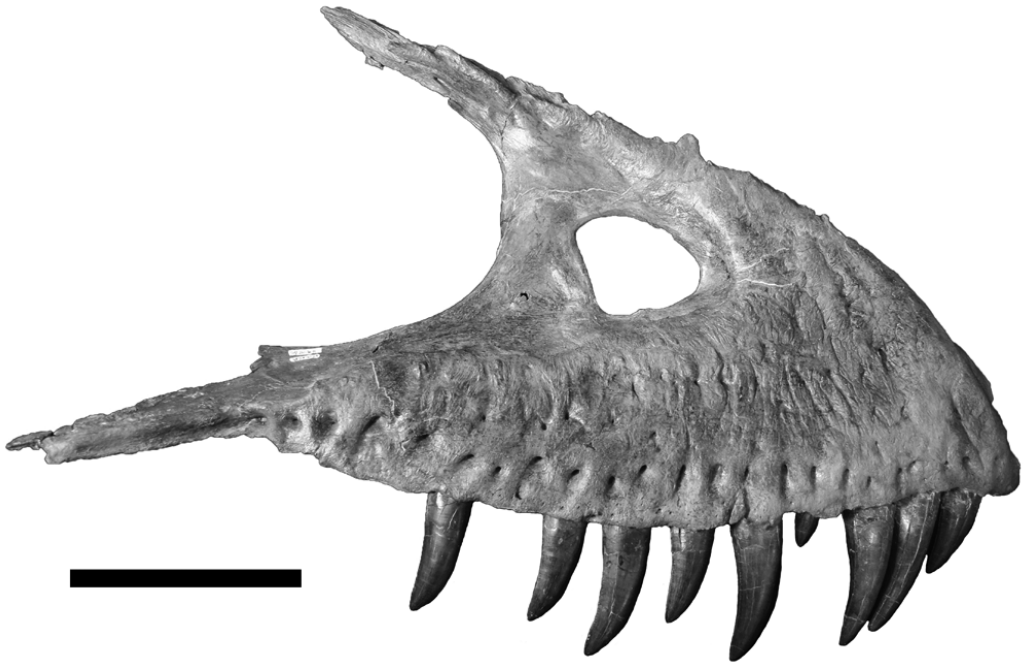

Fig. IV.11. Lateral view of the right maxilla of *Daspletosaurus* (TMP 2001.036.0001). Scale bar = 100 mm.

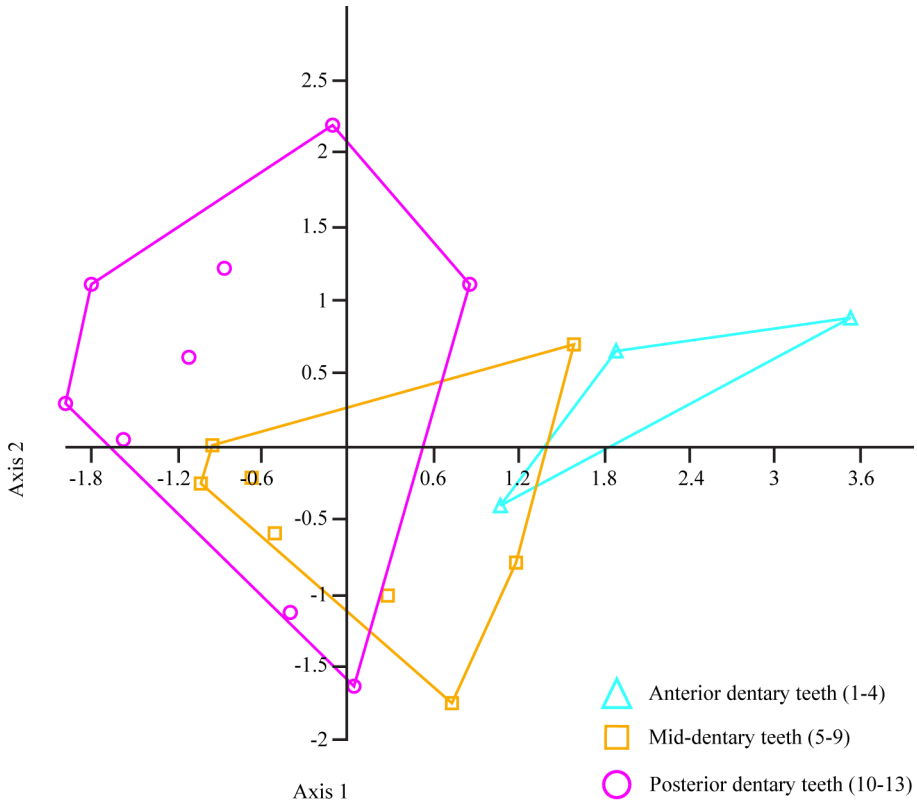

Fig. IV.12. Canonical variance analysis plots comparing tooth families of dentary teeth of *Gorgosaurus*. The plot shows good separation between anterior and posterior dentary teeth.

Discussion

Multivariate analyses of tyrannosaurid teeth provide powerful tools for studying different morphotypes and identifying how each measured component contributes to the variation in the dataset. In this study, the amount of variation in the dataset attributed to size (or PC1) is high compared to other measured variables. However, this is not surprising considering the size range encompassed by different tyrannosaurid taxa, as well as the variation of tooth size within the jaws of each taxon. For example in the *Tyrannosaurus* specimen BHI-3033, the ACH varies nearly six-fold depending on jaw position, from 88.7 mm in the first maxillary tooth to 15.2 mm in the thirteenth left dentary tooth.

According to the ordinance plot in Figure IV.2, PC2 shows a strong correlation between ANG and the FABL/BW ratio, which is in turn correlated with tooth proportions. Higher FABL/BW ratios indicate labiolingually flattened teeth, whereas lower FABL/BW ratios indicate labiolingually wide teeth. It becomes clear that the angles between carinae are more strongly correlated with tooth shape, rather than overall tooth size. For example, the angles between carinae in *Tyrannosaurus* are more variable when comparing premaxillary teeth with posterior maxillary teeth; the two types of teeth show significant differences in FABL/BW ratios, but not so much in ACHs. However, the difference in ACH is much greater when comparing anterior maxillary teeth with posterior maxillary teeth,

although fewer differences are observed in ANG, or FABL/BW ratios. This accords with Molnar's (1998) observation that the anterior and posterior maxillary teeth are similar in form even though there are significant differences in size. Farlow et al. (1991) also observed this by comparing the total crown height (TCH) and BW measurements of tyrannosaurid teeth and concluding that they are nearly linear functions of FABL. Indeed, by removing PC1 from the ordinance plot in the PCA (Fig. IV.3) the data overlap significantly, indicating that smaller teeth are generally miniatures of larger teeth. This is particularly true if the premaxillary data is removed (Fig. IV.13).

The teeth with the lowest FABL/BW ratios in the dataset occur in the premaxillary, anterior maxillary, and anterior dentary positions. These teeth also have the lowest angles between carinae. This could be a reflection of the function of the anterior dentition in tyrannosaurids, which is specialized for gripping and pulling on the prey. Enough bending resistance has been measured for these teeth to endure such mechanical stresses (Reichel 2010). The small angles between carinae, and the fact that they are located on the posterior (lingual) surface of these teeth, which are widened in a characteristic D-shape, makes them the perfect tools for defleshing carcasses. Lateral and posterior teeth have generally higher FABL/BW ratios and the carinae shift their positions to accommodate different functions for these teeth, such as slicing and cutting (Currie et al. 1990; Farlow et al. 1991; Molnar 1998; Smith 2005).

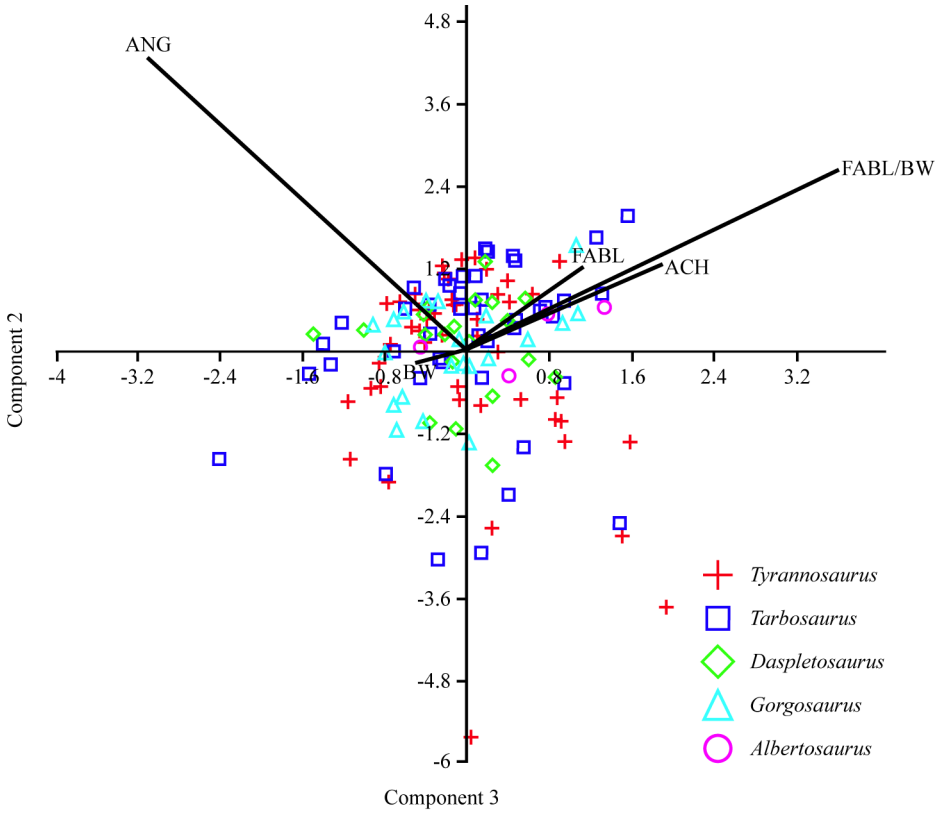

Fig. IV.13. Principal component analysis plot showing PC2 and PC3. Comparison between tooth measurements (excluding premaxillary teeth) of *Tyrannosaurus*, *Tarbosaurus*, *Daspletosaurus*, *Gorgosaurus*, and *Albertosaurus*. The data overlap between different taxa is increased when compared to Fig. 3, supporting the suggestion that a significant amount of the variation of the dataset can be attributed to size. Abbreviations as in the morphometric abbreviations section.

A characteristic *en echelon* (diagonally arrayed) tooth placement was observed by Smith (2005) in anterior maxillary teeth of *Tyrannosaurus*. This placement causes teeth to not line up along their anteroposterior axes. The carinae on these teeth are placed so that the angles between them are smaller and compensate for the lack of alignment on these teeth. Therefore, the anterior maxillary teeth in *Tyrannosaurus* served as gripping tools: while the carinae provided a posterolingual cutting edge, the en echelon placement of the anterior teeth prevented the meat from sliding forwards. Additionally, this placement causes the anterior area of the jaws to make wide cuts on the prey. The angles between carinae on lateral teeth are higher and more conservative in order to provide the slicing function to these teeth.

In addition to that, incrassate (labiolingually thickened) teeth are characteristic of advanced tyrannosaurids (Farlow et al. 1991; Holtz 2004). This feature provides the ability of individual teeth and their tooth rows to make wide cuts, as well as strengthening to resist lateral bending during feeding (Farlow et al. 1991; Abler 1992; Holtz 2002; Snively et al. 2006; Snively and Russell 2007*a*, 2007*b*; Reichel 2010). The FABL/BW proportions measured in the taxa analyzed here reveal how lateral teeth can be labiolingually wide, especially in adult specimens. These proportions influence the angles between carinae to a point. Until the point where that proportion reaches a value of about one, ANG values are generally smaller than 120 degrees. When the FABL/BW proportion is

higher than one, the range of ANG values significantly increases (Fig. IV.14), and the tooth position also plays a major role in determining ANG.

Another interesting revelation of the ordinance plot (Fig. IV.3) of the PCA is that the highest amount of variation in the FABL/BW ratio is associated with the *Tarbosaurus* data. Both juvenile (PIN 551-91) and adult specimens of this taxon were included in the analyses, suggesting that ontogeny in this taxon contributes to changes in tooth proportions to some degree. Tyrannosaurid juveniles are known to have zyphodonty (bladelike teeth) to a degree (Farlow et al. 1991; Holtz 2004). Buckley et al. (2010) demonstrated great morphometric separation between juvenile and adult teeth of *Albertosaurus sarcophagus*. This indicates that caution needs to be used when classifying theropod teeth by using multivariate analyses. However, in that same paper, analyses comparing adult and juvenile teeth of *Gorgosaurus libratus* showed that there was virtually no morphological separation between them (Buckley et al. 2010). This demonstrates that extra care has to be taken when handling datasets that may include juvenile specimens. The ontogenetic variations in tyrannosaurids are not yet fully understood, because of the rarity of juveniles. A detailed analysis including what is probably a *Tyrannosaurus* juvenile specimen (BMRP 2002.4.1) would be of great value to further explain this variability in the dataset.

The ANG variable is distributed in patterns that are similar for each taxon (Fig. IV.4). Therefore, this variable shows limited potential for

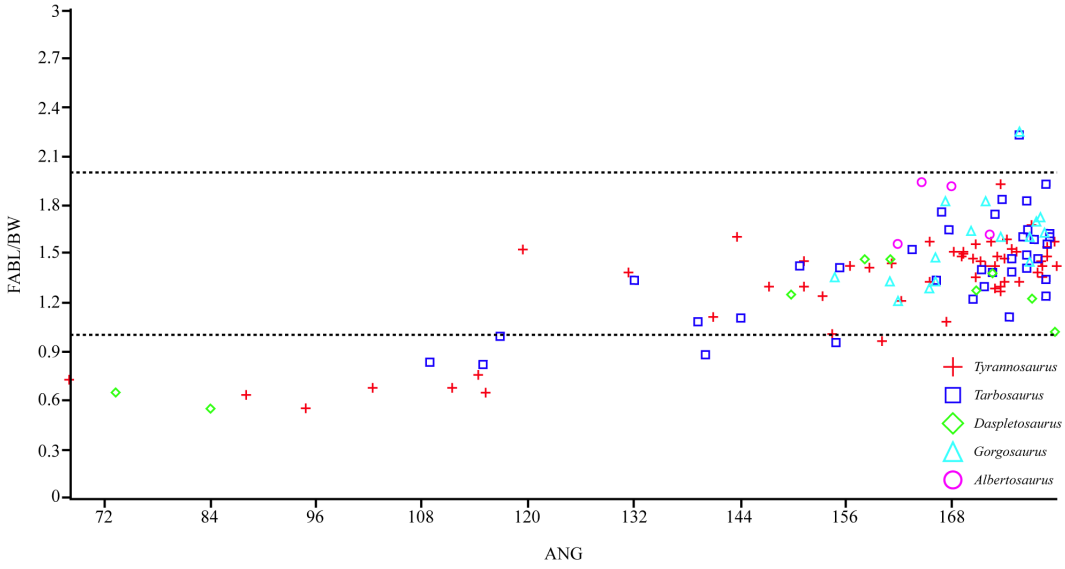

Fig. IV.14. Graph showing the variation of the FABL/BW proportion compared to the variation of angles between carinae. At a FABL/BW proportion of one or higher, the angles measured significantly increase.

taxonomic purposes at this stage, at least until more data can be collected from *in situ* teeth. However, there are well-defined patterns that are common to all tyrannosaurids that define how angles between carinae are distributed along the tooth rows. Therefore, this tool shows potential to help identifying tooth positions in isolated tyrannosaurid crowns.

DAs between most pairs of tyrannosaurid genera had less than 90% separation, which is not large enough to consider them as distinct morphotypes (Hammer and Harper 2006). This demonstrates that most tyrannosaurid teeth are similar and are not ideal for identifying taxa. However, this apparent uniformity may reflect the lack of *in situ* data. For example, although there are numerous isolated tooth crowns available for *Albertosaurus* (Buckley et al. 2010), there are dramatically fewer teeth still within jaws. This becomes obvious in the analyses done here, in which the only DAs that were not statistically significant at $p < 0.05$ included *Albertosaurus* data.

One interesting point is that the DA's done between *Tyrannosaurus* versus *Tarbosaurus* as well as *Daspletosaurus* scored the lowest percentage of separation between groups. This reveals that there is a stronger correlation between the tooth datasets of *Tyrannosaurus* and these two groups than with the remaining groups, which is in accordance with the phylogenetic proximity suggested for these three groups (Currie et al. 2003; Carr et al. 2005; Brusatte et al. 2010). It could, however, also be

a result of size-related scaling effects, because these taxa grow to large sizes when compared to other tyrannosaurids.

The CVAs done with all data combined (Fig. IV.5) also illustrate that point to an extent. It is clear that *Tarbosaurus* and *Tyrannosaurus* share many nodes, followed by *Daspletosaurus*. *Gorgosaurus* also shares a significant number of nodes with *Tarbosaurus* and *Daspletosaurus*, but only one node with *Tyrannosaurus*. It is important to note, however, that only dentary data were included for *Gorgosaurus* and that some of the nodes for this taxon occur in areas further away from the *Tarbosaurus*/*Tyrannosaurus* cluster than any other taxon. With the scarcity of data from *Albertosaurus*, it is premature to draw any conclusions from this analysis.

The results for the CVA of *Tyrannosaurus* teeth show good separation between most tooth families. These results are consistent with the way that carinal angles are distributed along the tooth row in this taxon (Fig. IV.4), in which each predetermined tooth family shows a characteristic range for measured angles between the anterior and posterior carinae.

The CVA for *Tarbosaurus* indicates further separation of different tooth families into clusters. The carinal angles observed in this taxon (Fig. IV.4) also show well-defined ranges for measured angles between carinae in each tooth family.

For *Daspletosaurus* and *Gorgosaurus* the CVA revealed a few discrete groupings; however, the amount of *in situ* data for these taxa was significantly less than for *Tyrannosaurus* and *Tarbosaurus*. The CVA groupings are reflected somewhat in the angles that occur between carinae in different tooth families (Fig. IV.4).

Based on the results of the CVAs for each taxon, it seems that *Tyrannosaurus* reveals the best segregation between tooth families, because each one of the tooth families in this taxon has a statistically significant amount of difference when compared to any of the other tooth families. Therefore, *Tyrannosaurus* has the highest degree of heterodonty when compared to the other tyrannosaurids analyzed here. D'Amore (2009) suggests that tooth position in relation to the jaw hinge is the only factor influencing variability in denticulation and apex orientation, and that the only function of those teeth is puncture cutting. If this is true, the apparent heterodonty in theropods is not significant, because of the lack of specialized functions for the different teeth. Farlow et al. (1991) also suggests that theropod teeth were multipurpose generalized instruments. However, several studies have demonstrated or quantified theropod heterodonty (Molnar 1998; Smith 2005; Reichel 2010), by suggesting that teeth in each region of the jaw were specialized for certain aspects of hunting, killing, and defleshing. The differential distribution of ANG along the tooth rows in tyrannosaurids suggests that different teeth had different functions, as also observable by bite mark evidences on dinosaur bones

(Jacobsen 1995; Erickson and Olson 1996). The findings about ANG distribution also reinforce the fact that heterodonty is present in these taxa, and helps quantifying the degree of heterodonty observed in them.

Conclusions

There are still blanks to fill in tyrannosaurid tooth data, especially when it comes to ontogenetic studies. The increasing amount of morphometric analyses in the last few years has greatly contributed to better understanding how tyrannosaurids develop as they grow, but this area of study is still at its infancy. Future studies of this nature would benefit greatly if they included specimens such as BMRP 2002.4.1, which is believed to be a juvenile *Tyrannosaurus*. The analyses done here helped better understanding a few aspects of tyrannosaurid tooth morphometrics, by testing the hypotheses proposed in the Introduction. Future analyses using the methods described in this analysis could also include CT scans of teeth, and the slice corresponding to the base of the anterior carina would be informative to obtain the data for calculation of the centroid and the angles between anterior and posterior carinae. The sample size represents important taxonomic groups and can be increased in future analyses. The preliminary results show the potential of this method for morphometric analyses of tooth function.

The first hypothesis, that the angles between carinae contribute significantly to the variation in the dataset, has been demonstrated by the

PCA, which revealed a high percentage of the variation in the dataset to be attributed to the ANG variable. This also becomes clear in Figure IV.4, which shows different ranges of angles between carinae in different tooth families.

The hypothesis that angles between carinae vary significantly between taxa is rejected at this point. Additional *in situ* data from taxa such as *Gorgosaurus* and *Albertosaurus* would greatly contribute to draw more conclusions about the potential of angles between carinae as a tool to aid in taxonomical studies.

The hypothesis that the variation of angles between carinae is a reflection of tooth function has been demonstrated by this study. The variation in ANG is strongly influenced by tooth proportions and tooth positions, and the angles observed in each tooth family are consistent with their functions. Therefore, this technique shows great potential to quantify heterodonty, and help better understand how tyrannosaurid tooth morphology varies.

References

Abler, W. L. 1992. The serrated teeth of tyrannosaurid dinosaurs, and biting structures in other animals. Paleobiology, **18**(2): 161–183.

Baszio, S. 1997. Investigations of Canadian dinosaurs: systematic palaeontology of isolated dinosaur teeth from the Latest Cretaceous of south Alberta, Canada. Courier Forschungsinstitut Senckenberg, **196**: 33–77.

Beatty, B.L., and Heckert, A.B. 2009. A large archosauriform tooth with multiple supernumerary carinae from the Upper Triassic of New Mexico (USA), with comments on carina development and anomalies in the Archosauria. Historical Biology, **21**(1): 57–65.

Brinkman, D.B. 1990. Paleoecology of the Judith River Formation (Campanian) of Dinosaur Provincial Park, Alberta, Canada: evidence from vertebrate microfossil localities. Palaeogeography, Palaeoclimatology, Palaeoecology, **78**(1–2): 37–54.

Brinkman, D.B. 2008. The structure of Late Cretaceous (late Campanian) nonmarine aquatic communities: a guild analysis of two vertebrate microfossil localities in Dinosaur Provincial Park, Alberta, Canada. *In* Vertebrate microfossil assemblages: their role in paleoecology and paleobiogeography. *Edited by* J.T. Sankey and S. Baszio. Indiana University Press, Bloomington, Ind., pp. 33–60.

Brusatte, S.L., Norell, M.A., Carr, T.D., Erickson, G.M., Hutchinson, J.R., Balanoff, A.M.; Bever, G.S., Choiniere, J.N., Makovicky, P.J., and Xu, X. (2010). Tyrannosaur paleobiology: new research on ancient exemplar organisms. Science, **329**(5998): 1481–1485.

Buckley, L.G. 2009*a*. Individual and ontogenetic variation in theropod dinosaur teeth: a case study of *Coelophysis bauri* (Theropoda: Coelophysoidea) and implications for identifying isolated theropod teeth. M.Sc. thesis, Department of Biological Sciences, University of Alberta, Edmonton, Alta.

Buckley, L.G. 2009*b*. Individual and ontogenetic variation in the dentition of *Coelophysis bauri*: implications for identifying isolated theropod teeth. Journal of Vertebrate Paleontology, **29**(3): 39A.

Buckley, L.G., Larson, D.W., Reichel, M., and Samman, T. 2010. Tooth and consequences: quantifying variation of teeth within a single population of *Albertosaurus sarcophagus* (Theropoda: Tyrannosauridae) from the Horseshoe Canyon Formation (Upper Cretaceous: Lower Maastrichtian) and implications for identifying isolated tyrannosaurid teeth in Maastrichtian-aged deposits. Canadian Journal of Earth Sciences, **45**: 1227–1251.

Carr, T.D., Williamson, T.E., and Schwimmer, D.R. 2005. A new genus and species of tyrannosauroid from the Late Cretaceous (middle

Campanian) Demopolis Formation of Alabama. Journal of Vertebrate Paleontology, **25**(1): 119–143.

Currie, P.J., Rigby, J.K. Jr., and Sloan, R.E. 1990. Theropod teeth from the Judith River Formation of Southern Alberta, Canada. *In*: Dinosaur Systematics: Approaches and Perspectives. *Edited by* Carpenter, K. and P. J. Currie (eds.). Cambridge University Press. pp. 107–125.

Currie, P.J., Hurum, J.H., and Sabath, K. 2003. Skull structure and evolution in tyrannosauris phylogeny. Acta Palaeontologica Polonica, **48**(2): 227 – 234.

D'Amore, D.C. 2009. A functional explanation for denticulation in theropod teeth. The Anatomical Record, **292**: 1297–1314.

Erickson, G.M. 1995. Split carinae on tyrannosaurid teeth and implications of their development. Journal of Vertebrate Paleontology, **15**(2): 268–274.

Erickson, G.M., and Olson, K.H. 1996. Bite marks attributable to *Tyrannosaurus rex*: preliminary description and implications. Journal of Vertebrate Paleontology, **16**: 175–178.

Farlow, J.O., Brinkman, D.L., Abler, W.L., and Currie, P.J. 1991. Size, shape and serration density of theropod dinosaur lateral teeth. Modern Geology **16**: 161–198.

Fiorillo, A.R., and Currie, P.J. 1994. Theropod teeth from the Judith River Formation (Upper Cretaceous) of south-central Montana. Journal of Vertebrate Paleontology, **14**: 74–80.

Fiorillo, A.R., and Gangloff, R.A. 2000. Theropod teeth from the Prince Creek Formation (Upper Cretaceous) of Northern Alaska, with speculations on Arctic dinosaur paleoecology. Journal of Vertebrate Paleontology, **20**(4): 675–682.

Hammer, O., and Harper, D.A.T. 2006. Palaeontological data analysis. Blackwell Publishing, Ltd., Malden, Mass.

Hammer, O., Harper, D.A.T., and Ryan, P.D. 2001. PAST: Paleontological Statistics software package for education and data analysis. Paleontologica Electronica, **4**(1): 1–9. Available from http://palaeo-electronica.org/2001_1/past/issue1_01.htm (last accessed 10 Aug. 2011).

Holtz, T.R., Jr. 2002. Theropod predation: evidence and ecomorphology. *In*: Predator-prey interaction in the fossil record. Topics in geobiology 17. *Edited by* Kelly, P.O.H., M. Kowelesky, and T.A. Hansen (eds). New York: Kluwer. pp 325–340.

Holtz, T.R., Jr. 2004. Tyrannosauroidea. *In* The Dinosauria. *Edited by* D.B. Weishampel, P. Dodson, and H. Osmolska. University of California Press, USA. pp. 111–136.

Jacobsen, A.R. 1995. Predatory behavior of carnivorous dinosaurs: ecological interpretation based on tooth marked dinosaur bones and wear patterns of theropod teeth. M.Sc. Thesis, University of Copenhagen, Copenhagen, Denmark.

Larson, D.W. 2008. Diversity and variation of theropod dinosaur teeth from the uppermost Santonian Milk River Formation (Upper Cretaceous), Alberta; a quantitative method supporting identification of the oldest dinosaur tooth assemblage in Canada. Canadian Journal of Earth Sciences, **45**(12): 1455–1468.

Larson, D.W. 2009. Multivariate analyses of small theropod teeth and implications for palaeoecological turnovers through time. Journal of Vertebrate Paleontology, **29**: 132A.

Molnar, R.E. 1998. Mechanical factors in the design of the skull of *Tyrannosaurus rex* (Osborn, 1905). *In* GAIA 15: Aspects of theropod paleobiology. *Edited by* B.P. Pérez-Moreno, T. Holtz, J.L. Sanz, and J.J. Mortalla. Museu Nacional de História Natural, Lisbon, Portugal. pp. 193–218.

Reichel, M. 2010. The heterodonty of *Albertosaurus sarcophagus* and *Tyrannosaurus rex*: biomechanical implications inferred through 3-D models. Canadian Journal of Earth Sciences, **47**: 1253–1261.

Samman, T. Powell, G.L., Currie, P.J., and Hills, L.V. 2005. Morphometry of the teeth of western North American tyrannosaurids and its applicability to quantitative classification. Acta Palaeontologica Polonica, **50**(4): 757–776.

Sankey, J.T. 2001. Late Campanian southern dinosaurs, Aguja Formation, Big Bend, Texas. Journal of Paleontology, **75**(1): 208–215.

Sankey, J.T. 2008*a*. Vertebrate paleoecology from microsites, Talley Mountain, Upper Aguja Formation, (Late Cretaceous), Big Bend National Park, Texas, USA. *In* Vertebrate microfossil assemblages: their role in paleoecology and paleobiogeography. *Edited by* J.T. Sankey and S. Baszio. Indiana University Press, Bloomington, Ind., pp. 61–77.

Sankey, J.T. 2008*b*. Diversity of Latest Cretaceous (late Maastrichtian) small theropods and birds: teeth from the Lance and Hell Creek formations, USA. *In* Vertebrate microfossil assemblages: their role in paleoecology and paleobiogeography. *Edited by* J.T. Sankey and S. Baszio. Indiana University Press, Bloomington, Ind., pp. 117–137.

Sankey, J.T., Brinkman, D.B., Guenthier, M., and Currie, P.J. 2002. Small theropod and bird teeth from the Late Cretaceous (Late Campanian) Judith River Group, Alberta. Journal of Paleontology, **76**(4): 751–763.

Smith, J.B., and Dodson, P. 2003. A proposal for a standard terminology of anatomical notation and orientation in fossil vertebrate dentitions. Journal of Vertebrate Paleontology, **23**(1): 1–12.

Smith, J.B. 2005. Heterodonty in *Tyrannosaurus rex*: implications for the taxonomic and systematic utility of theropod dentitions. Journal of Vertebrate Paleontology, **25**: 865–887.

Smith, J.B. 2007. Dental morphology and variation in *Majungasaurus crenatissimus* (Theropoda: Abelisauridae) from the Late Cretaceous of Madagascar. Journal of Vertebrate Paleontology Memoir, **8**(sp8): 103–126.

Smith, J.B., and Dodson, P. 2003. A proposal for a standard terminology of anatomical notation and orientation in fossil vertebrate dentitions. Journal of Vertebrate Paleontology, **23**(1): 1–12.

Snively, E. Henderson, D.M., and Philips, D.S. 2006. Fused and vaulted nasals of tyrannosaurid dinosaurs: implications for cranial strength and feeding mechanics. Acta Palaeontologica Polonica, **51**(3): 435–454.

Snively, E., and Russell, A. P. 2007*a*. Craniocervical feeding dynamics of *Tyrannosaurus rex*. Paleobiology, **33**: 610–638.

Snively, E., and Russell, A. P. 2007*b*. Functional morphology of the neck musculature in the Tyrannosauridae (Dinosauria, Theropoda) as

determined via a hierarchical inferential approach. Zoological Journal of the Linnean Society, **151**(4): 759–808.

Sweetman, S.C. 2004. The first record of velociraptorine dinosaurs (Saurischia, Theropoda) from the Wealden (Early Cretaceous, Barremian) of southern England. Cretaceous Research, **25**: 353–364.

Appendix 1: Tyrannosaurid tooth measurements

Taxon	Specimen	Tooth Position	FABL	BW	ACH	FABL/BW	ANG
Albertosaurus	TMP 1983.036.0100	LM7	19.6	12.6	?	1.56	162
Albertosaurus	TMP 1983.036.0100	LM8	21.9	11.4	44.3	1.93	164.8
Albertosaurus	TMP 1983.036.0100	LM10	17.3	9.1	32.8	1.91	168.1
Albertosaurus	TMP 1983.036.0100	LM11	14.6	9	27.6	1.62	172.4
Daspletosaurus	TMP 1997.012.0223	RM5	33.3	?	79.2	?	178.4
Daspletosaurus	TMP 1997.012.0223	RM8	29.4	?	59.4	?	173.9
Daspletosaurus	TMP 1997.012.0223	RM11	23.1	?	46.6	?	176.2
Daspletosaurus	TMP 2001.036.0001	RPM2	17	9.3	22.3	1.84	84.1
Daspletosaurus	TMP 2001.036.0001	RPM3	15.4	9.8	24.1	1.57	73.4
Daspletosaurus	TMP 2001.036.0001	RM2	19.9	?	41.5	?	?
Daspletosaurus	TMP 2001.036.0001	RM4	24.8	?	66.5	?	158.2
Daspletosaurus	TMP 2001.036.0001	RM5	30.5	?	85.4	?	170.8

Daspletosaurus	TMP 2001.036.0001	RM7	28	?	65.8	?	168.8
Daspletosaurus	TMP 2001.036.0001	RM8	29.5	?	66	?	172.3
Daspletosaurus	TMP 2001.036.0001	RM9	26.85	?	58.7	?	162.2
Daspletosaurus	TMP 2001.036.0001	RM10	24	?	47.8	?	171.9
Daspletosaurus	TMP 2001.036.0001	RM12	23.1	?	48.3	?	168.7
Daspletosaurus	TMP 2001.036.0001	LM1	19.9	?	41.6	?	159.9
Daspletosaurus	TMP 2001.036.0001	LM2	20.8	?	48	?	176
Daspletosaurus	TMP 2001.036.0001	LM3	24.4	23.8	70.4	1.02	179.8
Daspletosaurus	TMP 2001.036.0001	LM5	29.8	23.5	74.3	1.27	170.9
Daspletosaurus	TMP 2001.036.0001	LM7	25.8	20.8	?	1.24	149.8
Daspletosaurus	TMP 2001.036.0001	LM9	25.1	18.3	51.6	1.37	172.6
Daspletosaurus	TMP 2001.036.0001	LM13	15.4	10.5	24.6	1.47	161.1
Daspletosaurus	TMP 2001.036.0001	RD6	24	19.5	53.9	1.23	177.1
Daspletosaurus	TMP 2001.036.0001	RD15	16.9	11.6	27.9	1.46	158.2
Gorgosaurus	TMP 1967.009.0164	LD7	23.2	16.2	?	1.44	176.8
Gorgosaurus	TMP 1999.055.0170	LD4	18	15	39.3	1.20	162

Gorgosaurus	TMP 1999.055.0170	LD5	19.5	12.2	40.5	1.60	176.9
Gorgosaurus	TMP 1999.055.0170	LD9	17.8	10.9	33.2	1.63	170.3
Gorgosaurus	TMP 1999.055.0170	LD11	16.8	9.9	30.3	1.69	177.8
Gorgosaurus	TMP 1999.055.0170	LD12	16.8	9.2	27.7	1.82	171.9
Gorgosaurus	TMP 1999.055.0170	LD13	16.3	7.3	25.5	2.24	175.7
Gorgosaurus	TMP 1999.055.0170	LD14	14	8.8	22	1.59	173.7
Gorgosaurus	TMP 1999.055.0170	LD15	12.9	7.1	18.2	1.82	167.4
Gorgosaurus	TMP 1986.205.0001	LD3	24.5	18.6	56.5	1.32	166.3
Gorgosaurus	TMP 1983.036.0134	RD8	21.2	16.6	37.7	1.28	165.5
Gorgosaurus	TMP 1983.036.0134	RD10	21.1	15.7	34.1	1.35	154.9
Gorgosaurus	TMP 1983.036.0134	RD11	19.3	14.6	33.2	1.32	161.1
Gorgosaurus	TMP 1986.144.0001	RD4	12.6	8.6	24.3	1.47	166.2
Gorgosaurus	TMP 1986.144.0001	RD5	13.4	8.3	24.8	1.61	178.6
Gorgosaurus	TMP 1986.144.0001	RD10	12.7	7.4	22.7	1.71	178.1
Gorgosaurus	TMP 1994.012.0155	RD5	9.2	4.7	?	1.95	?
Gorgosaurus	TMP 1994.012.0155	RD9	8.7	4.2	13.5	2.06	?

Gorgosaurus	TMP 1994.012.0155	LD6	9	4.7	16.2	1.93	?
Gorgosaurus	TMP 1994.012.0155	LD10	9.4	4	15.5	2.33	?
Gorgosaurus	TMP 1994.012.0155	LD13	8.6	3.8	13	2.22	?
Tarbosaurus	UALVP 47949	LPM1	19.6	24.1	51.9	0.81	115.1
Tarbosaurus	UALVP 47949	LPM2	20.9	21.4	44.6	0.98	117
Tarbosaurus	UALVP 47949	LPM3	16.4	19.8	41.7	0.83	109.1
Tarbosaurus	UALVP 47949	LM1	35.4	26.5	?	1.33	132.3
Tarbosaurus	UALVP 47949	LM2	29	26.4	56.5	1.10	144.2
Tarbosaurus	UALVP 47949	LM3	36.3	25.7	70	1.41	155.6
Tarbosaurus	UALVP 47949	LM4	37.6	27.3	81.1	1.38	172.8
Tarbosaurus	UALVP 47949	LM6	37.3	23.9	68.6	1.56	179
Tarbosaurus	UALVP 47949	LM8	29.7	18	54.5	1.65	167.8
Tarbosaurus	UALVP 47949	LM10	34.2	18.6	79.3	1.83	173.9
Tarbosaurus	UALVP 47949	LM11	26.6	14.6	41.8	1.82	176.6
Tarbosaurus	UALVP 47949	LD5	33.4	22.8	59.6	1.46	175
Tarbosaurus	UALVP 47949	LD6	32.6	22.4	60.4	1.46	178

Tarbosaurus	UALVP 47949	LD8	29.2	21.3	?	1.37	?
Tarbosaurus	UALVP 47949	LD9	24	15.4	?	1.56	?
Tarbosaurus	UALVP 47949	LD13	22.7	12.7	29.1	1.79	?
Tarbosaurus	PIN 551-1	RM1	35.8	26.9	?	1.33	166.4
Tarbosaurus	PIN 551-1	RM3	35.2	26.2	64	1.34	178.7
Tarbosaurus	PIN 551-1	RM4	36	26.1	65.5	1.38	172.7
Tarbosaurus	PIN 551-1	RM5	37.6	23.4	60.8	1.60	179.1
Tarbosaurus	PIN 551-1	RM6	35.6	24.1	53	1.48	176.6
Tarbosaurus	PIN 551-1	RM7	32.2	20.3	47	1.59	177.4
Tarbosaurus	PIN 551-1	RM9	29.6	18	44.8	1.65	176.7
Tarbosaurus	PIN 551-1	RM10	22.6	14.1	34.2	1.60	176.3
Tarbosaurus	PIN 551-1	RD2	22.8	25.9	46.5	0.88	140.3
Tarbosaurus	PIN 551-1	RD7	28.2	21.7	41.7	1.30	171.9
Tarbosaurus	PIN 551-1	RD8	30.2	21.6	43.6	1.40	171.7
Tarbosaurus	PIN 551-1	RD9	29.1	20.6	44	1.41	176.8
Tarbosaurus	PIN 551-1	RD11	21.7	19.5	39.5	1.11	174.7

Tarbosaurus	PIN 551-1	RD12	22.8	13.1	29.4	1.74	172.94
Tarbosaurus	PIN 551-1	RD13	18	13	23	1.38	175.1
Tarbosaurus	PIN 551-1	RD14	13.8	8.5	14.1	1.62	179.2
Tarbosaurus	PIN 551-1	RD15	10.1	8.3	11	1.22	170.7
Tarbosaurus	PIN 551-1	LD1	17.7	16.5	?	1.07	139.4
Tarbosaurus	PIN 551-1	LD3	31	32.6	?	0.95	154.9
Tarbosaurus	PIN 551-1	LD4	30.2	24.6	?	1.23	178.9
Tarbosaurus	PIN 551-3	RM1	31.2	25.1	64.2	1.24	?
Tarbosaurus	PIN 551-3	RM3	38.6	26.5	92.3	1.46	?
Tarbosaurus	PIN 551-3	RM4	38.5	26.1	?	1.47	?
Tarbosaurus	PIN 551-3	RM5	35.8	24.3	67.8	1.47	?
Tarbosaurus	PIN 551-3	RM7	31.7	19.2	53	1.65	?
Tarbosaurus	PIN 551-3	RM8	29.1	16.3	45.2	1.79	?
Tarbosaurus	PIN 551-3	RM9	29.9	18	55.2	1.66	?
Tarbosaurus	PIN 551-91	RM2	15.7	?	35.1	?	?
Tarbosaurus	PIN 551-91	RM3	16.9	11.1	?	1.52	163.7

Tarbosaurus	PIN 551-91	RM6	17.4	8.2	30.5	2.12	?
Tarbosaurus	PIN 551-91	RM7	15.5	8	?	1.92	178.9
Tarbosaurus	PIN 551-2	RM2	18.1	12.7	?	1.43	151.1
Tarbosaurus	PIN 551-2	RM4	22.2	12.7	49.5	1.75	167
Tarbosaurus	PIN 551-2	RM6	21.5	9.7	?	2.23	175.8
Tyrannosaurus	UALVP 48586.21	RPM1	14.6	26.4	36.6	0.55	94.8
Tyrannosaurus	UALVP 48586.24	RPM2	18.4	28.4	38.1	0.65	115.3
Tyrannosaurus	UALVP 48586.15	RPM4	19.8	29.7	46.1	0.67	102.5
Tyrannosaurus	UALVP 48586.13	LPM1	16.2	25.7	37.4	0.63	88.1
Tyrannosaurus	UALVP 48586.19	LPM3	20.9	31.2	48.3	0.67	111.5
Tyrannosaurus	UALVP 48586.31	RM1	46.6	37.8	88.7	1.23	153.4
Tyrannosaurus	UALVP 48586.9	RM7	28.1	19.8	43.9	1.42	178.3
Tyrannosaurus	UALVP 48586.8	RM8	27.3	14.3	41.3	1.92	173.6
Tyrannosaurus	UALVP 48586.23	RM9	27.4	18.1	38.9	1.51	175.5
Tyrannosaurus	UALVP 48586.20	LM4	38.2	27.8	75.4	1.37	177.8
Tyrannosaurus	UALVP 48586.5	LM5	39.1	27.6	67.2	1.42	179.9

Tyrannosaurus	UALVP 48586.7	LM6	33.1	22.7	51.2	1.46	174.1
Tyrannosaurus	UALVP 48586.4	LM8	31.5	20.8	44.4	1.52	174.7
Tyrannosaurus	UALVP 48586.11	LM9	25	17.2	36.5	1.45	171.3
Tyrannosaurus	UALVP 48586.17	LM11	19.1	13.4	28.2	1.42	171.9
Tyrannosaurus	UALVP 48586.29	RD1	25.7	18.6	40.7	1.38	131.4
Tyrannosaurus	UALVP 48586.6	RD4	38.1	30	70.9	1.27	173.7
Tyrannosaurus	UALVP 48586.1	RD5	35.6	27.6	62.5	1.29	173.7
Tyrannosaurus	UALVP 48586.2	RD6	33.3	25.3	60.1	1.32	175.7
Tyrannosaurus	UALVP 48586.3	RD8	30.8	23.1	49.3	1.33	173.9
Tyrannosaurus	UALVP 48586.28	RD9	28.4	20	39.5	1.42	172.9
Tyrannosaurus	UALVP 48586.18	RD10	29.3	19.4	42.9	1.51	168.3
Tyrannosaurus	UALVP 48586.22	RD11	24.2	16.8	31.2	1.44	161.2
Tyrannosaurus	UALVP 48586.25	RD12	16.8	11.4	19.2	1.48	169.3
Tyrannosaurus	UALVP 48586.16	LD1	27.5	17.2	44	1.60	143.8
Tyrannosaurus	UALVP 48586.12	LD2	35.1	29.3	60.4	1.20	162.2
Tyrannosaurus	UALVP 48586.14	LD7	29.9	20.9	47	1.44	178.2

Tyrannosaurus	UALVP 48586.26	LD10	27	19.2	37.7	1.40	158.8
Tyrannosaurus	UALVP 48586.30	LD13	14.1	9.4	15.2	1.50	169.4
Tyrannosaurus	TMP 1981.006.0001	LPM4	17.5	24.3	34.4	0.72	68.1
Tyrannosaurus	TMP 1981.006.0001	RM2	36.3	28.1	71.2	1.29	151.3
Tyrannosaurus	TMP 1981.006.0001	RM3	44	29.5	77	1.49	169.6
Tyrannosaurus	TMP 1981.006.0001	RM5	38.6	26.2	70.1	1.47	170.4
Tyrannosaurus	TMP 1981.006.0001	RM6	35.9	24.2	54.6	1.48	178.8
Tyrannosaurus	TMP 1981.006.0001	RM7	33.8	21.6	54.2	1.57	179.8
Tyrannosaurus	TMP 1981.006.0001	RM8	33.6	21.4	53.6	1.57	172.5
Tyrannosaurus	TMP 1981.006.0001	RM10	28.6	18.1	38.5	1.58	174.4
Tyrannosaurus	TMP 1981.006.0001	LM1	35.6	27.4	61.2	1.30	147.5
Tyrannosaurus	TMP 1981.006.0001	LM3	40.6	27.3	77.6	1.48	173.2
Tyrannosaurus	TMP 1981.006.0001	LM4	36.4	23.7	64.4	1.54	178.8
Tyrannosaurus	TMP 1981.006.0001	LM7	30.8	18.4	46.3	1.67	177.1
Tyrannosaurus	TMP 1981.006.0001	RD1	15.3	20.4	27	0.75	114.4
Tyrannosaurus	TMP 1981.006.0001	RD2	23.9	21.5	41.2	1.11	141.1

Tyrannosaurus	TMP 1981.006.0001	RD3	31.3	29.2	56	1.07	167.5
Tyrannosaurus	TMP 1981.006.0001	RD6	30.7	21.2	47.5	1.45	151.2
Tyrannosaurus	TMP 1981.006.0001	RD9	30.4	23.8	43.8	1.28	172.9
Tyrannosaurus	TMP 1981.006.0001	RD10	27.8	17.9	?	1.56	170.8
Tyrannosaurus	TMP 1981.006.0001	RD11	23.9	15.4	?	1.56	165.5
Tyrannosaurus	TMP 1981.006.0001	LD1	17.4	11.5	25.1	1.52	119.5
Tyrannosaurus	TMP 1981.006.0001	LD2	22.7	22.8	41.1	1.00	154.6
Tyrannosaurus	TMP 1981.006.0001	LD3	22.3	23.3	?	0.96	160.2
Tyrannosaurus	TMP 1981.006.0001	LD4	32.9	24.1	?	1.36	178.3
Tyrannosaurus	TMP 1981.006.0001	LD5	30.4	22.4	53.7	1.36	170.8
Tyrannosaurus	TMP 1981.006.0001	LD6	29	21.9	56.3	1.33	165.4
Tyrannosaurus	TMP 1981.006.0001	LD7	30.7	21.6	46	1.42	156.5

Chapter 5

Enamel microstructures in theropod dinosaurs and other reptiles: a functional approach

Introduction

Studies on mammal enamel microstructure are facilitated because their characteristic prismatic structures are easily visible under optical microscopes with polarized light. Unfortunately the same is not true for non-mammalian amniotes. One of the few exceptions is the lizard *Uromastyx*, which has been reported as having prismatic structures (Cooper and Poole 1973). Buffetaut et al. (1986) suggest a simple form of 'prisms' present in some theropod dinosaur taxa, however these 'prisms' are similar to the microstructures commonly found in reptile enamel, described by Sander (1999, 2000) and Hwang (2005). These findings suggest that prismatic enamel is not necessarily associated with a reduced rate of tooth replacement (as suggested by Grine et al. 1979), or complex masticatory systems and precise dental occlusion, and that the function of the prisms and other microstructures in enamel needs further research.

Scanning electron microscopy analyses done with a chondrichthyan, a teleost, a urodele amphibian, an anuran amphibian, two lepidosauria, and two mammals showed that all these taxa have distinct

basal laminae – or basal unit layers (Hwang 2005). This layer represents the first depositional activity of ameloblasts, and consists of fairly unorganized enamel crystals. Subsequent stages of enamel biomineralization showed highly organized enamel crystals in mammals, lepidosaurians, the anuran, and the chondrichthyan, while amorphous or randomly oriented crystals were found in the teleost and the urodele (Diekwisch et al. 2002).

Sander (1999) conducted an extensive study about reptile enamel microstructures, in which he covered a significant range of taxa. This study was followed by a study by Hwang (2005), in which a comprehensive range of dinosaur taxa was analyzed using Scanning Electron Microscopy (SEM). This technique proved itself effective to capture images of organized microstructures on non-mammalian amniote enamel. Hwang (2005) pointed out the significance of microstructure of tooth enamel to the taxonomy of major groups of dinosaurs. Both authors described in detail microstructures that strongly resemble the structures described as ‘prisms’ in theropods by Buffetaut et al. (1986).

The terminology created by Sander (1999) for describing reptile enamel microstructures is appropriate for this study; the hierarchical levels for reptilian enamel are: crystallite, module, enamel type, schmelzmuster, and dentition. The simplest level is that of the crystallite. Crystallites can be arranged in different ways relative to the enamel-dentine junction. Crystallites can be parallel, divergent, or convergent. Incremental lines

often occur with parallel crystallites, and are caused by changes in crystallite morphology (Hwang 2005). The next level – modules of enamel (Sander 1999) – describes the repeatable units formed by crystallites. The modules can be defined by crystallite discontinuities in parallel crystallites or the columnar units of diverging crystallites, for example. The enamel types are continuous volumes of enamel made up of the same modules or crystallites. The schmelzmuster is a combination of enamel types, which can be taxon-specific (Hwang 2005). Finally, the dentition level describes at which jaw position a certain type of schmelzmuster may be found for each tooth (Fig. I.1).

Some authors demonstrated that the three-dimensional arrangements of enamel types within a single tooth – the schmeltzmusters – can be diagnostic for exclusive monophyletic clades of reptiles as they are in mammals (Dauphin et al. 1998; Hwang 2005; Stokosa 2005). Others would argue that similarities between schmeltzmusters of distantly related taxa are indicative of the biomechanical properties of a given arrangement of enamel microstructures and are thus only useful for identifying general ecomorphotypes (Sander 1999, 2000). The influence of the different enamel microstructures on biomechanics has not been addressed with much detail yet. A study on modern crocodilians (Creech 2004) describes different enamel microstructures found in a range of 23 extant species. This study provided new data on material properties of crocodilian enamel.

In this project, biomechanical aspects of the enamel microstructure patterns in isolated tooth crowns of theropod dinosaurs are described. Additionally, two Late Cretaceous mosasaurid reptiles are represented, by a *Platecarpus* indeterminate Cope, 1869 (UALVP 53595) tooth, and a second tooth (UALVP 51744) that has characteristics similar to what has been described as *Platecarpus ptychodon* (Arambourg 1952). Finally, the varanid lizard *Varanus komodoensis* was also analyzed. The mosasaurids and *Varanus komodoensis* have their enamel microstructures described for the first time and are included for comparisons with theropod dinosaurs. Theropods, mosasaurids, and varanid lizards represent different ecomorphotypes, but have carinate teeth at least at one stage of their development (Fig.V.1).

Because changes in the enamel microstructure of adjacent teeth can occur in heterodont animals (Sander 2000; Hwang 2005), the conservative and homodont dentition of *Platecarpus* indeterminate (UALVP 53595) is ideal for inferring the arrangements of enamel types throughout their marginal dentition from a single tooth (Russell 1967; Konishi and Caldwell 2007). In the case of theropods, *Platecarpus ptychodon* (UALVP 51744) and *Varanus komodoensis*, this is not true, because heterodonty has been recognized in some taxa (Currie et al. 1990; Farlow et al. 1991; Smith 2005; Reichel 2010), and differences in enamel microstructures along the tooth row were described for some theropods, including *Troodon* (Hwang 2005).

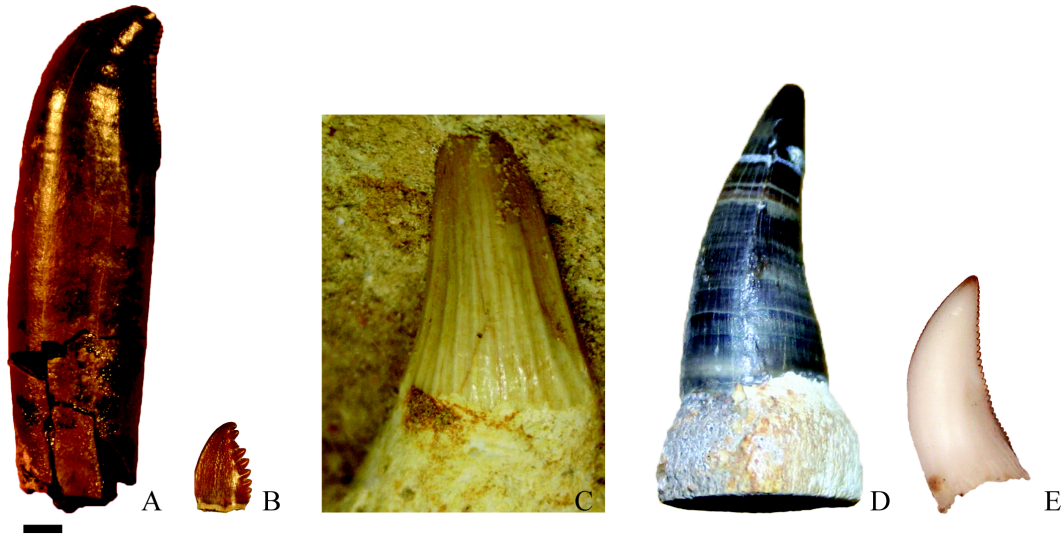

Fig. V.1. Photographs of teeth representing each of the taxa in this analysis. (A) a tyrannosaurid (*Albertosaurus sarcophagus* TMP 2004.56.19), (B) a troodontid (*Troodon* sp. AMNH 22669), (C) *Platecarpus ptychodon* (UALVP 51744), (D) *Platecarpus* indeterminate (UALVP 53595), and (D) *Varanus komodoensis* (UALVP 53481). Scale bar = 2 mm.

The hypothesis tested in this project is that enamel microstructures offer structural support for the tooth in response to different environmental pressures and thus are distinct in different ecomorphotypes, offering mechanical support for different types of stress inflicted to teeth.

Materials and Methods:

The theropod dinosaurs analyzed in this project include an unidentified isolated tyrannosaurid tooth (UALVP 53361), as well the small theropod *Troodon* (UALVP 53358). Two Late Cretaceous mosasaurid taxa were included for comparisons in this project. One isolated tooth from *Platecarpus* indeterminate (UALVP 53595) (previously longitudinally sectioned for petrographic slides) and one from *Platecarpus ptychodon* (UALVP 51744) were analyzed. Finally, *Varanus komodoensis* teeth donated by the Toronto Zoo (UALVP 53481) were also included in this analysis for further comparisons.

The specimens were embedded in epoxy resin (with the exception of *Platecarpus* indeterminate) and sectioned transversely and longitudinally in a microtome. After that, their exposed surfaces were polished with 220 – 600 grit sand paper. They were then etched with HCl 5% for 15 – 60 seconds. Finally, all samples were subject to an ultrasonic bath for at least 30 seconds, in order to remove lose debris from the

surfaces being analyzed. Most samples were coated with carbon (with the exception of *Platecarpus* indeterminate) prior to being analyzed in the scanning electron microscope (SEM). The analyses were done on a JEOL 6301F field emission SEM at the SEM Lab in the Earth and Atmospheric Sciences Department at the University of Alberta.

Three-dimensional models representing the parallel and diverging enamel crystallites (Fig. V.2) were made using the 3-D modeling software Rhino®. Two models representing diverging crystallites were created, so that the different angles found in the crystallites could be tested. One had crystallites diverging in an angle of 20º in relation to the central axis of the column, and the second model had crystallites diverging in an angle of 30º. The third model represents parallel crystallites. All models were scaled and analyzed with the FEA software Strand7®. The material properties of enamel were applied to them. The values for enamel material properties used in this study were based on research done on reptiles wherever possible. However the scarcity of such studies on reptiles made it so that some of the data had to be based on research done with mammalian enamel. The Young's Modulus, a measure of stiffness (Boresi and Schmidt 2003), was used in this analysis and the value of 6.04 e10 Pascals (Pa) is based on that of fresh crocodilian teeth (Creech 2004). The Poisson's ratio (the transverse versus axial strain) describes how a structure bulges under compression and thins under tension (Boresi and Schmidt 2003), and the value used in this analysis is 0.3, based on that of

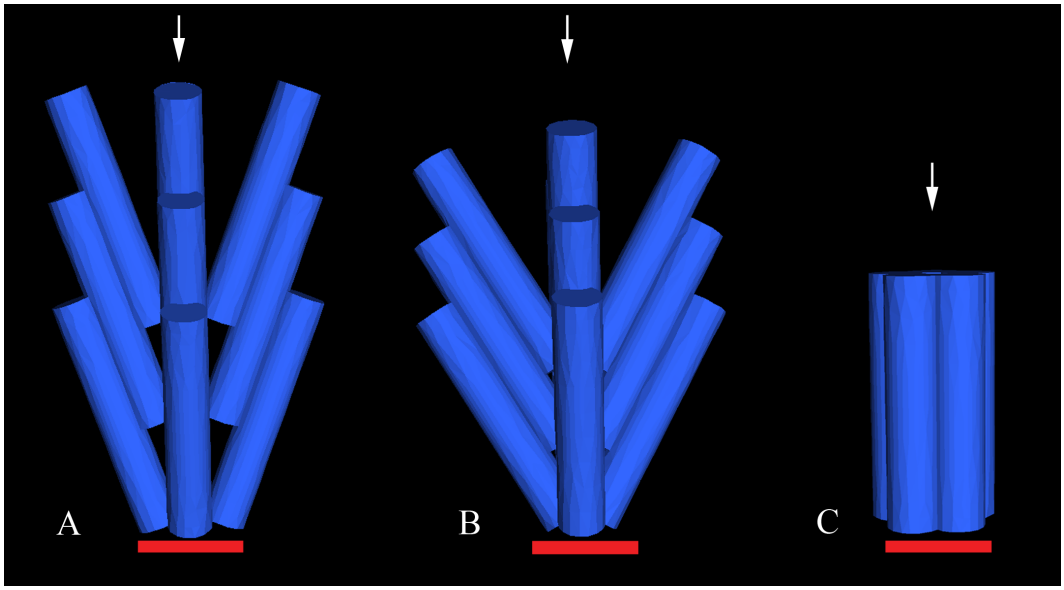

Fig. V.2. Three-dimensional models of enamel microstructures found in the taxa in this analysis. First scenario, with restraints (red lines) applied to the base of each model, and forces (white arrows) applied at a normal angle to the vertical axis of each model. (A) Model with crystallites diverging at a 20º angle in relation to the vertical axis of the model, (B) Model with crystallites diverging at a 30º angle in relation to the vertical axis of the model, (C) Model with parallel crystallites.

human teeth (Rees and Hammadeh 2004). The enamel density used in this analysis [2800 kilograms per cubic meter (kg/m^3)] is also based on that of human enamel (Manly et al. 1939).

The models were tested in two scenarios. In the first one, the models were constrained at their bases and a force was applied at an angle normal to the main axis of the model (Fig. V.2). In the second scenario, the models were restrained at their base and laterally, to simulate the presence of other columns beside the model tested (Fig. V.3). In this scenario, the force was applied at a 45° angle. That way, the arrangement of the 3-D objects representing enamel crystallites could be tested under different circumstances during chewing, because teeth receive forces from a variety of angles. The results were visualized using the von Mises yield criterion, which evaluates the proximity to yield within a structure, and consequently, the stress and strain energy density. The von Mises yield criterion is appropriate for tooth analyses, because dental tissues are ductile under moderate, gradually applied loads (Bell et al. 2009). In summary, the von Mises yield criterion indicates which parts of a structure are more likely to fail when forces are applied to it. The force applied to all models was 2000 N, which is the estimated bite force for teeth in mid-jaw position of *Albertosaurus sarcophagus* (Reichel 2010). The models in this analysis were not evaluated for their ability to sustain this specific force, but rather for how effective they are in absorbing any

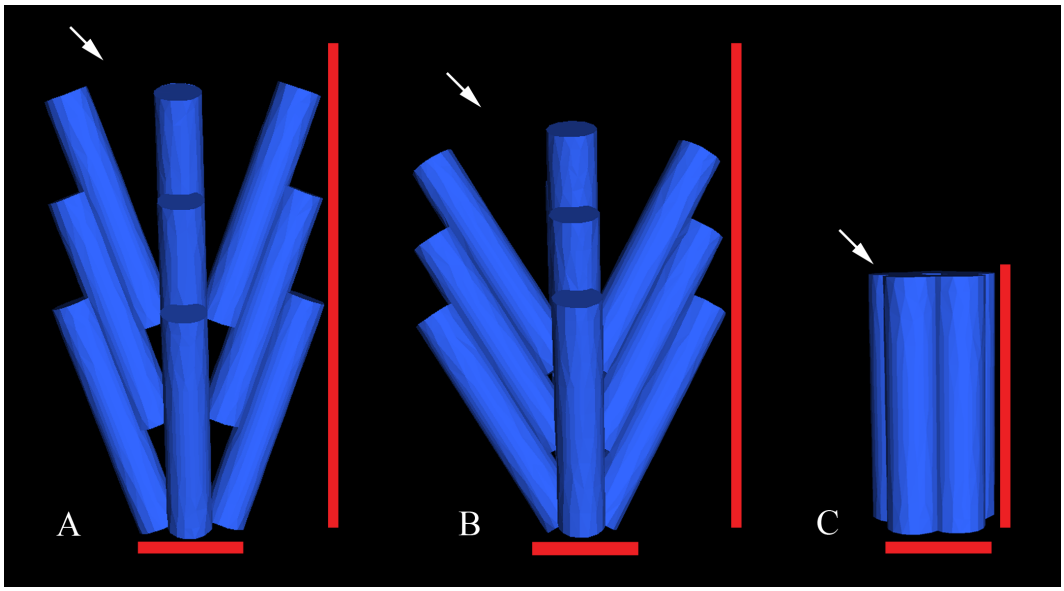

Fig. V.3. Three-dimensional models of enamel microstructures found in the taxa in this analysis. Second scenario, with restraints (red lines) applied to the base and lateral surface of each model, and forces (white arrows) applied at a 45º angle to the vertical axis of each model. (A) Model with crystallites diverging in a 20º angle in relation to the vertical axis of the model, (B) Model with crystallites diverging in a 30º angle in relation to the vertical axis of the model, (C) Model with parallel crystallites.

force at all, and how different stresses and strains are distributed within each structure.

Results:

The enamel thickness of the tyrannosaurid tooth (UALVP 53361) section (Fig. V.4) is approximately 90 μm. Two different layers of enamel microstructures were observed: diverging crystallites organized in columns and parallel crystallites (near the outer surface of the enamel) with faint incremental lines. Similar results were observed by Hwang (2005). The width of each column of diverging enamel crystallites ranges from 12 to 16 μm. The width of these columns increases towards the outer enamel surface. The angle measured between the central axis of each column and the insertion of crystallites ranges from 15 to 25 degrees.

In the *Troodon* tooth (UALVP 53358) section (Fig. V.5), the enamel thickness is about 15 μm. The crystallites are arranged in a parallel pattern. The brittle nature of the enamel layer in this specimen caused it to flake off at different levels, which is fortunate in this analysis, because it revealed that the parallel crystallites were deposited in slightly different angles at each level. No incremental lines were observed.

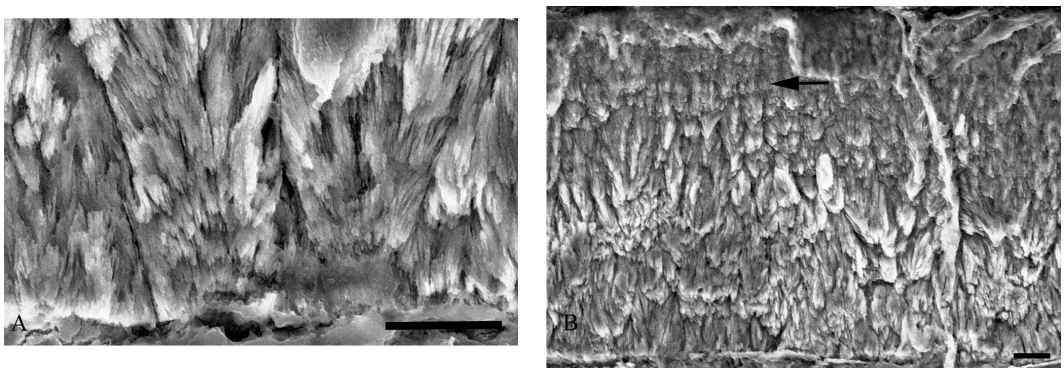

Fig. V.4. SEM photomicrograph of the enamel layer of a tyrannosaurid. (A) Columnar enamel with diverging crystallites. (B) Diverging crystallites (bottom), and parallel crystallites with faint incremental lines (arrow). Enamel-dentine junction is at the bottom of each picture. Scale = 10 μm.

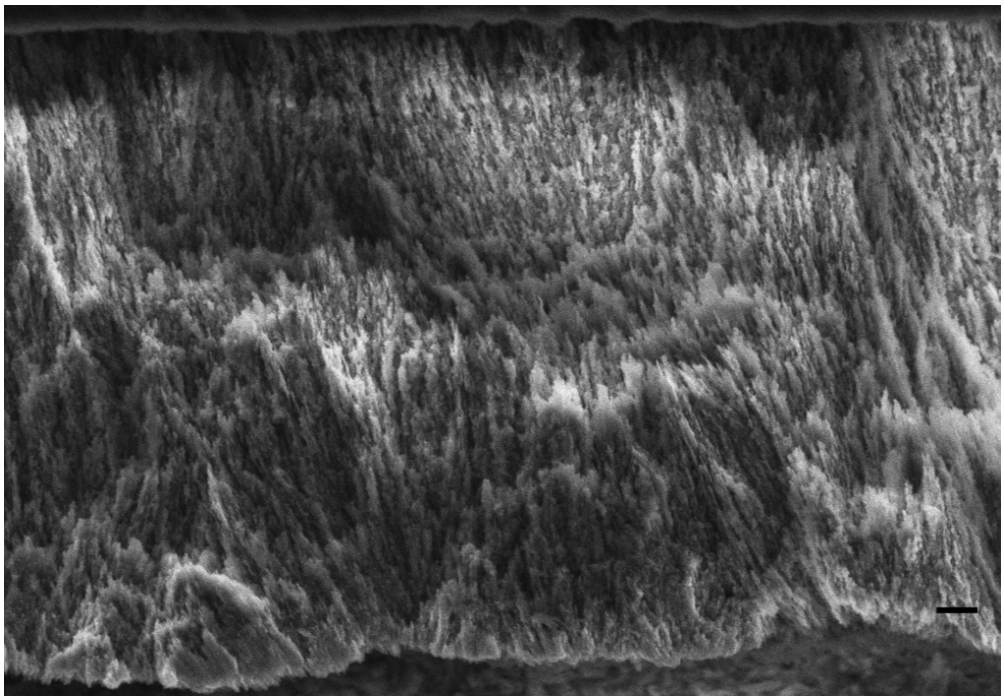

Fig. V.5. SEM photomicrograph of the enamel layer of a troodontid, with parallel crystallites. Enamel-dentine junction is at the bottom of the picture. Scale = 1 μm.

In the section of the *Platecarpus ptychodon* tooth (UALVP 51744, Fig. V.6), the enamel thickness is around 30 to 50 μm (near the base of the tooth, the tip of the tooth is broken). Diverging enamel crystallites organized in columns are found throughout the enamel of this taxon. The width of the diverging crystallite columns ranges from 12 to 14 μm. As in the tyrannosaurid tooth, the width of the columns also tends to increase towards the outer enamel surface. However, the angle between the central axis of each column and the insertion of the crystallites ranges from 25 to 30 degrees.

The SEM analysis revealed that the enamel thickness observed in a *Platecarpus* indeterminate tooth (UALVP 53595, Fig. V.7) is about 20 μm. The enamel crystallites are parallel to one another. The crystallites are loosely arranged, and lack the incremental lines. The quality of preservation of this specimen does not allow the observation of crystallites being deposited at different angles in different levels.

The *Varanus komodoensis* section (UALVP 53481, Fig.V.8) indicates that the enamel thickness in this specimen is about 10 μm. As in *Troodon* and *Platecarpus* indeterminate, the crystallites are parallel, and this specimen also shows well-preserved incremental lines in the enamel. It does not appear, however, that the parallel crystallites in *Varanus komodoensis* were deposited at different angles in different levels, as previously described for *Troodon*.

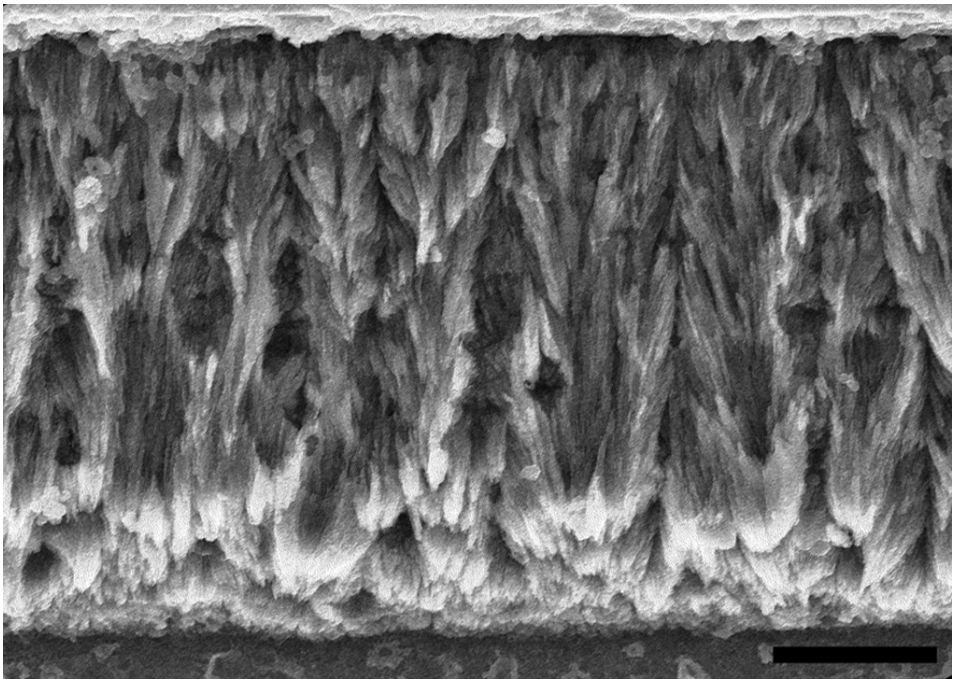

Fig. V.6. SEM photomicrograph of the enamel layer of *Platecarpus ptychodon*, with columnar diverging crystallites. Enamel-dentine junction is at the bottom of the picture. Scale = 10 μm.

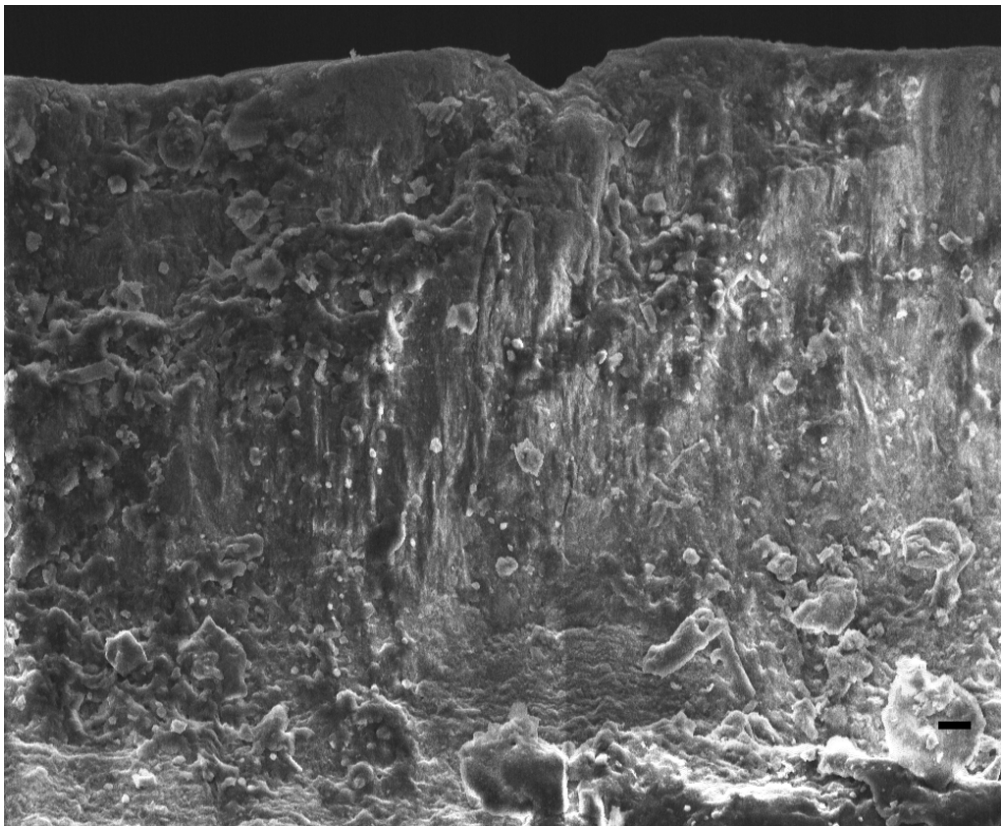

Fig. V.7. SEM photomicrograph of the enamel layer of *Platecarpus* indet, with parallel crystallites. Enamel-dentine junction is at the bottom of the picture. Scale = 1 μm.

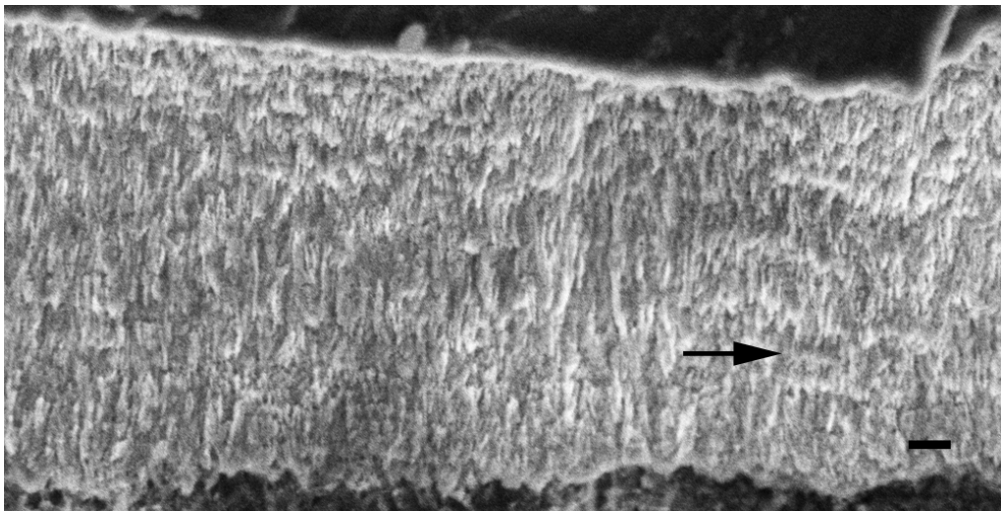

Fig. V.8. SEM photomicrograph of the enamel layer of *Varanus komodoensis*, with parallel crystallites, and incremental lines (arrow). Enamel-dentine junction is at the bottom of the picture. Scale = 1 μm.

The 3-D models (Figs. V.9–V.11) of the three different microstructure arrangements were tested in two different scenarios. In the first one, a 2000 N force was applied to the top of each model, at a normal angle with the main axis of the model. In the second scenario, the 2000 N force was applied at an inclined angle (approximately 45º to the model axis). The measured values for stresses of Von Mises (in Pascals) in each case are outlined in Table V.1. The graph in Fig. V.12 summarizes the percentages of stress transferred to different parts of each model.

In the first scenario (with the force applied at a normal angle), the model representing diverging crystallites at a 30º angle (as described for *Platecarpus ptychodon*) had the highest raw value for strain density (Fig. V.9) near the site where the force was applied (2.5 x 10^{16} Pa). However, this model also had the lowest percentage of this amount transferred to the base of the model (14%).

The model representing diverging crystallites in a 20º angle (as described for tyrannosaurid enamel) had the highest value for stress density (Fig. V.10) measured at the base of the model. The model representing parallel crystallites (as described for *Troodon*, *Platecarpus* indeterminate, and *Varanus komodoensis*) (Fig. V.11) had the lowest stress values measured near the site where the force was applied (1.9 x 10^{15} Pa), but the highest percentage of the initial stress value was transferred to the base of the model (31%). However, the raw stress value

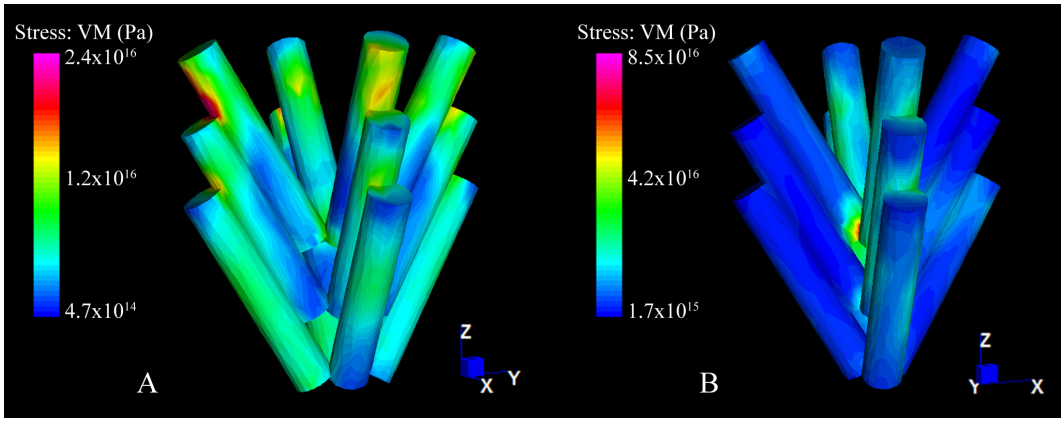

Fig. V.9. FEA results for the 3-D model representing diverging crystallites at a 30° angle. (A) First scenario, with forces applied at a normal angle, (B) second scenario, with forces applied at a 45° angle. Scales indicate Von Mises stresses measured in Pascals (Pa).

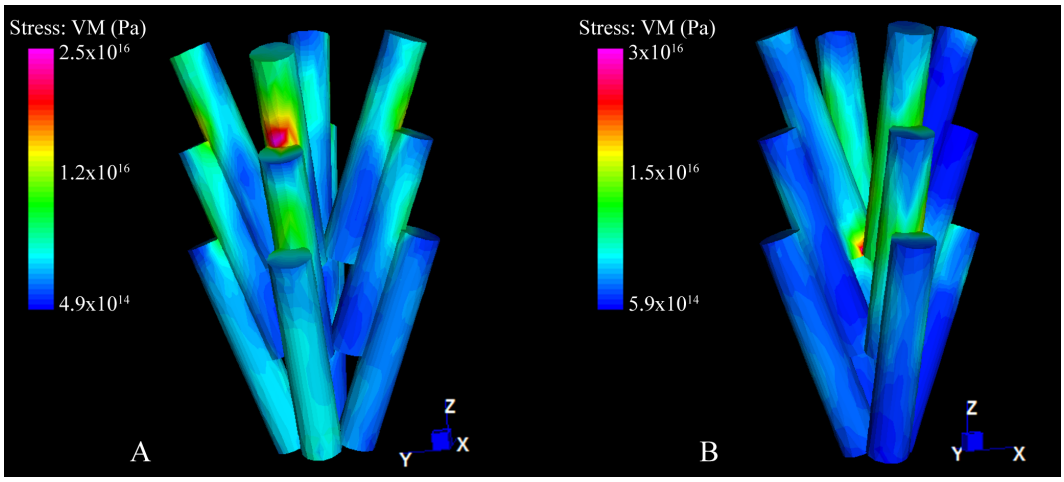

Fig. V.10. FEA results for the 3-D model representing diverging crystallites at a 20° angle. (A) First scenario, with forces applied at a normal angle, (B) second scenario, with forces applied at a 45° angle. Scales indicate stresses of Von Mises measured in Pascals (Pa).

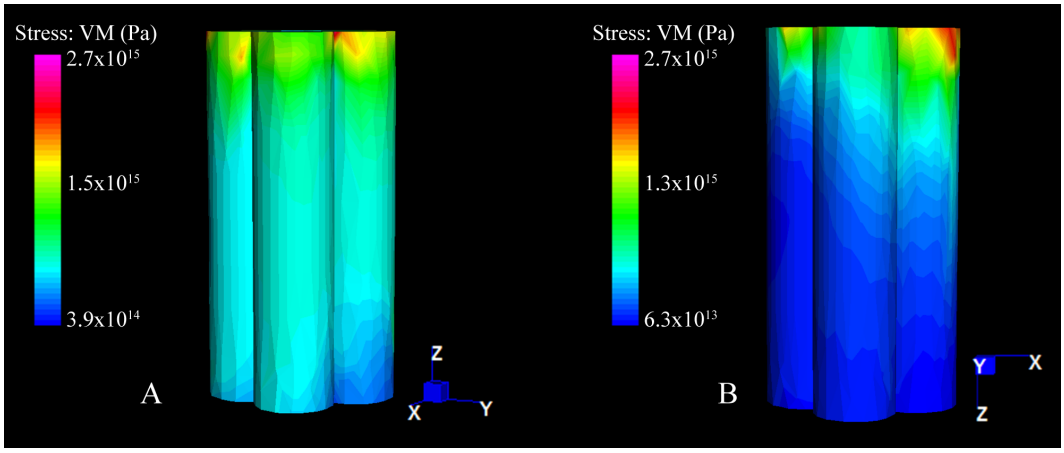

Fig. V.11. FEA results for the 3-D model representing parallel crystallites. (A) First scenario, with forces applied at a normal angle, (B) second scenario, with forces applied at a 45° angle. Scales indicate stresses of Von Mises measured in Pascals (Pa).

Table V.1. Stresses of Von Mises (VM) in Pascals (Pa) and percentages of stress measured in each model in two scenarios with forces applied at different angles.

Direction of force applied to model	Model	VM stress measured at the site where force was applied (Pa)	VM stress measured at the base of the model (Pa)	VM stress measured at the center of diverging crystallite columns (Pa)*	VM stress measured at the opposite side of where force was applied (Pa)*	Percentage of stress measured at top transferred to base of model	Percentage of stress measured at top transferred to center of diverging [illegible]	Percentage of stress measured at top transferred to opposite side of model*
Normal	crystallites Diverging at 20°	2.1×10^{16}	4.4×10^{15}			21%		
	crystallites Diverging at 30°	2.5×10^{16}	3.6×10^{15}			14%		
	Parallel crystallites	1.9×10^{15}	5.9×10^{14}			31%		
45° angle	crystallites Diverging at 20°	4.6×10^{15}	8.8×10^{14}	3×10^{16}	3.7×10^{14}	19%	652%	8%
	crystallites Diverging at 30°	1.1×10^{16}	4.2×10^{15}	4.7×10^{16}	8.3×10^{15}	38%	427%	75%
	Parallel crystallites	5.1×10^{14}	8.7×10^{13}	N/A	2×10^{15}	17%	N/A	392%

*Relevant measurements only in scenario with force applied at a 45° angle

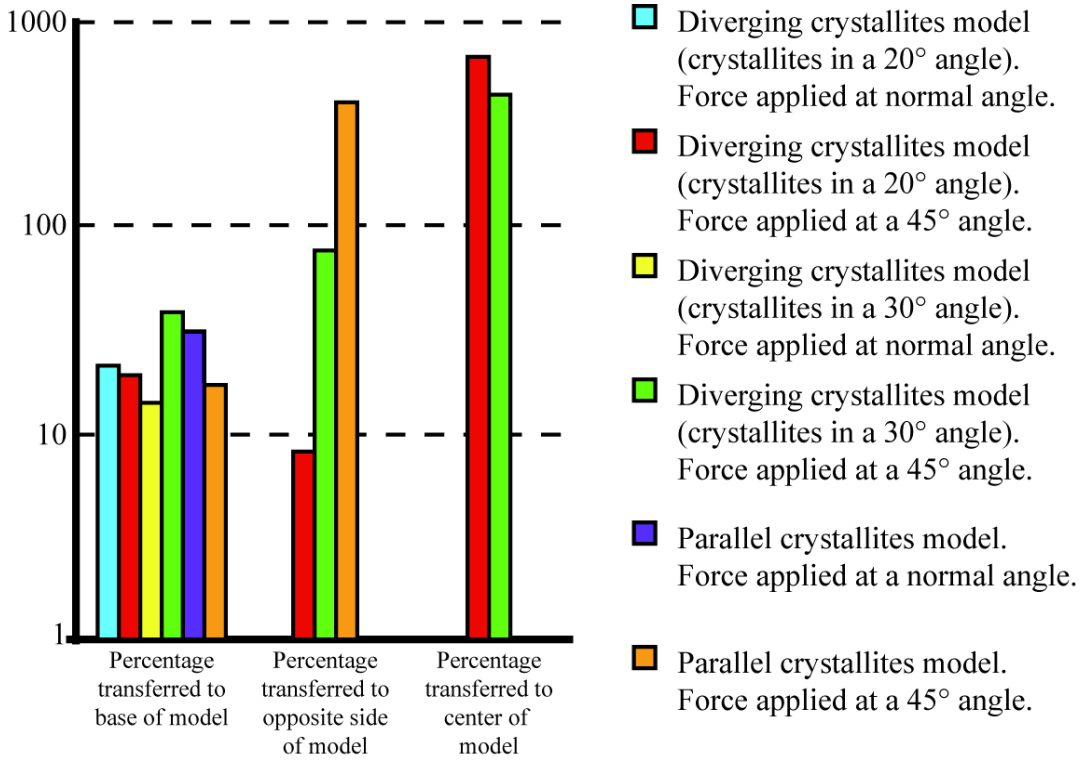

Fig. V.12. Log-transformed percentages of initial stresses transferred to different areas of each model in both scenarios tested.

measured at the base of this model is still the lowest of all three (5.9×10^{14} Pa).

In the second scenario (with a 45º angled force applied to all models, and additional restraints added to the lateral surface of each model), the model representing diverging crystallites at a 30º angle (Fig. V.9) had the highest stress density at the site where the force was applied (1.1×10^{16} Pa), whereas the model representing parallel crystallites had the lowest (5.1×10^{14} Pa) (Fig. V.11). The model representing diverging crystallites in a 30º angle had the highest value for stress density measured at the base of the model (4.2×10^{15} Pa), whereas the parallel crystallites model had the lowest (8.7×10^{13} Pa). All models successfully decreased the percentage of stress that reached the base of the model (representing the enamel-dentine contact), and the most successful model in doing so is the one with parallel crystallites (with only 17% of the initial stress being measured at the base of the model). The diverging crystallite models directed most of the initial stress into the center of the columnar structure (Figs. V.9–V.10), in which high stress densities were measured. However, these models were successful in not transferring the initial stress onto the opposite side of the model, and therefore showed potential to continuously reduce stress density from one column to the next. The parallel crystallites model increased the stress density nearly four times the initial value towards the opposite side of the model, suggesting that this structure is less effective at maintaining the enamel layer integrity

when forces are applied at inclined angles, even though the amount of stress transfer to the base of the model (and towards deeper layers in the tooth) is minimal.

Discussion

The samples studied added significant information about reptile enamel microstructures to the intensive analyses done by Hwang (2005) and Sander (1999; 2000). These authors recognized the phylogenetic value of these structures, especially Hwang (2005), in which it was demonstrated that in many cases, the schmeltzmuster might characterize dinosaur clades to the family level. However, the functional significance of different types of enamel microstructures had been only superficially explored, leaving many questions unanswered.

The results obtained indicate that a significant portion of the force initially applied to a tooth is absorbed in the enamel layer, which forms an effective barrier to prevent stresses and strains from being transferred to the more internal layers of the tooth, depending on the angle at which the force is applied.

In previous descriptions of tyrannosaurid enamel, it has been recognized that this taxon is characterized by the presence of at least two enamel types: columnar and parallel crystallites (Hwang 2005). This is also observed in the specimen UALVP 53361, and some functional

inferences can be made. The models tested with FEA indicated that parallel crystallites are effective at reducing the percentage of stresses transferred to more internal layers of the tooth in both scenarios. In the scenario with forces applied at a 45° angle to the axis of the model, the stress reduction at the base of the model was the highest of all; however, the lateral transfer of stress (onto adjacent crystallites) was increased. Additionally, when looking at the percentage of stress transferred to the base of the model in the scenario with forces applied at right angles, the diverging crystallites described for tyrannosaurids (with crystallites placed at a 20° angle in relation to the main axis of the column) outperformed the parallel crystallites. That way, this combination of enamel types in tyrannosaurids could have ensured that once a certain force was applied to the tooth, it had two different 'barriers' to dissipate that energy. The exceptional morphology of tyrannosaurid teeth (labiolingually expanded when compared to other theropods) and their unique biomechanics (Reichel 2010) may have further contributed as an adaptation to resist lateral bending. Additionally, Hwang (2005) suggested that the parallel crystallite enamel represents a more primitive stage than columnar structures; tyrannosaurids may have retained this structure, which is commonly found in less specialized primitive zyphodont teeth, such as those of dromaeosaurids.

The troodontid tooth (UALVP 53358) has only parallel crystallites without incremental lines. It has been observed that this taxon has a range

of enamel types that may occur in its teeth, and that is likely due to its unquestionable heterodonty (Hwang 2005). The crystallites in the specimen used in this study were deposited in different directions at each level (Fig. V.5). This feature increases the range of stresses that the enamel can sustain, because by constantly changing the direction of the parallel crystallite deposition, the tooth can receive stresses from a variety of directions with a lower risk of breakage. The heterodonty in *Troodon* also explains different types of enamel in different tooth positions because each region of the jaws is specialized for different functions that have different biomechanical challenges, as observed in heterodont dentitions of tyrannosaurids (Reichel 2010).

The teeth in *Varanus komodoensis* (UALVP 53481) have simple zyphodont morphology and the presence of parallel crystallite enamel is not surprising. The incremental lines indicate slight changes in crystallite deposition and these discontinuities add another aspect to the mechanics of enamel. The discontinuities in the enamel could cause the more superficial layers to flake off under situations of great mechanical stress (especially when considering the tendency of the parallel crystallites models to transfer stresses laterally). This is still more advantageous than propagating a crack into the deeper layers of the tooth, and possibly causing its early loss. The tyrannosaurid (UALVP 53361) analyzed also had faint incremental lines, which suggests that this adaptation also worked for this taxon. In fact, intense flaking of enamel has been observed

in shed and *in situ* tyrannosaurid teeth (for example in *Daspletosaurus* maxillary teeth, TMP 2001.036.0001, Fig. V.13), and also described by Schubert and Unguar (2005), indicating that these animals often had to face problems associated with the brittle nature of enamel. Because most of the columns in the enamel would be oriented perpendicularly to the vertical axis of the tooth (except for the ones near the tip), the addition of the columnar enamel layer increases the strength of tyrannosaurid teeth in both labiolingual and anteroposterior directions. The differentiation of enamel into two different types in tyrannosaurids could therefore be the result of a strong selective pressure towards reinforced teeth with increased bending resistance, as also suggested by Farlow et al. (1991), Snively et al. (2006), and Reichel (2010). Craniocervical mechanics in tyrannosaurids suggests powerful anteroposterior movements during feeding (Snively and Russell 2007*a*, 2007*b*). The reinforced enamel would also allow behaviors such as holding struggling prey and rapid head movements to deflesh carcasses, which may cause lateral stresses on teeth.

An interesting find is the significant difference between the teeth of *Platecarpus* indeterminate and *Platecarpus ptychodon*. These two specimens (UALVP 53595 and UALVP 51744, respectively) show significant differences on their external morphology (Fig. V.1). These differences include the fact that *Platecarpus ptychodon* has ornamentation on the surface of the enamel, which is not present in the *Platecarpus*

Fig. V.13. An *in situ* tooth with an intensively worn crown in a *Daspletosaurus* (TMP 2001.036.0001) left maxilla. Scale bar = 50 mm.

indeterminate specimen. The SEM images from these specimens show further differences in the enamel types of each taxon. *Platecarpus* indeterminate has crystallites arranged in a parallel pattern, whereas *Platecarpus ptychodon* clearly shows columns of diverging crystallites. The *Platecarpus ptychodon* tooth is more labiolingually expanded (similarly to tyrannosaurid teeth) and the presence of columns of diverging crystallites in the enamel is a convergent adaptation to what is seen in tyrannosaurids. The angle between crystallites is slightly larger, and that caused the columnar enamel in *Platecarpus ptychodon* to be more resistant to stresses in situations where forces are applied at a right angle to the columns of crystallites, while still being effective at reducing the amount of stress that is transferred to deeper layers of the tooth when forces are applied at a 45° angle. As previously mentioned, these columns increase the bending resistance of a tooth, suggesting that this animal also had an increased capacity to withstand the stresses generated by large struggling prey, or lateral head movements during feeding. Additionally, the microstructure in teeth of *Mosasaurus* has been described by Torii (1998), and although no SEM images are available from that study, the diagrams suggest that the enamel microstructure in *Mosasaurus* is also composed of diverging crystallites. The more slender tooth of *Platecarpus* indeterminate has the basic parallel crystallite arrangement, which is effective in preventing stresses from reaching

deeper layers of the tooth, at the cost of a higher chance of enamel flaking off when forces are applied at certain angles.

Conclusions:

In summary, comparing the taxa studied, the combination of enamel microstructures found in tyrannosaurids is the most effective in preventing the transfer of stresses to the dentine layer of their teeth. The outer layer of parallel crystallites transfers low percentages of stress to deeper layers, although it has a tendency to shatter due to lateral transfer of strain to adjacent crystallites. The next layer, with columns of diverging crystallites, is effective at preventing lateral transfer of strain (to adjacent columns), making it less likely to shatter. This deeper layer further reduces the amount of stresses transferred to the dentine layer of the tooth. In *Platecarpus ptychodon*, the only microstructures in the enamel are columns with crystallites diverging at slightly higher angles than in the diverging crystallites of tyrannosaurid enamel. They still offer good protection against lateral transfer of stresses to adjacent columns and are also effective at preventing stresses to reach deeper layers of the tooth, even without the additional layer of parallel crystallites found in tyrannosaurids. Finally, the taxa that have parallel crystallite enamel (*Platecarpus* indeterminate, the troodontid, and *Varanus komodoensis*) still benefit from the protection provided by the enamel, because the parallel crystallites transfer low percentages of the initial stresses to

deeper layers of the tooth. The potential to transfer stresses laterally to adjacent crystallites (and possibly shattering pieces of enamel) is reduced by the presence of incremental lines, or slight changes in the angle at which the crystallites are deposited in different layers of enamel. These discontinuities help prevent cracks from propagating.

Therefore, the main hypothesis that enamel microstructures offer structural support for the tooth in response to different environmental pressures is accepted to be true. The biomechanical importance of different enamel microstructures is demonstrated, in addition to their potential phylogenetic value demonstrated by previous authors (Dauphin et al 1988; Sander 1999; Hwang 2005). It seems that heterodont taxa especially offer good potential for the study of the functionality of enamel microstructures. Future analyses should include the premaxillary teeth of tyrannosaurids, troodontids and *Varanus komodoensis* in order to test if these teeth have similar adaptations in these taxa. Additionally, further sampling of *Platecarpus ptychodon* teeth would be invaluable, because some level of heterodonty is present in this taxon (UALVP 51744).

The notable differences in the enamel microstructure patterns of *Platecarpus* indeterminate and *Platecarpus ptychodon* suggest separation between these taxa. However, further sampling of mosasaurid taxa must be done to support the claim that enamel microstructures can be incorporated into phylogenetic analyses of this group. The only previous

description of enamel microstructures in mosasaurs is a preliminary one of *Mosasaurus* by Torii (1998).

References:

Arambourg, C. 1952. Les vertébrés fossils des gisement de phosphates (Maroc-Algerie-Tunisie). Service Géologique au Maroc, Notes et Mémoires, **92**: 1–372.

Bell, P.R., Snively, E. and Shychosky, L. 2009. A comparison of the jaw mechanics in hadrosaurid and ceratopsid dinosaurs using finite element analysis. The Anatomical Record, **292**: 1338–1351.

Boresi, A.P. and Schmidt, R. J. 2003. Advanced mechanics of materials. John Wiley and Sons, 681 pp.

Buffetaut, E., Dauphin, Y., Jaeger, J.J., Martin, M., Mazin, J.M., and Tong, H. 1986. Prismatic dental enamel in theropod dinosaurs. Naturwissenschaften, **73**: 326–327.

Cooper, J.S., and Poole, D.F.G. 1973. The dentition and dental tissues of the agamid lizard, *Uromastix*. Journal of Zoology (London), **169**: 85–100.

Currie, P.J., Rigby, J.K. Jr., and Sloan, R.E. 1990. Theropod teeth from the Judith River Formation of Southern Alberta, Canada. *In*: Dinosaur Systematics: Approaches and Perspectives. *Edited by* Carpenter, K. and P.J. Currie (eds.). Cambridge University Press. pp. 107–125.

Creech, J. E. 2004. Phylogenetic character analysis of crocodylian enamel microstructure and its relevance to biomechanical performance. Unpublished Masters Thesis, Florida State University, Tallahassee, 59 pp.

Dauphin, Y., and Jaeger, J. -J., and Osmolska, H. 1988. Enamel microstructure of ceratopsian teeth (Reptilia, Archosauria). Geobios, **21**: 319 – 327.

Dieckwisch, T.G.H., Berman, B.J., Anderton, X., Gurinsky, B., Ortega, A.J., Satchell, P.G., Williams, M., Arumugham, C., Luan, X., McIntosh, J.E., Yamane, A., Carlson, D.S., Sire, J.-Y., and Shuler, C.F. 2002. Membranes, minerals, and proteins of developing vertebrate enamel. Microscopy research and technique, **59**: 373–395.

Farlow, J.O., Brinkman, D.L., Abler, W.L., and Currie, P.J. 1991. Size, shape and serration density of theropod dinosaur lateral teeth. Modern Geology **16**: 161–198.

Grine, F.E., Vrba, E.S., and Cruickshank, A.R.I. 1979. Enamel prisms and diphyodonty: linked apomorphies of Mammalia. South African Journal of Science, **75**: 114–120.

Hwang, S. H. 2005. Phylogenetic patterns of enamel microstructure in dinosaur teeth. Journal of Morphology, **266**: 208 – 240.

Konishi, T., and Caldwell, M. W. 2007. New specimen of *Platecarpus planifrons* (Cope, 1874) (Squamata: Mosasauridae) and a revised taxonomy of the genus. Journal of Vertebrate Paleontology, **27**: 59-72.

Manly, R. S., Hodge, H. C. and Ange, L. E. 1939. Density and refractive index studies of dental hard tissues: II. Density distribution curves 1,2. Journal of Dental Research 18: 203–211.

Rees, J. S. and Hammadeh, M. 2004. Undermining of enamel as a mechanism of abfraction lesion formation: a finite element study. European Journal of Oral Sciences 112: 347–352.

Reichel, M. 2010. The heterodonty of *Albertosaurus sarcophagus* and *Tyrannosaurus rex*: biomechanical implications inferred through 3-D models. Canadian Journal of Earth Sciences, **47**: 1253–1261.

Russell, D.A. 1967. Systematics and morphology of American mosasaurs (Reptilia, Sauria). Peabody Museum of Natural History, Yale University, Bulletin, **23**: 1-241.

Sander, P.M. 1999. The microstructure of reptilian tooth enamel: terminology, function, and phylogeny. München Geowissenschaft Abhandlungen (Reihe A), **38**: 1 – 102.

Sander, P.M. 2000. Prismless enamel in amniotes: terminology, function and evolution; pp. 92 – 106 in M. F. Teaford, M. M. Smith, M. W. J.

Ferguson (eds.), Development, function and evolution of teeth. Cambridge University Press.

Schubert, B.W., and Unguar, P.S. 2005. Wear facets and enamel spalling in tyrannosaurid dinosaurs. Acta Palaeontologica Polonica, **50**: 93–99.

Smith, J.B. 2005. Heterodonty in *Tyrannosaurus rex*: implications for the taxonomic and systematic utility of theropod dentitions. Journal of Vertebrate Paleontology, **25**: 865–887.

Snively, E., and Russell, A.P. 2007*a*. Craniocervical feeding dynamics of *Tyrannosaurus rex*. Paleobiology, **33**: 610–638.

Snively, E., and Russell, A.P. 2007*b*. Functional morphology of the neck musculature in the Tyrannosauridae (Dinosauria, Theropoda) as determined via a hierarchical inferential approach. Zoological Journal of the Linnean Society, **151**(4): 759–808.

Snively, E., Henderson, D.M., and Phillips, D.S. 2006. Fused and vaulted nasals of tyrannosaurid dinosaurs: Implications for cranial strength and feeding mechanics. Acta Palaeontologica Polonica, **51**: 435–454.

Torii, S. 1998. Origin of enamel prisms and Hunter-Shreger bands in reptilian enamel. Connective tissue research, **38**: 45 – 51.

Chapter 6

Case study: a model for the bite mechanics in *Stegosaurus*[1]

Introduction

The clade Stegosauria was erected by Marsh in 1877, the same year he described the genus *Stegosaurus*. In spite of over 130 years of studies, little has been described about the detailed tooth morphology for this taxon. Generally, each *Stegosaurus* tooth is subtriangular in labial view, has a prominent cingulum, and has a variable number of rounded denticles, ranging from seven to fifteen (Galton and Upchurch 2004; Barrett 2001). A *Stegosaurus* tooth also has a complex network of secondary longitudinal ridges (Galton and Upchurch 2004). The descriptions of stegosaur teeth are not detailed enough to group them into separate species, nor do they include interpretations about the functions of the structures observed.

Aspects of feeding in stegosaurs have been addressed, however. It has been suggested that this taxon may have had cheeks, supported by a pronounced dorsolateral ridge on the maxilla (Galton and Upchurch 2004),

---

[1] A version of this chapter has been published. Reichel, M. 2010. Case study: a model for the bite mechanics in *Stegosaurus* (Ornithischia, Stegosauridae). Swiss Journal of Geosciences, **103**: 235–240.

and may have had a horny beak or ramphotheca (Czerkas 1998, 1999; Papp and Witmer, 1998). Tooth wear has been described as being the result of tooth-food contact (Galton and Upchurch 2004). The wear facets occur on the occlusal surface of the crown, are generally horizontal, and are sometimes angled slightly posteriorly. The jaw action is described as strictly orthal (Barrett 2001).

These inferences about the bite and chewing behaviour in *Stegosaurus* have yet to be tested biomechanically. In this paper, the bite force of *Stegosaurus* is estimated based on cranial proportions, and its ability to bite through plant materials of different thicknesses is tested. Additionally, complex enamel structures, such as denticles and longitudinal ridges, are tested for their influence on overall tooth performance under normal stresses related to bite forces. The main method used in this study is Finite Element (FE) analysis, which reveals the structural performance of a realistically modeled object subdivided into a mesh of small elements.

Materials and Methods

The FE analyses are based on 3D models made with the software ZBrush®. The 3D models are based on measurements and the general morphology of tooth crowns from cf. *Stegosaurus armatus* (DS-RCR2003-02, ‘Sarah’ Fig.VI.1), and *Stegosaurus stenops* (USNM 4934), both from

Fig. VI.1. Photograph of the *Stegosaurus armatus* specimen DS-RCR2003-02 (‘Sarah’), isolated tooth number 269. Photograph is a courtesy of Jean-Paul Brillon-Bruyat. Scale bar equals 2mm.

the Morrison Formation of Wyoming, USA. CT scans were not used in this analysis. Even though CT scans provide finer details, the emphasis of this study is in the proportions observed in the specimens, which are reflected in the simplified 3D models, and how objects with such proportions respond to stresses similar to those in stegosaur jaws. CT scans will be a good tool for comparisons in the future, especially for studies focusing on morphological differences within or between stegosaur specimens.

Two digital models were made for a generalized *Stegosaurus* tooth. Because the dentition of *Stegosaurus* is essentially homodont, it is irrelevant to make different models for different tooth positions. One model is plain (Fig. VI.2A), without the denticles or vertical ridges, and the other model (Fig. VI.2B) has the external features that are observed in the original specimens, such as vertical ridges and denticles. The models were not given a cingulum at this stage, and the significance of this structure is not addressed in this paper. The models are 5.0mm tall (from the base to the tip of the crown), 3.2mm labiolingually wide (at the base of the crown), and 5.0mm anteroposteriorly wide (at the base of the crown).

After building the 3D models, they were converted to NASTRAN format through the software Mimics®, and imported into Strand7® for FE meshing and analysis. The models were given material properties of enamel, because the thickness of the enamel layer in ornithischian

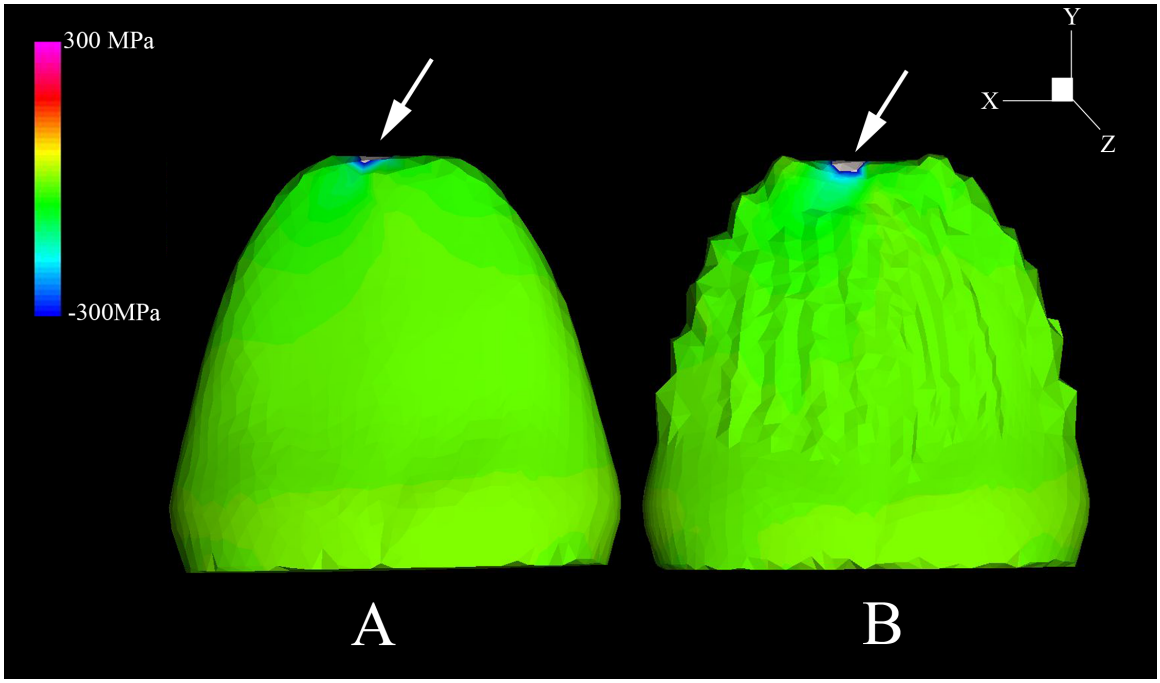

Fig. VI.2. 3D models of a *Stegosaurus* tooth. *A*, without the external features. *B*, with external features, such as denticles and ridges. White arrows indicate the direction and area where loads were applied. Note the dark area of higher compression surrounding a small white area (indicating enamel failure) where the load was applied.

dinosaurs is significantly high, reaching about 50μm in Ankylosauria (Hwang 2005). The forces were applied to the occlusal surfaces of the crowns and the models were constrained along the X, Y, and Z axes at their bases. The constraint was both translational and rotational, so that the condition observed in the jaws (in which teeth have virtually no movement) was simulated.

Four material and structural performance properties dictate how a 3D object will react to the forces applied to it. There are not many studies on comparative values for those enamel properties among vertebrates, but reptiles and mammals share some developmental characteristics for the enamel, such as its ectodermal origin (Edmund 1969). The values used in this analysis were based on reptile studies where possible, but the rarity of such studies on reptile enamel forced some of the data to be based on mammalian research. The elastic or Young's Modulus is a ratio of stress to strain and a thus a measure of stiffness (Boresi and Schmidt 2003). The Young's Modulus value used in the analyses is 6.04 e10 Pascals (Pa), and is based on the value measured in fresh crocodylian teeth (Creech 2004). Poisson's Ratio (transverse versus axial strain) describes how a structure deforms perpendicularly to the direction of force, by bulging transversely under compression and thinning under tension (Boresi & Schmidt 2003). The Poisson's ratio used in the analyses was 0.30, which is the same as in human teeth (Rees and Hammadeh 2004). The density -

2800 kilograms per cubic meter (Kg/m^3) – assigned to the models is that of human enamel (Manly et al. 1939). Finally, the model's yielding point (or failure stress) indicates the breaking point of the material, and sets an upper level for the structure's performance. The failure stress of enamel (for compressive stress) was estimated at values that average 300 megapascals (MPa) by Currey (2002) and Waters (1980). Waters (1980) also estimated the yielding point for enamel as an average of 35 MPa (for tensile stress), and 80 MPa (for shear stress). The scale on the models was therefore set as a maximum of 300 MPa to reflect the maximum compressive stress that can be yielded by tooth enamel.

An additional 3D model was made to simulate a tree branch (Fig. VI.3), in order to test how efficient the estimated *Stegosaurus* bite forces were at breaking plant materials. This model consists of a hollow cylinder (the hollow core represents the air and water content in the branch). The material properties given to that model were those of green timber (default settings by Strand7© for white cypress). The Young's Modulus for the model is 9.1 e9 Pa, and the density is 8.5 e-7 Kg/mm^3. The failure stress (compressive strength) has been measured in juvenile wood of *Taiwania cryptomerioides* (a species of modern timber) by Lin et al. (2006), and is 25.3 MPa, parallel to grain. This value was used to set the upper limit for the material failure stress in all models. The same model geometry was tested in four different diameters of 4mm, 8mm, 12 mm, and 24 mm. The

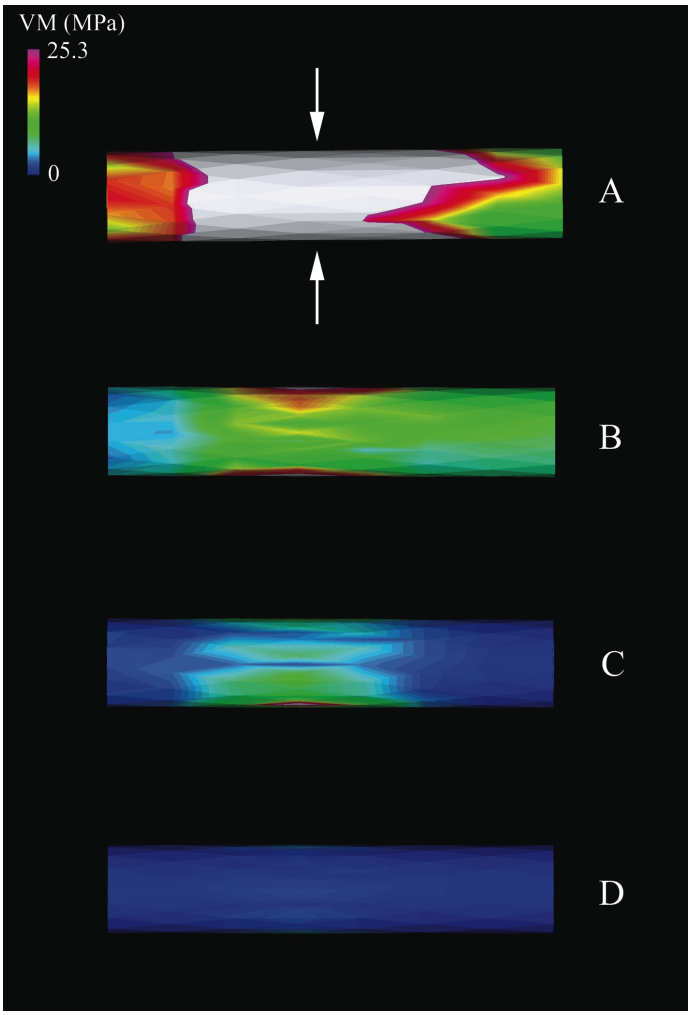

Fig. VI.3. Three-dimensional models of cylinders with plant material properties. The forces applied in all models are as represented by the white arrows in *A*. Constraint in all models was applied to the right end. Models have diameters of *A*, 4mm; *B*, 8mm; *C*, 12mm; *D*, 24mm. Models are not to scale. The white area in *A* indicates failure of the material. Dark areas in *C* and *D* indicate low von Mises (VM) stresses.

length of the cylinders increased proportionately to the increase in diameter, starting with 20mm for the smallest model.

The forces were applied transversely to the cylinder on the midsection of the model. All models were restrained along the X, Y and Z axes (translational and rotational constraint) on one end of the cylinder to simulate the site of attachment of the branch to the plant. The results were viewed with the von Mises yield criterion, which is appropriate for wood because it is ductile under moderate, gradually applied loads. The von Mises criterion evaluates relative proximity to yield within the structure, as a reflection of strain energy density (Farke 2008). The results are shown as a summation of principal components of stress, and not a characterizable force/area, and they are therefore not informative for determining types of stress (Bell et al. 2009).

The bite forces for *Stegosaurus* imposed on its teeth and food were estimated following the method used by McHenry (2009) for *Kronosaurus queenslandicus*. The cross-sectional area of bite muscles through the subtemporal fenestra was calculated as 19.7 cm^2, based on ventral images of USNM 4934 (*Stegosaurus stenops*) from Ostrom and McIntosh (1966). The skull of the specimen ‘Sarah’ (DS-RCR2003-02) is disarticulated and therefore not appropriate for the measurements needed in this analysis. The jaw proportions necessary for calculating forces at the

teeth were also measured from *Stegosaurus stenops* (USNM 4934). The "in lever" (from the jaw articulation to the center of the jaw muscle insertions) measures 7.42 cm. The "out lever" is the distance from the centre of the jaw muscle insertions to specific positions along the tooth row (Fig. VI.4). In *Stegosaurus stenops*, respective out levers for the anterior, middle, and posterior teeth are 29.5, 22.5, and 15.0 cm. The angle between the muscle insertion and the dentary bone was estimated to be approximately 45°. Based on these measurements, the bite force calculations were done as follows. The concentric specific tension (as a muscle shortens) is generally equivalent to 20N per square centimeter (Bamman et al. 2000; Snively and Russell 2007). This multiplied by the cross sectional area gives the muscle force (F_y). The total vertical force (F_{in}) applied by the temporal muscles to its point of attachment (in this case, to the jaw) is given by the following formula:

$F_{in} = sin \propto . F_y$ (in which $\propto = 45°$, the muscle's angle of pull relative to the vertical).

The overall line of pull for each the temporal muscles is in the same sagittal plane as its insertion on the mandible, so medial or lateral components of the force were judged to be insignificant for calculating the F_{in}.

After F_{in} is known, it is possible to calculate the bite forces for each part of the jaw using the following formula:

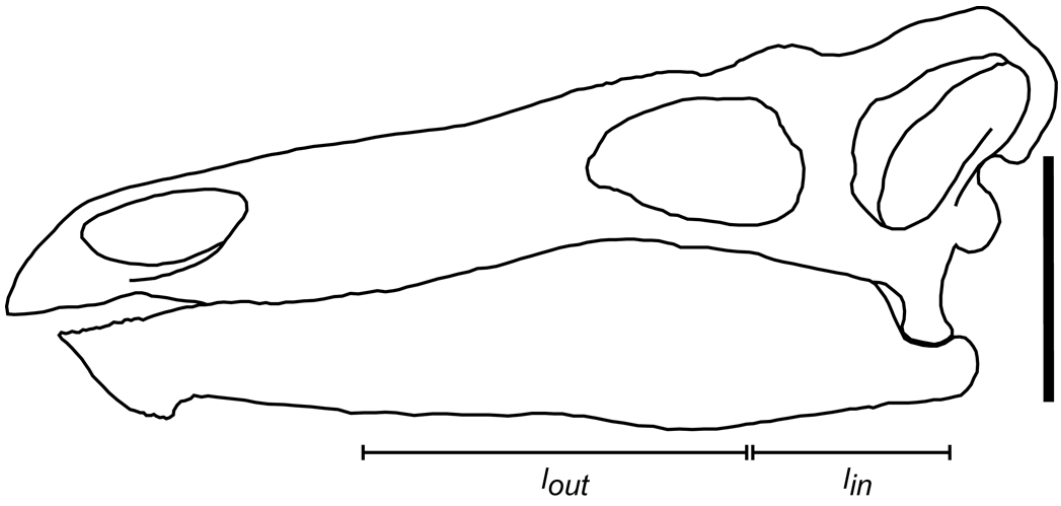

Fig. VI.4. The skull of *Stegosaurus stenops* with lines indicating the measurements for the “in lever” (l_{in}) and “out lever” (l_{out}). Scale bar equals 100mm.

$I_{in} \cdot F_{in} = I_{out} \cdot F_{out}$ (in which I_{in} and I_{out} are, respectively, the "in lever" and the "out lever" (measured previously in centimeters), and F_{in} and F_{out} are, respectively, the concentric force applied by the muscle to its point of attachment and the bite force at the measured point of the jaw).

There were three sets of FE analyses. In the first set, the calculated bite forces for anterior, middle and posterior teeth were applied directly to the tooth model. In the second set, smaller forces were applied to the model, taking into consideration the number of teeth in each of the anterior-, mid- and posterior-sections, and dividing the calculated bite force for each area by the number of teeth in the same area. In the third set of analyses, the bite force (the highest one) calculated for the posterior portion of the jaw was applied to plant 3D models with varying diameters.

Results

The calculated bite force for *Stegosaurus stenops* is 140.1N on the anterior teeth, 183.7N on the middle teeth, and 275N on the posterior teeth. Any of these forces, when applied straight to both 3D models of the tooth, caused failure of the enamel around the area where the force was applied (considering the 300 MPa yielding point for compressive stress in enamel). The load was applied to a small area of the model and therefore this localized enamel failure may be an artifact. The highest stress levels

are found around the tip, and significantly lower stress levels are found near the base. The main stresses are compressive. In all models, values lower than 1% of the stress observed at the tip were found at the base, indicating an efficient dissipation of compressive stresses associated with the load on the tooth. The presence of denticles and ridges did not seem to offer an advantage or disadvantage to the overall stress handling of the models.

The maximum bite force (275N) was applied to the plant models. The force was applied transversely to the cylinder. In the model with a 4mm diameter, the stresses caused by the bite force were high enough to cause the plant material to fail throughout the diameter of the cylinder. In the 8mm diameter model, the force was enough to cause the plant model to fail near the nodes where the load was applied, but the stresses were significantly lower and the failure did not follow throughout the whole diameter, as in the first case. In the 12mm diameter model, there was a significantly smaller area in which the plant model failed, immediately around the nodes where the load was applied. In the 24mm diameter model, the plant model did not fail.

Discussion

The bite forces calculated for *Stegosaurus* (140.1N, 183.7N, and 275N for anterior, middle and posterior teeth, respectively) are relatively low when

compared to those estimated by Erickson et al. (1996) for the posterior portion of the jaws of Labrador dogs (550N), humans (749N), or wolves (1,412N). However, the calculated bite forces of *Stegosaurus* suggest that this taxon had the ability to bite through smaller branches and leaves. The plant models show *Stegosaurus* had the potential to break smaller branches, but did not have enough force in its jaws to crush a thick (more than 12 mm in diameter) object with the material properties of green timber, even when using its highest biting forces, measured at the position of the last tooth in the maxilla. Any larger plant parts could be incorporated into the diet only if *Stegosaurus* was capable of biting more efficiently than predicted in this analysis. Parrish et al. (2004) describe the Morrison Formation flora as dominated by herbaceous, short-lived plants, characteristic of a seasonal environment. *Stegosaurus* probably took advantage of the abundance of smaller, fast growing plants. More tests with different material properties from other plants, such as modern ferns, would further inform about dietary preferences in *Stegosaurus*.

The tooth wear observed by Galton and Upchurch (2004) is mainly attributed to tooth-food contact, and indicates some ability to chew. But it is also true that the wear facets are neither common nor extensive, which suggests that this may have been an occasional, rather than a repetitive behavior in *Stegosaurus*. The models did not show potential for enamel failure near the denticles at any of the forces applied. It seems therefore that the overall morphology of the tooth is structurally sound enough to

carry denticulate edges, which increase the efficiency of teeth in cutting food materials (Abler 1992). The stresses were effectively distributed on the tooth crown, so that the denticles did not receive a significant amount of strain.

The fact that small failure areas appeared in all tooth models around the area where the force was applied suggests a few points:

1. *Stegosaurus* was not using its full potential bite force, especially when considering the small amount of wear observed in teeth.

2. *Stegosaurus* had a high tooth replacement rate, and therefore the small amount of wear observed is a result of the fact that each tooth does not stay in use for long.

3. The tooth models with material properties of enamel are more brittle than what is observed in reality.

The second option seems unlikely due to the rarity of isolated shed crowns in the fossil record, although that could be due to preservational bias. Additional studies in stegosaur tooth replacement rates would reinforce this conclusion. The first possibility is more likely, and can be combined with the fact that *Stegosaurus* could be using a beak (Galton and Upchurch 2004) during most of its foraging behaviour. In that case, the teeth would receive less stress attributed to bite forces. However, the anterior part of the jaws is capable of inflicting the least amount of force. If *Stegosaurus* was indeed making use of its beak most of the time, the

plants it fed on would have even thinner branches than predicted in this analysis, or different material properties.

The third point is also to be taken into consideration. Future analyses should test the same tooth models with layers of dentine and enamel in order to verify if the failure areas are due to the brittle nature of enamel.

Another point not addressed in this paper is the presence of a cingulum in stegosaur teeth. This structure has been reported as an important feature for reducing strains near the base of mammalian teeth (Anderson et al. 2009). However, even without the addition of a cingulum to the stegosaur tooth models, only small stresses are concentrated at the base. It would still be interesting to study the function or systematic distribution of this structure within Stegosauria in the future.

Conclusions

In conclusion, this analysis shows that *Stegosaurus* had bite forces lower than those measured on posterior tooth positions of Labrador dogs (550N) (Erickson et. al 1996) and that the tooth morphology is efficient in dissipating the compressive stresses generated during bite, so that a minimal amount of stress is transferred to the jaw bones, or to the valuable denticles, which increase the cutting ability of the teeth.

This study also shows that the morphology and biomechanics of *Stegosaurus* teeth can give clues about the feeding habits of this taxon and some indication about plant preferences. More data on stegosaur tooth morphology and variations along the tooth row are needed, as well as more data on tooth wear and jaw and tooth replacement rates. Microwear studies, which have a great potential for plant preference studies, also would improve this analysis. Additionally, using those methods on models with material properties equivalent to the plants described for the Morrison Formation would help to pin down the taxa that could likely be part of the diet of *Stegosaurus*.

This paper's methods have potential for studies with other herbivorous taxa and could provide tools to quantify morphological differences between closely related taxa. This particular study demonstrated that the relatively small teeth of *Stegosaurus* could participate in the food processing of plants, but the small amount of wear observed in most specimens suggests that a significant percentage of the bite stresses could have been concentrated on the beak.

References

Anderson, P., Gill, P. & Rayfield, E. 2009. How the cingula of basal mammal teeth may alleviate strain in the enamel caused by a soft food diet. Journal of Vertebrate Paleontology, **29** (suppl. 3): 54A.

Abler, W. L. 1992. The serrated teeth of tyrannosaurid dinosaurs, and biting structures in other animals. Paleobiology, **18**(2): 161–183.

Bell, P.R., Snively, E. & Shychosky, L. 2009. A comparison of the jaw mechanics in hadrosaurid and ceratopsid dinosaurs using finite element analysis. The Anatomical Record, **292**: 1338–1351.

Boresi, A. P. & Schmidt, R. J. 2003. Advanced mechanics of materials. John Wiley and Sons, 681 pp.

Bamman, M. W., Newcomer, B. R., Larson-Meyer, D., Weisner, R. L. & Hunter, G. R. 2000. Evaluation of the strength-size relation *in vivo* using various muscle size indices. Medicine and Science in Sports and Exercise, **32**: 1307–1313.

Barrett, P. M. 2001. Tooth wear and possible jaw action of *Scelidosaurus harrisonii* Owen and a review of feeding mechanisms in other thyreophoran dinosaurs. *In* The armored dinosaurs. *Edited by* Carpenter, K. (Ed.). Indiana University Press, Bloomington, IN, 25–52.

Creech, J. E. 2004. Phylogenetic character analysis of crocodylian enamel microstructure and its relevance to biomechanical performance. Unpublished Masters Thesis, Florida State University, Tallahassee, 59 pp.

Currey, J.D. 2002. Bones: structure and mechanics. Princeton University Press, N.J. 436 pp.

Czerkas, S. 1998. The lips, beaks, and cheeks of ornithischians. Journal of Vertebrate Paleontology, **18**: 37A.

Czerkas, S. 1999. The beaked jaw of stegosaurs and their implications for other ornithischians. *In*: Gillette, D. D. (ed.). Vertebrate paleontology in Utah - Miscellaneous Publications of Utah Geological Survey, **99**: 143–150.

Edmund, A.G. 1969. Dentition. *In* Biology of the Reptilia – Volume 1, Morphology A. *Edited by* C. Gans, A.d'A. Bellairs, and T.S. Parsons. Academic Press, London, UK. pp. 117–200.

Erickson, G.M., Van Kirk, S.D., Su, J., Levenston, M.E., Caler, W.E., and Carter, D.E. 1996. Bite-force estimation for *Tyrannosaurus rex* from tooth-marked bones. Nature, **382**:706–708.

Farke, A.A. 2008. Frontal sinuses and head-butting in goats. Journal of Experimental Biology, **211**: 3085–3094.

Galton, P. M. & Upchurch, P. 2004. Stegosauria. *In* The Dinosauria. Second Edition. *Edited by* D.B. Weishampel, P. Dodson, and H. Osmólska (Eds.). University of California Press. pp. 343–362.

Hwang, S.H. 2005. Phylogenetic patterns of enamel microstructure in dinosaur teeth. Journal of Morphology, **266**: 208–240.

Lin, C.-J., Wang, S.-Y., Yang, T.-H., and Tsai, M.-J. 2006. Compressive strength of young Taiwania (*Taiwania cryptomerioides*) with different thinning and pruning treatments. Journal of Wood Science, **52**(4): 337–341.

Marsh, O. C. 1877. New order of extinct Reptilia (Stegosauria) from the Jurassic of the Rocky Mountains. American Journal of Science 14: 513–514.

Manly, R. S., Hodge, H. C. & Ange, L. E. 1939. Density and refractive index studies of dental hard tissues: II. Density distribution curves 1,2. Journal of Dental Research, **18**: 203–211.

McHenry, C. R. 2009. Devourer of gods: the paleoecology of the Cretaceous pliosaur *Kronosaurus queenslandicus*. Unpublished Ph. D. dissertation, Department of Earth Sciences, University of Newcastle, Newcastle, N.S.W., Australia, 635 pp.

Ostrom, J. H. & McIntosh, J. S. 1966. Marsh's dinosaurs - the collections from Como Bluff. Yale University Press, New Haven and London, 388 pp.

Papp, M. J. & Witmer, L. 1998. Cheeks, beaks or freaks: A critical appraisal of buccal soft-tissue anatomy in ornithischian dinosaurs. Journal of Vertebrate Paleontology **18**: 69A.

Parrish, J. T., Peterson, F. & Turner, C. E. 2004. Jurassic "savannah" – plant taphonomy and climate of the Morrison Formation (Jurassic, western U.S.A.). Sedimentary Geology, **167**: 139–164.

Rees, J. S. & Hammadeh, M. 2004. Undermining of enamel as a mechanism of abfraction lesion formation: a finite element study. European Journal of Oral Sciences 112: 347–352.

Snively, E., and Russell, A. P. 2007. Craniocervical feeding dynamics of *Tyrannosaurus rex*. Paleobiology, **33**: 610–638.

Waters, N.E. 1980. Some mechanical and physical properties of teeth. In: Society of Experimental Biology, 34th Symposium. The mechanical properties of biological materials. Cambridge University Press, Cambridge, 99–135.

Chapter 7

General discussion and conclusions

Discussion

Animals are naturally destructive. They feed on large molecules built by other organisms, such as plants, from simple molecules. Vertebrates are especially known for attacking the largest structures, and most of them rely on their teeth for doing so. It is only logical that vertebrates such as ourselves would seek deeper knowledge into the way teeth function, whether it is because we heavily depend on our own teeth or because we all have an admiration (or fear) of large predators that could easily sink their teeth into our bodies.

Most vertebrates evolved teeth for aiding ingestion, in the sense that they aid the process of taking food into the mouth. However, most of the real breakdown of food happens chemically, within the guts. Although mammals are known to have advanced mechanisms of chewing (initiating a mechanical breakdown prior to the chemical breakdown of food), reptiles also developed amazing structures and adaptations in their teeth to aid the process of obtaining food and getting it into their mouth.

The development of teeth is similar in reptiles and mammals. The two main tissues, enamel and dentine, have different origins: enamel originates from the ectoderm, whereas dentine originates from the

mesoderm (Peyer 1968). However, the external structures observed in mammalian and reptilian teeth differ greatly. Mammalian dentitions are characterized by being heavily heterodont and members of the Carnivora have teeth that are modified for cutting. These teeth are called carnassials and they are the enlarged fourth upper pre-molar and lower first molar, which act as longitudinal blades that shear across each other as an efficient cutting mechanism. Although reptiles generally achieved lower degrees of heterodonty than mammals, they did develop structures to increase the efficiency of their teeth, by adding multiple cusps, carinae and sometimes denticles onto the cutting edges of their teeth. Carinae are fairly simple structures with low energetic costs to develop, when compared to the multi cusped teeth in some reptiles, and molars and premolars of mammals. Also, teeth with multiple cusps require precise dental occlusion to be functional, and therefore adaptations in the jaw articulations and musculature to provide this precision. An interesting case is that of *Arctocyon ferox*, in which some of the teeth with multiple cusps in the lower jaw have denticulate edges (personal observation of AMNH 2456) (Fig. VII.1).

It has been demonstrated that carinae (and denticles) develop at the enamel-dentine junction (Abler 1996; Sander 2000). It has been argued that the intrusion of carinae into the enamel-dentine junction is dependent on the thickness of the enamel (Sander 2000), or at least on the size of the carinae. However, in Chapter 2 it has been demonstrated

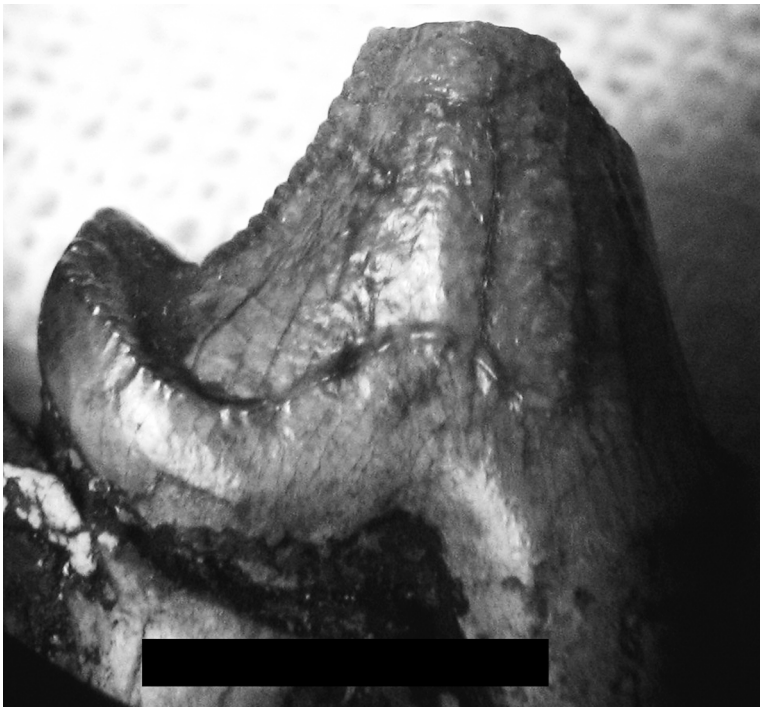

Fig. VII.1. A tooth of the mammal *Arctocyon ferox* (AMNH 2456), with denticulate edges. Scale bar = 5 mm.

that carinae influence the enamel-dentine contact in taxa with enamel as thin as 10 μm (such as *Varanus komodoensis*) or as thick as 56 μm (tyrannosaurids). It becomes clear, especially in specimens in which sections of teeth in early stages of development are available (such as *Varanus rudicollis*), that the carinae already develop in the dentine before enamel is deposited. Beatty and Heckert (2009) suggested that carinae develop at the dentinogenesis stage in crowns with supernumerary carinae; if this is the case, then it is reasonable to assume that the inner surface of the basal membrane influences the development of the morphology of carinae. In this case, the thickness of the enamel would have little to no influence in the development of carinae because carinae start developing before enamel deposition. Additionally, the enamel thickness within a taxon (and even within a tooth) varies greatly; and assuming that the presence or absence of carinae in teeth is a result of the enamel thickness is risky, to say the least. The enamel, therefore, conforms to the morphology dictated by the dentine. In cases where carinae have denticles, each one of the denticles is analogous to a tooth within a tooth (Abler 1996). Each denticle has its own internal structure formed by a cylindrical radix of dentine, and a local change in dentine growth rates, which extends from the deeper layers of the dentine all the way to the enamel (Abler 1996), at least in theropods. The local changes in dentine growth rates caused by the presence of denticles starts early in

tooth development, and may extend as far as the pulp cavity in some cases, influencing the internal surface of the tooth. An example of this can be observed in *Tyrannosaurus* (SMNH 2523.8), in which a premaxillary tooth has what appears to be denticles on the matrix filling the pulp cavity that correspond with the denticles on the outer surface of the tooth. These false denticles on the matrix infilling are formed in depressions in the dentine below each enamel-capped denticle on the outside of the tooth. They are referred to as “denticle shadows” in this study, and are probably the result of the presence of internal structures of denticles, such as radices.

It appears that the more simplified denticles in *Varanus komodoensis* are more primitive than the ones seen in theropod dinosaurs, because the internal structures of denticles, or changes in local dentine growth rates are not visible. However, the resulting external morphology, and the development of denticles at the enamel-dentine contact in both taxa suggest considerable adaptive value of denticulate carinae for these groups. Although each group shows different levels of complexity in their denticles, the functionality of the denticles is analogous. The presence of denticulate carinae is not limited to reptiles, however. Mammals (for example *Arctocyon ferox* and *Oxyaena forcipata*), birds (Currie and Coy 2008), and fish (especially sharks), are also known for the presence of denticulate carinae on their teeth; this indicates selective pressure for the development of such structures at least in carnivorous

taxa. Convergent evolution of enamel surface morphologies in reptiles has been suggested (Sander 1997). The findings described here go further and suggest the convergent evolution of a structure formed by both enamel and dentine in teeth of a range of carnivore vertebrates.

The presence of high concentrations of anteroposteriorly directed dentinal tubules near posterior carinae suggests high nutrient transport to these areas. This has been observed in the taxa studied in Chapter 2 (theropods, *Varanus komodoensis*, and *Varanus rudicollis*), and is consistent with the presence of larger posterior carinae (and denticles) in teeth of these taxa. In one of the sections of an unerupted *Varanus rudicollis* tooth, the anterior portion of the tooth had predentine (indicating that this area was not fully mineralized at the time of death), whereas the posterior portion of the tooth is completely mineralized. The pulp cavity is posteriorly placed in most teeth, so that the anterior portion of the tooth has a thicker layer of dentine. The differential growth of these teeth could be the cause of the curvature that characterizes zyphodont teeth in the taxa analyzed. Therefore, the dentine deposition in the anterior portion of the tooth takes longer than in the posterior portion, and that is visible through the lag between mineralization in the posterior and anterior portions of the tooth. The extent of the lag is unknown, but it is likely to be related to the degree of curvature in each tooth. Differential growth of dentine is only visible in late developmental stages, which is when the teeth start to acquire the proportions at their final stage of development.

The dentine is equally distributed (including dentine tubules) and equally developed in teeth in their early stages of development in *Varanus rudicollis*, in which the overall tooth shape is still a generalized cone.

The increased amount of nutrient transport to the posterior half of the tooth (suggested by the concentration of dentinal tubules near the posterior carina in teeth in later stages of development) could promote faster growth and mineralization for the posterior carinae, as well as larger carinae and denticles. Posterior carinae endure high stresses during feeding, associated with behaviors such as pulling carcasses while defleshing them, as in tyrannosaurids (Snively and Russell 2007*a*, 2007*b*) and *Varanus komodoensis* (Moreno et al. 2008). In a tyrannosaurid premaxillary tooth, the high concentrations of anteroposteriorly directed dentine tubules occur near both carinae, which are positioned on the posterior side of the tooth. This suggests that the reinforcement of posterior carinae can be associated with feeding behaviors that cause stresses in an anteroposterior direction (such as pulling movements).

The presence of denticles in some taxa, but not others can be explained by a number of factors. First, the most obvious inference would be that size determines the presence of denticles. It has been previously noted that smaller teeth generally lack such structures (Currie and Coy 2008). However, exceptions do exist. For example, in theropods, although most small taxa have denticulate teeth, large-sized theropod spinosaurid teeth (which are large compared to dromaeosaurid and troodontid teeth)

lack denticles. Additionally, in some taxa such as *Troodon* not all teeth have both anterior and posterior carinae with denticles. The premaxillary teeth of the tyrannosaurid *Aublysodon* have also been suggested to lack serrations. Although this may be due to wear, digestion, or postmortem erosion (Brochu 2002; Carr and Williamson 2004), it is more probable that it represents an ontogenetic stage characteristic of tyrannosaurine tyrannosaurids (Currie 2003). More exceptions to the statement that smaller teeth lack denticles, when compared to larger teeth can be found in crocodilians. Whereas the teeth of the medium sized *Sebecus* are found to have denticles (Legasa et al. 1994), the giant *Sarcosuchus* lacks this feature (Sereno et al. 2001). Modern crocodilians, such as *Alligator* and *Crocodylus* also lack denticles in their teeth.

Therefore, other factors could play an important role in determining the presence or absence of denticles, such as phylogenetic relationships. Phylogeny could partially explain the retention of this character in taxa with smaller teeth (such as troodontid and dromaeosaurid theropods), which are derived forms when compared to the more basal Ceratosauria, in which many taxa already have denticulate carinae. Still, ancestry alone does not explain the presence of denticulate carinae in such a diversity of taxonomic groups, including some varanid lizards, some carnivorous mammals, and some fish. The biomechanics of teeth associated with behaviors such as pulling on carcasses (causing high anteroposterior stresses), biting through bone (causing high stresses in a number of

directions), or holding struggling prey (causing high labiolingual stresses) requires adaptations in morphology of the crowns and roots (Reichel 2010). Perhaps the most noticeable of these adaptations is the widening of teeth labiolingually. However, a labiolingually wide tooth sacrifices its cutting ability if it is a smooth (non - serrated) blade, and the solution for this problem is the presence of denticles, because they improve the cutting ability of a blade (Farlow et al. 1991). Indeed, the only taxon studied in Chapter 2 that does not have denticles on its teeth is *Varanus rudicollis*. This small animal feeds mostly on invertebrates and small vertebrates that can be swallowed whole (Losos and Greene 1988) and has small, labiolingually flat teeth. The other varanid lizard, *Varanus komodoensis* has been known for a long time to feed on larger prey (Losos and Greene 1988), and uses pulling behavior to remove meat from carcasses. Theropods, especially tyrannosaurids, may have behaved in similar ways while feeding (Snively and Russell 2007*a*, 2007*b*), and their labiolingually widened teeth strongly suggest that they were adapted to sustain high lateral bending stresses to sustain the stresses involved with struggling prey and biting through bones.

The biomechanical implications for tyrannosaurid teeth during feeding behaviors are described in Chapter 3, which is an examination of the biomechanics of teeth in *Albertosaurus sarcophagus* and *Tyrannosaurus rex*. The bite forces were estimated for these two taxa, based on a method developed by McHenry (2009). The estimates suggest

Tyrannosaurus had a bite force about four times that of *Albertosaurus*, and reaching a force of up to 13,876N in the posterior region of its jaws.

The tooth mechanics in these taxa varies significantly. In *Tyrannosaurus*, the teeth with most labiolingual bending resistance are the mid-maxillary, anterior dentary, and posterior dentary ones. In *Albertosaurus*, the teeth with highest lateral bending resistance are the ones in the mid-maxillary, mid-dentary, and posterior dentary positions. In both taxa, the teeth with the highest lateral bending resistance are found in the mid-maxillary position. However, in the dentary, the teeth with the highest lateral bending resistance are found in the mid-dentaries of *Albertosaurus*, whereas in *Tyrannosaurus* they are found in the anterior and posterior dentary positions.

The root proportions in these taxa also differ significantly. The percentage of root length within a tooth in *Albertosaurus* is generally lower than in *Tyrannosaurus*. However in both taxa the premaxillary teeth have proportionately long roots compared to the rest of the dentition. It is surprising that the shortest root proportions are found in mid-maxillary and mid-dentary teeth of *Albertosaurus*. Their high labiolingual bending resistance in the FEA suggests, however, that the crown morphology efficiently deflects shear stresses that could potentially cause the breakage of the crown, reducing the mechanical need for longer roots in these teeth. In *Tyrannosaurus*, the shortest roots are found in the posterior dentary teeth. These teeth also have high lateral bending resistance,

suggesting that tall roots are not associated with lateral bending resistance. The upper and lower teeth of *Albertosaurus* and the upper teeth of *Tyrannosaurus* have a well-defined pattern of tooth biomechanics that suggests that their anterior and posterior teeth were adequate for pulling on prey. An example of this behavior is when they use their teeth for defleshing carcasses, and their powerful neck muscles aided that behavior (Snively and Russell 2007*a*, 2007*b*).

The mid-maxillary teeth in both taxa and the mid-dentary teeth only in *Albertosaurus* were important tools to hold onto struggling prey, or to pull sideways on a carcass, behaviors that cause high labiolingual shear stresses. Powerful lateral movements of the head during feeding have been suggested (Snively and Russell 2007*a*, 2007*b*), after studies in craniocervical dynamics. This is also supported by the presence of large lateral semicircular canals in tyrannosaurids (Witmer and Ridgely 2009).

The upper dentitions of theropods, including tyrannosaurids, overbite the lower dentitions. The differences found in the lower jaw of *Tyrannosaurus* when compared to *Albertosaurus* may be a reflection of the noticeable overbite in these taxa. It is currently not known whether the degree of overbite varies significantly between different tyrannosaurid groups; however, the finite element analysis shows that the biomechanics of anterior dentary teeth in *Tyrannosaurus* are more consistent with lateral maxillary teeth than with premaxillary teeth. This observation makes sense

because the anterior dentary teeth align with the anterior maxillary teeth, rather than with premaxillary ones.

Based on the range of values obtained for the shear stress proportions measured in each taxon, it seems that *Albertosaurus* has a higher variety of biomechanical responses from each jaw region. Consequently the teeth are more specialized for different functions. In the FEA, the teeth in *Tyrannosaurus* have less fluctuation in the XY/Z values (the proportion of stresses in the anteroposterior and apicobasal versus labiolingual stresses), demonstrating that its teeth have more homogenous biomechanical responses. This could be a consequence of the fact that *Tyrannosaurus* has teeth that are labio-lingually wider than *Albertosaurus*. Therefore, *Tyrannosaurus* has teeth that are efficient at resisting shear stresses in a wider range of directions. A similar study has been done with carnivorous mammals, in which canids have been shown to have more laterally compressed canines relative to those of felids or hyaenids. Canids have shallow, slashing bites, compared with the deep bites of felids and hyaenids, which often result in tooth-bone contact (Van Valkenburgh and Ruff 1987). The labiolingually wider teeth of felids and hyaenids are able to sustain the stresses and labiolingual bending caused by this behavior, whereas the teeth of canids fail the same test.

The FEA results in Chapter 3 showed that the different functions demonstrated for each tooth family in tyrannosaurids is a reflection of their heterodonty; however, it does not quantify the degree of heterodonty

found in each taxon. A study on external morphologies of teeth is more adequate for that purpose, because it is more comparable across different taxa.

Therefore, in Chapter 4, multivariate analyses were done to compare a set of different measurements taken from tyrannosaurid teeth in order to test the utility of carina placement as a measure of quantification of heterodonty. When dealing with tyrannosaurids, one of the biggest challenges is the great variation in size, which can obscure other variables in multivariate analyses. A few measures to counter that effect include log transforming data and using, whenever possible, rates instead of raw values (for example FABL/BW ratios to describe tooth proportions). The use of rates makes it clear that the angle measured between the anterior and posterior carinae (ANG) is more related to tooth shape (FABL/BW) than to the overall tooth size. This also correlates ANG to function, because the premaxillary and anterior dentary teeth of all taxa clearly show distinct patterns for this measurement (when compared to lateral teeth). Premaxillary teeth that have been demonstrated previously to have a specific function and biomechanics associated with pulling and defleshing carcasses. The FABL/BW proportion seems to influence ANG values up until when the FABL/BW proportion reaches a value of about one. At values higher than that, the range of ANG values significantly decreases, and tooth position plays a more significant role in determining ANG.

The anterior maxillary teeth of *Tyrannosaurus* have lower ANGs compared to the mid-maxillary and posterior maxillary teeth, and may be a reflection of the *en echelon* tooth placement described by Smith (2005). This tooth placement is characterized by teeth that do not line up along their anteroposterior axes, but instead line up diagonally. These teeth have smaller ANGs to compensate for this misalignment. This suggests that the anterior maxillary teeth of *Tyrannosaurus* could serve as efficient gripping tools, because the carinae provided a posterolingual cutting edge, and the *en echelon* placement of the teeth would have prevented the meat from sliding forwards, because the diagonal alignment of teeth, along with carinae placed somewhat posteriorly, offers resistance for the meat to slide anteriorly. In addition to that, a capability for making wider cuts in the food could also result from this morphology. These characteristics would also make these teeth efficient tools for scraping meat off bones, functioning in a similar way to incisors and forcing the meat into the mouth. It is common to see anterior maxillary teeth with broken or worn tips, suggesting this behavior did indeed happen (Schubert and Unguar 2005).

The ANGs in mid-maxillary teeth are larger, providing an anteroposterior slicing function to these teeth, which is consistent with the biomechanics described previously; mid-maxillary teeth in tyrannosaurids have strong anteroposterior axes, and increased bending resistance in this direction. It seems that ANG values at this point are of limited use for taxonomy, because the distribution patterns of ANGs along the tooth rows

observed in tyrannosaurids are, at the current sample size, too similar. However, this measurement has shown great potential for identifying tooth positions in isolated tyrannosaurid crowns. There is a range of angles that are characteristic for each tooth family. The best separation between tooth families was found in *Tyrannosaurus*, which leads to the conclusion that this is the taxon with the highest degree of heterodonty, at least from a carinal placement point of view. However, this high degree of heterodonty could be size related, because the *Tyrannosaurus* teeth were the largest among the specimens studied. The analysis of ontogenetic sequences could help to verify this point further.

Another aspect to tooth reptile biomechanics to be taken into consideration is the role of enamel microstructure in theropods and other reptiles. Mammals have developed complex enamel prisms, which are efficient structures that add great mechanical resistance to teeth. Reptilian enamel strengthens teeth as well, but the microstructures have not been studied nearly as much as mammalian enamel prisms. It is clear that reptile enamel microstructure has phylogenetic value, as suggested by Sander (1999, 2000) and Hwang (2005). Especially when looking at the schmeltzmuster level, all taxa in the analysis in Chapter 5 were distinct. Tyrannosaurid teeth have columnar enamel with diverging crystallites (at angles of about 20° in relation to the main axis of the column of crystallites) near the contact with dentine, and parallel crystallites with faint incremental lines near the outer surface of the enamel. Troodontid teeth

have parallel crystallites without incremental lines. However, in different layers of the enamel of the specimen studied, the parallel crystallites were deposited at slightly different angles. The tooth (UALVP 53595) of the mosasaurid *Platecarpus* also has parallel crystallites, although it did not appear that there were any incremental lines or varying angles of deposition of crystallites at different layers. The tooth of the mosasaurid *Platecarpus ptychodon* (UALVP 51744) has columnar enamel with diverging crystallites (with crystallites inclined at an angle of about 30° in relation to the main axis of the column of crystallites) throughout the whole width of the enamel. Finally, the varanid lizard *Varanus komodoensis* tooth (UALVP 53481) has parallel crystallites with well-defined incremental lines. Although the differences in the schmeltzmuster of enamel in the different specimens are probably taxonomically influenced, the biomechanics associated with each of the structures differs significantly.

The structures observed in tyrannosaurids provide a layer of protection in the outermost enamel, in which parallel crystallites greatly reduce stresses that are transferred into the deeper layers of the tooth. However, if forces are applied to that layer at certain angles (in one of the case studies, 45°), the parallel crystallites in this layer have a tendency to fail, and may flake off. The presence of incremental lines helps prevent cracks from propagating farther into the tooth. The columnar structures with diverging crystallites near the dentine perform much better when forces are applied at inclined angles, because the columns absorb much

of the impact, preventing it from propagating to adjacent columns or towards the dentine. This configuration provided increased bending resistance in tyrannosaurid teeth.

Although the troodontid specimen does not have multiple types of enamel microstructure, the parallel crystallites seen in the SEM indicate a unique arrangement. Parallel crystallites deposited at different angles provide mechanical reinforcement, because they increase the ability of that enamel to receive forces from a variety of angles. It has been demonstrated, however, that *Troodon* has different enamel microstructures in different tooth families (Hwang 2005), and further testing with this variability in mind will allow a better understanding of troodontid feeding habits and behaviors.

The microstructure of enamel in a *Varanus komodoensis* tooth has a similar configuration to the outer layer of tyrannosaurid enamel. The parallel crystallites provide great stress resistance at right angles; however, at inclined angles they are more fragile, and the incremental lines play an important role of preventing cracks from propagating into deeper layers of the tooth.

The teeth of the mosasaurid taxa studied have distinct enamel microstructures. One *Platecarpus* tooth (UALVP 53595) has parallel crystallites, but a detailed analysis of these crystallites was hindered by the poor quality of the specimen, whereas the *Platecarpus ptychodon* tooth (UALVP 51744) has clearly defined columnar structures with

diverging crystallites. FEA analyses of the 3-D models representing parallel and diverging crystallites show the tooth biomechanics in these two specimens differ significantly. The angles of diverging crystallites in tyrannosaurid and mosasaurid taxa vary, and this variation influences the capability of these structures to withstand stresses. Crystallites diverging at a 30° angle from the main axis of the column of crystallites (such as the ones observed in *Platecarpus ptychodon*) seem to be more efficient at sustaining stresses generated when a 45° angled force is applied to them than the ones found in tyrannosaurids. This makes sense when considering that in *Platecarpus ptychodon* these columns extend from the outer layer of the enamel to the enamel-dentine junction, and receive any forces (and stresses) directly from the external environment. In contrast, tyrannosaurids have an extra layer of protection provided by parallel crystallites closer to the outer enamel surface, which diminishes the levels of mechanical stress that is transmitted to the layer with columnar enamel. This “filter” creates different selective pressures, compared to what is seen in the mosasaurid tooth, resulting in wider angles for crystallite deposition in tyrannosaurid enamel, and narrower angles for crystallite deposition in the mosasaurid enamel. It is likely that the teeth in *Platecarpus ptychodon* had great bending resistance as a result of the presence of these microstructures, which is a convergent adaptation to what is seen in tyrannosaurids.

In order to further investigate the applicability of the techniques developed in Chapter 3, a tooth from a herbivorous taxon, *Stegosaurus*, was also analyzed in Chapter 6. The bite forces calculated using the method by McHenry (2009) indicated that the jaws of *Stegosaurus* were relatively weak (275N in the posterior region of the jaws, which is the strongest). This would have been sufficient for these animals to feed on thin branches and herbaceous plants, characteristic of the seasonal environments described for the Morrison Formation flora (Parrish et al. 2004). When these biting forces were applied to a 3-D model representing a *Stegosaurus* tooth, some material failure was observed near the tip of the tooth, suggesting that this area has the highest potential for breakage and/or wear. However, this taxon also has structures on the cutting edges of its teeth that are reminiscent of the denticles in theropods, and these "denticles" show little potential to break under the biting forces attributed to *Stegosaurus*. Denticulate edges increase the efficiency of teeth in cutting food (Abler 1992), and in a taxon with low biting forces such as the ones calculated for *Stegosaurus*, the mechanical advantage of a serrated edge is significant. The efficient distribution of stresses in the 3-D model representing a *Stegosaurus* tooth suggests that stegosaur teeth had high bending resistance, similar to tyrannosaurid teeth. In addition to that, the overall morphology of the crowns in *Stegosaurus* efficiently distributes the stresses caused by forces applied to it, at least enough so to prevent the denticles from breaking. The denticles in *Stegosaurus* are also

proportionately large, when compared to the ones in theropods, which makes them even stronger and more efficient for cutting fibrous materials such as plants.

Conclusions

The complex denticles observed in theropods (with their own internal structures) are not found in *Varanus komodoensis*; however, the denticles in both taxa develop at the enamel-dentine junction, and the basic tooth developmental processes that produce carinae are similar. Although the tooth morphologies of *Varanus komodoensis* and theropod dinosaurs differ at the denticular level, the presence of denticulate carinae in these two distantly related taxa suggests that similar biomechanics and feeding behaviors created similar selective pressures for the development of such structures.

When considering tooth biomechanics at the microscopic level, enamel microstructures in reptiles are a great tool to make inferences about functional aspects of the dentition. It is clear that different enamel microstructures, whether they are parallel crystallites or columnar diverging crystallites, offer different mechanical solutions to prevent tooth failure under different circumstances. It is only natural that in heterodont taxa, different combinations of enamel microstructures reflect the different functions of each tooth family. The tooth biomechanics observed in tyrannosaurids demonstrate that each tooth family has a crown

morphology that reflects its function. In a taxon such as *Tyrannosaurus*, the alignment of the jaws could explain why the teeth in the dentary have different biomechanics than those in *Albertosaurus*, indicating that heterodonty in tyrannosaurids is taxon-specific and dependant on skull proportions. When comparing angles between anterior and posterior carinae of five tyrannosaurid taxa (*Albertosaurus*, *Daspletosaurus*, *Gorgosaurus*, *Tarbosaurus*, and *Tyrannosaurus*), it became clear that *Tyrannosaurus* had the highest degree of heterodonty because it had the greatest range of differences between tooth families defined by the angles measured between anterior and posterior carinae. This is probably related to the gigantism observed in this taxon, as well as jaw proportions and alignment. Most importantly, the tooth biomechanics observed in the taxa studied indicates that the bending resistance is provided mostly by the labiolingual thickening of teeth. The same is true for herbivorous taxa, such as *Stegosaurus*, which has a crown morphology that efficiently distributes stresses to help prevent the denticles (important for improving the cutting ability of the teeth) from breaking, by ensuring that most of the stresses that occur during an average bite are reduced in the areas with denticles.

It is suggested that the presence of labiolingually thickened teeth can be related to behaviors that cause great lateral stresses on teeth during feeding. The labiolingual thickening of teeth sacrifices the cutting ability of smooth (unserrated) edges; however, the presence of denticulate

carinae increases the cutting ability of labiolingually thickened teeth and is a solution developed by multiple taxa that encounter this problem.

Although there is still need for numerous additional analyses to improve the understanding of tooth development in reptiles, the main goal of this project, to determine why and how carinae (and denticles) develop in such a variety of taxa, has been reached. It seems that there are a number of reasons to explain the development of such structures, and that biomechanics and function play a significant role in determining their presence.

The hypothesis that carinal and denticle development are similar in a variety of taxa and this represents an adaptive convergence is probably true. The comparisons between tooth development in theropod dinosaurs and varanid lizards outlined in Chapter 2 demonstrated that although different levels of complexity may be found in the denticles of these taxa, the basic processes that determine the presence of carinae and denticles are similar. Therefore, the external morphology and function of denticulate carinae in these distantly related taxa is a convergent adaptation to improve the cutting efficiency of teeth while maintaining good labiolingual bending resistance through the labiolingual thickening of teeth.

The hypothesis that carinal positions, along with other measurable variables in tooth morphometrics influence tooth function, its biomechanics, and make heterodonty quantifiable is also accepted. It becomes clear with Chapters 3 through 6 that although there is a strong

phylogenetic aspect to tooth morphology, there is also a clear functional relationship that can be assessed through the analyses of the biomechanics of simplified structures. Although analyses of heterodonty in reptiles are uncommon and perhaps controversial, there have been an increasing number of studies, especially with tyrannosaurids (Currie et al. 1990; Molnar 1998; Holtz 2004; Smith 2005). As more specimens are discovered, the subtle differences in the dentitions of these animals become more evident, and the contribution of biomechanical analyses of teeth to behavioral analyses is significant.

Future analyses of juvenile reptile taxa, as well as birds, mammals and fish would further improve the results discussed. The analysis of ontogenetic sequences is especially important in tyrannosaurid taxa. Furthermore, there is a wide range of sizes, and understanding the morphometric changes in gigantic taxa (such as *Tarbosaurus* and *Tyrannosaurus*) will help separate adaptations that occur due to differences in behavior from those due to allometric constraints.

Another prospect for the future is a morphometric study of taxa that have serrated teeth, and to compare these with closely related taxa that have unserrated teeth. Such an analysis will help determine whether there are any measurable variables that may influence the presence or absence of denticulate edges.

Finally, a detailed developmental study of an ontogenetic series of a *Varanus komodoensis* would be invaluable for better understanding the

fine details regarding the development of carinae and denticles in this taxon. These analyses will have great potential for comparisons with theropod taxa, even though the denticles are more complex structures in theropod teeth. The feeding behaviors in *Varanus komodoensis*, such as inertial feeding and the use of neck muscles to pull meat from carcasses are comparable to what has been suggested for tyrannosaurids. Therefore, *Varanus komodoensis* teeth make good analogs for functional and developmental analyses.

It is clear that the study of biomechanics is a growing field in paleontology, especially with the increasing ease of access to resources such as CT-scans and Finite Element Analysis software. The exchange of information is facilitated, because sending files between computers, rather than loaning original specimens can grant access to 3-D images that have a level of detail many times comparable to that of the original fossil. Besides that, CT-scans allow the analysis of internal structures of any given object, without the need for destructive procedures. This shift in paleontological research has facilitated the analysis of structural mechanics in teeth and bones, and therefore we are now able to test hypotheses about behaviors previously suggested for a variety of groups. This thesis is an addition to this field. Perhaps the most important conclusion drawn from the research in Chapters 2 to 6 is that reptile teeth are not featureless, laterally compressed blades, but rather an invaluable

source of information about the daily lives and habits of extinct and extant animals.

References

Abler, W. L. 1992. The serrated teeth of tyrannosaurid dinosaurs, and biting structures in other animals. Paleobiology, **18**(2): 161–183.

Beatty, B.L., and Heckert, A.B. 2009. A large archosauriform tooth with multiple supernumerary carinae from the Upper Triassic of New Mexico (USA), with comments on carina development and anomalies in the Archosauria. Historical Biology, **21**(1): 57–65.

Brochu, C.A. 2002. Osteology of *Tyrannosaurus rex*: Insights from a nearly complete skeleton and high-resolution computed tomographic analysis of the skull. Memoirs of the Society of Vertebrate Paleontology, **7**: 1–138.

Carr, T.D., and Williamson, T.E. 2004. Diversity of late Maastrichtian Tyrannosauridae (Dinosauria: Theropoda) from western North America. Zoological Journal of the Linnean Society, **142**(4): 479–523.

Currie, P.J. 2003. Allometric growth in tyrannosaurids (Dinosauria: Theropoda) from the Upper Cretaceous of North America and Asia. Canadian Journal of Earth Sciences, **40**: 651–665.

Currie, P.J., and Coy, C. 2008. *In* Vertebrate Microfossil Assemblages: their role in palaeoecology and palaeobiogeography. *Edited by* Sankey,

J.T., and Baszio, S. (eds.). Indiana University Press, Bloomington. pp. 159–165.

Farlow, J.O., Brinkman, D.L., Abler, W.L., and Currie, P.J. 1991. Size, shape and serration density of theropod dinosaur lateral teeth. Modern Geology **16**: 161–198.

Hwang, S.H. 2005. Phylogenetic patterns of enamel microstructure in dinosaur teeth. Journal of Morphology, **266**: 208–240.

Legasa, O., Buscalioni, A.D., and Gasparini, Z. 1994. The serrated teeth of *Sebecus* and the iberoccitanian crocodile, morphological and ultrastructural comparison. Studia Geologica Salmanticensia, **29**: 127–144.

Losos, J.B., and Greene, H.W. 1988. Ecological and evolutionary implications of diet in monitor lizards. Biological Journal of the Linnean Society, **35**: 379–407.

McHenry, C. R. 2009. Devourer of gods: the paleoecology of the Cretaceous pliosaur *Kronosaurus queenslandicus*. Unpublished Ph. D. dissertation, Department of Earth Sciences, University of Newcastle, Newcastle, N.S.W., Australia, 635 pp.

Moreno, K., Wroe, S., Clausen, P., McHenry, C., D'Amore, D.C., Rayfield, E., and Cunningham, E. 2008. Cranial performance in the Komodo

dragon (*Varanus komodoensis*) as revealed by high-resolution 3-D finite element analysis. Journal of Anatomy, **212**: 736–746.

Parrish, J. T., Peterson, F. and Turner, C. E. 2004. Jurassic “savannah” – plant taphonomy and climate of the Morrison Formation (Jurassic, western U.S.A.). Sedimentary Geology 167: 139–164.

Peyer, B. 1968. Comparative odontology. The University of Chicago Press, Chicago, USA. 347 pp.

Reichel, M. 2010. The heterodonty of *Albertosaurus sarcophagus* and *Tyrannosaurus rex*: biomechanical implications inferred through 3-D models. Canadian Journal of Earth Sciences, **47**: 1253–1261.

Sander, P. M. 1997. Non-mammalian synapsid enamel and the origin of mammalian enamel prisms: the bottom-up perspective. *In* Koenigswald, W.v. and Sander, P. M. (eds) Tooth enamel microstructure. Balkema, Rotterdam, Netherlands. Pp. 41–62.

Sander, P.M. 1999. The microstructure of reptilian tooth enamel: terminology, function, and phylogeny. München Geowissenschaften Abhandlungen (Reihe A), **38**: 1–102.

Sander, P. M. 2000. Prismless enamel in amniotes: terminology, function, and evolution. *In* Development, function and evolution of teeth. *Edited by* M.F. Teaford, M.M. Smith, and M.W.J. Ferguson. Cambridge University Press, Cambridge, UK, pp. 92–106.

Schubert, B.W., and Unguar, P.S. 2005. Wear facets and enamel spalling in tyrannosaurid dinosaurs. Acta Palaeontologica Polonica, **50**: 93–99.

Sereno, P.C., Larsson, H.C.E., Sidor, C.A., and Gado, B. 2001. The giant crocodyliform *Sarcosuchus* from the Cretaceous of Africa. Science, **294**: 1516–1519.

Smith, J.B. 2005. Heterodonty in *Tyrannosaurus rex*: implications for the taxonomic and systematic utility of theropod dentitions. Journal of Vertebrate Paleontology, **25**: 865–887.

Snively, E., and Russell, A. P. 2007*a*. Craniocervical feeding dynamics of *Tyrannosaurus rex*. Paleobiology, **33**: 610–638.

Snively, E., and Russell, A. P. 2007*b*. Functional morphology of the neck musculature in the Tyrannosauridae (Dinosauria, Theropoda) as determined via a hierarchical inferential approach. Zoological Journal of the Linnean Society, **151**(4): 759–808.

Van Valkenburg, B., and Ruff, C.B. 1987. Canine tooth strength and killing behaviour in large carnivores. Journal of Zoology, London, **212**: 379 – 397.

Witmer, L.M., and Ridgely, R.C. 2009. New insights into the brain, braincase, and ear region of tyrannosaurs (Dinosauria, Theropoda),

with implications for sensory organization and behavior. The Anatomical Record, **292**: 1266 –1296.